NASA
Technical
Paper
2644

February 1987

Flight Investigation of the Effect of Tail Configuration on Stall, Spin, and Recovery Characteristics of a Low-Wing General Aviation Research Airplane

H. Paul Stough III,
James M. Patton, Jr.,
and Steven M. Sliwa

NASA

NASA Technical Paper 2644

1987

Flight Investigation of the Effect of Tail Configuration on Stall, Spin, and Recovery Characteristics of a Low-Wing General Aviation Research Airplane

H. Paul Stough III,
James M. Patton, Jr.,
and Steven M. Sliwa

Langley Research Center
Hampton, Virginia

National Aeronautics
and Space Administration

Scientific and Technical Information Branch

CONTENTS

LIST OF FIGURES

SUMMARY

Flight tests were performed to investigate the stall, spin, and recovery characteristics of a low-wing, single-engine, light airplane with four interchangeable tail configurations. The four tail configurations were evaluated for the effects of varying mass distribution, center-of-gravity position, and control inputs. Stalls were characterized by predominant roll-off tendencies accompanied by slight nose-down pitching motions. Variations in tail configuration produced spins at angles of attack from 40° to 60° and turn rates of about 145 to 208 deg/sec. Deflecting the ailerons with the spin tended to steepen the spin, reduce the yaw rate, and increase the magnitude of oscillations in roll rate and pitch rate; deflecting ailerons against the spin had the opposite effect. The steady spin was not noticeably affected by entry conditions or power level. Increasing the mass of the wing did not appreciably change the spin mode, but it did degrade spin recovery. Asymmetries in wing mass distribution caused the airplane to spin flatter and to recover more slowly when spinning toward the lighter wing. A center-of-gravity shift of nine percent of the mean aerodynamic chord had little effect on spin characteristics. Some unrecoverable flat spins were encountered which required the use of the airplane spin chute for recovery. For recoverable spins, antispin rudder followed by forward wheel with centered ailerons provided the quickest spin recovery. For all four tail configurations, the moderate spin modes of the airplane agreed very well with those predicted from spin-tunnel model tests. The flat spin encountered was at a lower angle of attack and at a slower turn rate than predicted from spin-tunnel model tests. Results indicate that the 1947 NACA tail design criterion cannot be used alone to predict airplane spin recovery characteristics.

INTRODUCTION

In response to the need for improving the stall/spin characteristics of general aviation airplanes, the National Aeronautics and Space Administration (NASA) is conducting a comprehensive program to develop new stall/spin technology for this class of airplane (ref. 1). The program incorporates spin-tunnel model tests, radio-controlled flying model tests, static- and rotary-balance wind-tunnel tests, analytic studies, and airplane flight tests for a number of configurations representative of typical general aviation airplanes.

Airplane flight-test results provide a reference base for correlation of theoretical predictions and model test results. Four single-engine airplanes are being or have been tested in the NASA stall/spin program: (1) a low-wing airplane with four interchangeable tails (ref. 2), (2) a low-wing airplane with wing-tip rockets for control augmentation (ref. 3), (3) a high-wing airplane (ref. 4), and (4) a low-wing airplane with a T-tail (refs. 5 and 6).

Spin-tunnel model tests (ref. 7) have been conducted to explore the effects of tail design on the spin and recovery characteristics of a typical low-wing, single-engine, light general aviation airplane and to evaluate a tail design criterion for satisfactory spin recovery for light airplanes. These tests showed that in addition to the tail configuration, other geometric characteristics of the airplane configuration could appreciably affect the spin and recovery characteristics. It was concluded in reference 7 that the "tail design criterion for light airplanes, which uses

the tail damping power factor (TDPF) as a parameter, cannot be used to predict spin-recovery characteristics. However, certain principles implicit in the criterion are still valid and should be considered when designing a tail configuration for spin recovery. It is important to provide as much damping to the spin as possible (area under the horizontal tail), and it is especially important to provide as much exposed rudder area at spinning attitudes as possible (unshielded rudder volume coefficient (URVC)) in order to provide a large antispin yawing moment for recovery."

To validate the model test results reported in reference 7, an airplane was modified to accommodate tail configurations selected from those tested on the model, and flight tests were conducted to determine the spin and recovery characteristics. This report presents results for flight tests of the low-wing airplane with four interchangeable tails. Stall, incipient spin, developed spin, and recovery characteristics are presented, including the effects of mass distribution, center-of-gravity position, and control inputs. Results from related model tests are presented in references 7 to 9. This report is primarily a presentation of flight-test results; however, a brief comparison of airplane and model spin characteristics is included. (See also ref. 10.) Although it was not a variable for the tests reported herein, wing leading-edge design can have a strong effect on airplane stall/spin characteristics, as shown in references 2 and 11.

SYMBOLS AND ABBREVIATIONS

Measurements are referred to the set of body axes with the origin at the airplane center of gravity, as shown in figure 1. Measurements were made and quantities are presented in U.S. Customary Units. Symbols in parentheses refer to labels on computer generated figures.

a_N	(NORM ACC)	normal acceleration at center of gravity (positive in negative Z_b direction), g units
	(ALTITUDE)	pressure altitude, ft
b		wing span, ft
$\bar{c}$		mean aerodynamic chord, ft
c.g.		center-of-gravity location, percent $\bar{c}$
FS		fuselage station, longitudinal coordinate measured along a water line, positive moving aft (wing leading edge is at FS 68.03), in.
g		acceleration due to gravity, 32.2 ft/sec^2
I_X, I_Y, I_Z		moment of inertia about X_b, Y_b, and Z_b body axis, respectively, slug-ft^2
IYMP		inertia yawing-moment parameter, $\frac{I_X - I_Y}{mb^2}$
L		distance from center of gravity of airplane to centroid of fuselage area S_F, ft (see fig. 5)

L_1		distance from center of gravity of airplane to centroid of rudder area S_{R1}, ft (see fig. 5)
L_2		distance from center of gravity of airplane to centroid of rudder area S_{R2}, ft (see fig. 5)
	(LAT ACC)	lateral acceleration at center of gravity (positive in positive Y_b direction), g units
	(LAT FORCE)	lateral wheel force (positive for forces tending to rotate wheel clockwise), lb
	(LONG ACC)	longitudinal acceleration at center of gravity (positive in positive X_b direction), g units
	(LONG FORCE)	longitudinal wheel force (positive for forces tending to pull wheel aft), lb
m		mass of airplane, slugs
	(MPR)	engine manifold pressure, in. Hg
p	(ROLL RATE)	roll rate (positive for right wing down), deg/sec
	(PROP SPEED)	propeller and engine speed, rpm
q	(PITCH RATE)	pitch rate (positive for nose up), deg/sec
r	(YAW RATE)	yaw rate (positive for nose right), deg/sec
R		spin radius, approximately $\frac{g}{\Omega^2 \tan \alpha}$, ft
R/S		rate of sink, ft/sec
	(RES ACC)	resultant linear acceleration, (LONG ACC^2 + LAT ACC^2 + NORM ACC^2)$^{1/2}$, g units
	(RUD FORCE)	rudder pedal force (positive for forces tending to push right pedal forward), lb
S		wing area, ft^2
S_F		fuselage side area under horizontal tail, ft^2 (see fig. 5)
S_{R1}		unshielded rudder area above horizontal tail, ft^2 (see fig. 5)
S_{R2}		unshielded rudder area below horizontal tail, ft^2 (see fig. 5)
T		period of spin, approximately $\frac{360°}{\Omega}$, sec
TDPF		tail damping power factor (see fig. 5)
TDR		tail damping ratio (see fig. 5)

u,v,w		velocity component in X_b, Y_b, and Z_b direction, respectively, ft/sec (see fig. 1)
URVC		unshielded rudder volume coefficient (see fig. 5)
V	(SPEED)	true airspeed, ft/sec (see fig. 1)
WL		water line, vertical coordinate in airplane plane of symmetry measured perpendicular to reference line (reference line is WL 45.00 and passes through propeller center line), in.
X_b,Y_b,Z_b		body axes through airplane c.g. (see fig. 1)
x		distance rearward from leading edge of mean aerodynamic chord to center of gravity, ft
y		distance between center of gravity and fuselage center line (positive when center of gravity is right of center line), ft
z		distance between center of gravity and fuselage reference line (positive when center of gravity is below line), ft
α	(ALPHA CG)	true angle of attack at airplane center of gravity, deg (see fig. 1)
α'		angle between fuselage reference line and relative wind (approximately equal to absolute value of angle of attack at plane of symmetry), deg
α_m		measured angle of attack at instrumentation boom, deg
α_T		true angle of attack at instrumentation boom, deg
β	(BETA CG)	angle of sideslip at airplane center of gravity, deg (see fig. 1)
β_m		measured angle of sideslip at instrumentation boom, deg
β_T		true angle of sideslip at instrumentation boom, deg
δ_a	(AILERON)	average aileron deflection (positive for right aileron trailing edge down), $\frac{1}{2}$ (Right aileron deflection + Left aileron deflection), deg (see fig. 1)
δ_e	(ELEVATOR)	elevator deflection (positive for trailing edge down), deg (see fig. 1)
δ_r	(RUDDER)	rudder deflection (positive for trailing edge left), deg (see fig. 1)
ϕ		bank angle (positive for right wing down), deg
μ		airplane relative density coefficient, $\frac{m}{\rho Sb}$
ρ		air density, slugs/ft^3

Ω (TURN RATE) total angular velocity of airplane, $(p^2 + q^2 + r^2)^{1/2}$ with sign of r, deg/sec

DESCRIPTION OF AIRPLANE

Baseline Configuration

The test airplane was a two-place, single-engine, low-wing, fixed-gear design. This airplane was a one-of-a-kind research airplane, but was considered representative of this class of aircraft. A photograph and three-view drawing of the baseline configuration are presented as figures 2 and 3, respectively. The wing incorporated an NACA 64_2-415 airfoil section (modified to remove lower-surface reflex near the trailing edge) and had plain flaps and ailerons. The baseline configuration, referred to as tail 4, had a low, aft-mounted horizontal tail, and the rudder extended from the top of the vertical tail to the top of the fuselage. Elevator, rudder, and aileron trim could not be varied in flight. Brackets for adding ballast at the wing tips and at the firewall enabled variation of airplane mass and moments of inertia while maintaining a fixed center-of-gravity position. Fuel was carried in a 10-gallon tank mounted in the cockpit near the airplane center of gravity to reduce fuel movement during spins. The airplane was equipped with a spin-recovery parachute system (ref. 12), the size of which was based on tests in the Langley Spin Tunnel (ref. 13). Baseline airplane characteristics are presented in table 1.

Tail Configurations

To study the effect of tail configuration on stall, spin, and recovery characteristics, the horizontal tail was relocated and the rudder length was changed to produce the four tail arrangements shown in figure 4. The tail configurations were selected based on spin-tunnel tests of nine different tails on a model of the test airplane. Tail configurations 2, 3, 4, and 6 (the identification numbers used in the model tests of reference 7 are used herein) were chosen because they were thought to be typical of current production designs, because they were the easiest to implement on the test airplane, and because model tests indicated they would yield a wide range of spin characteristics.

The various tail configurations consisted of three locations for the horizontal tail and either a long or a short rudder. Geometric characteristics of the four tails are given in table 2. Both tails 2 and 3 had the horizontal stabilizer mounted at the top of the fuselage. Tail 2 had a short rudder; tail 3 had a long rudder. Tail 4, the baseline configuration, had a low, aft-mounted horizontal tail and a short rudder. Tail 6 had the horizontal tail mounted above the fuselage on the vertical stabilizer and had a long rudder. Horizontal and vertical tail incidences were kept constant at -3° and 0°, respectively.

Variation of only the tail configuration provided an opportunity to evaluate the validity of the tail damping power factor (TDPF), a spin-recovery design criterion presented by the National Advisory Committee for Aeronautics (NACA) in 1947 and described in reference 14. The historical development and the method of calculation are given in reference 7. As shown in figure 5, TDPF is the product of the tail damping ratio (TDR) and the unshielded rudder volume coefficient (URVC). The criterion assumes the airplane spin mode is a function of TDR and the airplane spin-recovery control power is a function of URVC; hence, the overall spin-recovery characteristics are expected to be a function of TDPF. A wide range of tail damping

characteristics for the test airplane was obtained with the four tail configurations, as shown in table 3. The TDPF of each of the four tails is plotted in figure 6 against the inertia yawing-moment parameter (IYMP) values tested to relate these designs to the 1947 NACA design guideline for satisfactory spin recovery.

Mass Distribution

To investigate the effect of tail configuration alone, the mass characteristics of the airplane were carefully controlled and are listed in table 4. For the baseline loading tested, the overall weight of the airplane at test altitude varied from 1530 to 1538 lb, which was slightly above the normal gross weight limit of the airplane. The center-of-gravity position was nominally 26 percent of the mean aerodynamic chord ($0.26\bar{c}$); the normal aft center-of-gravity limit for the test airplane is 27 percent of the mean aerodynamic chord ($0.27\bar{c}$), as shown in figure 7. Considering the equations of motion for a rigid body, important mass characteristics for spin recovery are the IYMP and the airplane relative density coefficient μ. The IYMP was maintained at about -50×10^{-4}; μ varied from about 9.7 at an altitude of 5000 ft to 11.3 at an altitude of 10 000 ft.

To determine the effects of varying mass distribution on spin and recovery characteristics, additional tests were performed with tails 2, 3, and 4 at IYMP values of 0 and 50×10^{-4}. Ballast was added to make the airplane neutrally loaded (IYMP = 0) and wing heavy (IYMP = 50×10^{-4}) while maintaining the center of gravity at $0.26\bar{c}$. Gross weight and relative density μ were increased slightly by the ballast addition. These airplane loadings are also presented in table 4. The combinations of TDPF and IYMP tested are displayed graphically in figure 6 along with the criterion boundaries for spin recovery for $\mu = 11$.

Center of Gravity

Aft movement of the center of gravity normally enables an airplane to penetrate the stall more deeply and therefore can be detrimental to spin characteristics. To study the effect of center-of-gravity location on spin and recovery characteristics, the baseline configuration (tail 4) was tested at center-of-gravity positions of $0.26\bar{c}$ to $0.35\bar{c}$. It was not possible to add sufficient ballast or to relocate enough equipment to move the center of gravity forward of $0.26\bar{c}$. The IYMP varied from -53×10^{-4} to -61×10^{-4} during these tests of center-of-gravity effects.

INSTRUMENTATION

The test airplane was instrumented to measure and record flow angles and true airspeed ahead of each wing tip, linear accelerations along the body axes, angular rates about the body axes, control surface positions, control wheel and rudder pedal forces, engine power parameters, altitude, and spin-recovery parachute load. The onboard data system was supplemented by ground-based telephoto video and movie cameras and by wing-tip and cockpit mounted movie cameras. Pilot comments were recorded on the ground videotape. All data were time correlated and provided a continuous time history from spin entry through recovery. Data were telemetered to a ground station and monitored in real time along with a video display of the spinning airplane. For debriefing purposes, the videotape and telemetry records were reviewed shortly after each flight.

Linear accelerations and flow measurements were corrected to indicate conditions at the airplane center of gravity. The measured values of angle of attack and angle of sideslip were corrected for upwash and sidewash based on flow angle corrections determined from wind-tunnel tests of full-scale and small-scale models which duplicated the flight-test instrumentation boom installation (ref. 15). The correction equations are as follows:

For $\alpha_m \leq 53°$,

$$\alpha_T = 0.8776\,\alpha_m + 0.0170\,\beta_m - 0.80 \quad \text{(at left wing tip)}$$

$$\alpha_T = 0.8776\,\alpha_m - 0.0170\,\beta_m - 0.80 \quad \text{(at right wing tip)}$$

For $\alpha_m > 53°$,

$$\alpha_T = 0.8984\,\alpha_m - 0.0244\,\beta_m - 0.85 \quad \text{(at left wing tip)}$$

$$\alpha_T = 0.8984\,\alpha_m + 0.0244\,\beta_m - 0.85 \quad \text{(at right wing tip)}$$

For all α_m,

$$\beta_T = 0.9873\,\beta_m - 0.0956\,\alpha_m - 0.11 \quad \text{(at left wing tip)}$$

$$\beta_T = 0.9873\,\beta_m + 0.0956\,\alpha_m - 0.11 \quad \text{(at right wing tip)}$$

Detailed descriptions of the instrumentation system and the data reduction procedures can be found in references 16 and 17.

EVALUATION PROCEDURE

The results of the investigation were based on pilot comments, time history records of airplane motions and controls, and films and videotapes of the tests. All maneuvers were flown by the same pilot, thus minimizing differences in maneuvering caused by variation in pilot technique.

The initial flight tests were conducted with tail 6, followed by tests with tails 2, 3, and 4 in that order. This order of testing corresponded to a progression from the most favorable to the least favorable spin and recovery characteristics indicated by the model tests of reference 7. Airplane stall and departure characteristics were evaluated with tail 6. Maneuvers included 1g and accelerated (banked) stalls with flaps retracted for various combinations of engine power, bank angle, and sideslip angle, as shown in table 5. An abbreviated series of stalls were performed with tails 2, 3, and 4. For each tail configuration, elevator effectiveness was

determined from gradual airspeed acceleration-deceleration maneuvers at 1g with idle power, and rudder effectiveness was determined from steady-heading sideslips at constant airspeed.

The spin tests were performed at the NASA Wallops Flight Facility. The test altitudes ranged from 10 000 to 5000 ft. Reynolds number (based on $\bar{c}$) at the stall was about 2.5×10^6. Spin entry conditions included combinations of acceleration, roll, pitch, yaw, and power. Controls anticipated to be prospin (i.e., in the direction of the spin) were applied at or just before the stall. The control positions at entry were wheel back with rudder in the direction of the spin or neutral and ailerons either neutral with the spin (right wheel for a right spin), or against the spin (left wheel for a right spin). All spins were performed with the flaps retracted. Spins were allowed to develop for 1, 3, 6, and, in some instances, 10 or more turns. Recovery control inputs investigated included the following:

1. Normal recovery controls, defined as full antispin rudder followed by full trailing-edge-down elevator with ailerons neutralized

2. Simultaneous recovery controls, defined as simultaneous application of full antispin rudder and full trailing-edge-down elevator with ailerons neutralized

3. Rudder only, defined as full antispin rudder alone

4. Neutral recovery controls, defined as neutralized rudder, elevator, and ailerons

5. Elevator only, defined as full trailing-edge-down elevator with prospin rudder and aileron deflections maintained

For each major configuration change, spins were conducted to both the left and right; the most critical (faster, flatter, etc.) direction was then used for the remainder of spin tests in that configuration. Spins were performed with the wingtip cameras removed, the wheel pants removed, and the propeller rotation stopped to assess possible effects on airplane spin and recovery characteristics.

RESULTS AND DISCUSSION

Comparison of Tail Effectiveness

Elevator effectiveness, as determined from idle-power acceleration-deceleration maneuvers, and rudder effectiveness, as determined from steady-heading sideslips at constant airspeed with power on, are presented in figures 8 and 9, respectively, for the four tail configurations. For a given airplane angle of attack, tails 2 and 3 consistently operated with more positive (trailing edge down) elevator deflection and tail 4 operated with more negative elevator deflection than the other tails. At cruise angles of attack, tail 4 operated with the elevator in a near-neutral position. For the center-of-gravity position tested ($0.26\bar{c}$), all four tails had more than sufficient elevator deflection to fully stall the airplane. With power on, approximately 5° of right rudder deflection was needed to trim the airplane for straight and level flight with zero sideslip. Results from tests of a full-scale model of the subject airplane with tail 4 in the Langley 30- by 60-Foot Tunnel (ref. 18) agree well with the flight-test results, as indicated in figures 8 and 9.

Stall Characteristics With Baseline Loading

The airplane stall characteristics with tail 6 are presented in table 5. Table 6 presents the stall characteristics of the airplane for tails 2, 3, 4, and 6. The airplane stall characteristics are illustrated by means of time histories in figures 10 to 15.

The airplane with tail 6 stalled at an angle of attack of about 18°. For the baseline loading tested, slow deceleration (1 mph/sec) to a 1g, wings-level stall at idle power with flaps retracted produced a stall at an indicated airspeed of 72 mph and a trailing-edge-up elevator deflection of about 8° with the rudder centered. Stall warning in the form of a light buffeting preceded the stall airspeed by about 2 to 3 mph and was judged to be inadequate. The addition of maximum power reduced the elevator deflection needed to stall the airplane to about 4° trailing edge up and reduced both the warning and stall airspeeds by about 4 mph.

Idle-power stalls with tail 6.- Slow deceleration to a 1g, wings-level stall with near-zero sideslip and with the controls held fixed at the stall (fig. 10) resulted in a tendency for the airplane to roll-off slowly. Pulling the wheel full aft (maximum elevator deflection) and then holding the controls fixed (fig. 11) produced a more pronounced tendency to roll-off and to autorotate to the left. With the wheel pulled full aft, the roll-off tendency could be countered with judicious anticipatory use of the rudder, but eventually the pilot would lose control of the airplane.

Stalls from coordinated 30° banked turns produced mild wing-rock or wing-drop motions. Figure 12 illustrates a stall from an idle-power, 30° banked right turn. At the stall, the left wing started dropping. To counter this left roll, right aileron was applied while maintaining neutral rudder deflection. The airplane then rolled off to the right. Left aileron and rudder inputs were unable to stop this roll-off until the airplane was unstalled by reducing the elevator deflection. Stalls from coordinated 60° banked turns produced a more pronounced tendency to roll to the left and to autorotate.

When stalled with sideslip, the airplane rolled away from the sideslip; that is, right sideslip produced a left roll. Figure 13 illustrates idle-power stalls with both left and right sideslip.

Power-on stalls with tail 6.- When stalled with maximum power and near-zero sideslip, the airplane tended to roll to the right (fig. 14). Pulling the control wheel full aft at the stall accentuated the right roll-off tendency; however, use of full aileron control inputs was effective in countering the roll-off tendency. Stalls from coordinated 30° and 60° banked left and right turns resulted in roll-offs to the right.

When stalled with sideslip, the airplane rolled away from the sideslip. Figure 15 illustrates a stall in a slipping, 60° banked left turn. At the stall, the airplane abruptly rolled to the right "over the top."

Stalls with tails 2, 3, and 4.- The results of the limited stall investigations performed with tails 2, 3, and 4 (see table 6) were generally similar to those of the more extensive investigation with tail 6. Stall departures were characterized by roll-off tendencies. When stalled with sideslip, the airplane tended to roll away from the slip. Tails 3 and 6, which had long rudders, could produce much larger sideslip angles at the stall than tails 2 and 4 and had more pronounced roll-offs with sideslip than tails 2 and 4.

When the airplane with tail 6 was stalled at idle power with full right rudder deflection (large negative angle of sideslip), the pilot sensed from the ensuing motion that the vertical tail was stalling, an undesirable characteristic for light airplanes. Tails 2, 3, and 4 did not exhibit any such tendency to lose directional stability.

Spin Characteristics With Baseline Loading

The results are based on 385 spins totalling 2540 turns. A total of 398 spins were attempted, but in 13 attempts the airplane did not enter a spin. The number of spins performed for each tail configuration is presented in table 7. Spin characteristics ranged from slow and steep to fast and flat, as shown in figure 16. In some instances, the spin-recovery parachute was required to recover the airplane from flat spins.

1-turn spins.- In the United States, certification of general aviation airplanes in the normal and utility categories requires the demonstration of recovery from a 1-turn spin or from a 3-sec spin, whichever takes longer, within 1 additional turn following the application of recovery controls (ref. 19). This requirement is intended to address only airplane characteristics in an abused stall condition, that is, when the airplane is stalled with controls in a prospin direction and corrective control inputs are delayed. Compliance with this standard does not clear an airplane for intentional spins.

With this standard in mind, 58 1-turn, idle-power spins were studied to address the abused stall and incipient spin for the airplane with tails 2, 3, 4, and 6 at $IYMP = -50 \times 10^{-4}$. Angle of attack and turn rate at the initiation of recovery from 1-turn spins are presented in figure 16. Representative time histories of 1-turn spins are presented in figures 17 to 20 for the four tail configurations tested. Using normal recovery controls, the airplane always recovered within the 1-turn guideline.

The first turn following application of any combination of prospin controls required from 3.4 to 9.3 sec, with the average being 5.2 sec. Altitude loss varied from 50 to 450 ft, with the average being 210 ft. In general, a 1-turn spin to the right took less time than the same spin to the left; however, looking at each spin individually, less time did not necessarily correspond to less altitude loss.

Altitude loss during recovery from a 1-turn spin ranged from 200 to 500 ft and averaged 340 ft when normal recovery controls were used. Recovery took from 1.5 to 2.5 sec and averaged 1.9 sec.

Following recovery from a spin, the airplane entered a dive. The altitude lost in the dive was dependent upon how abruptly the pilot pulled the airplane out of the dive. An abrupt pullout, limited by the airplane maximum positive load factor of 3.8, resulted in less loss of altitude than a more gentle pullout, limited by the airplane never-exceed speed of 195 mph. In a sample of 57 recovery dives, performed within these limitations following recovery from 1-turn spins, altitude loss ranged from 200 to 1150 ft and averaged 550 ft. The duration of the dives ranged from 1.7 to 6.5 sec and averaged 4.3 sec.

Taken as a whole, from stall through incipient spin, recovery, and pullout to level flight, a 1-turn spin could require from 450 to 2100 ft of altitude and last

from 6.6 to 18.3 sec. An average 1-turn spin could be expected to result in a cumulative loss of 1100 ft and last 11.4 sec. Therefore, a stall followed by departure into an incipient spin at a typical airport traffic pattern altitude of 800 to 1000 ft above ground level would require prompt and proper action by the pilot to recover before ground impact.

Fully developed spins.- Table 8 summarizes characteristics of representative fully developed spins as a function of aileron deflection for the four tail configurations tested at IYMP = -50×10^{-4}. Figures 17 to 21 present time histories of representative idle-power, ailerons-neutral spins for the four tails tested. The spin usually became fully developed after about 4 to 5 turns.

With ailerons neutral, the baseline configuration (tail 4) had two spin modes, one moderate ($\alpha = 43°$) and one flat ($\alpha = 60°$), as shown in figure 21. Changing the tail design from the baseline configuration eliminated the flat spin and produced moderate spins for tails 2 ($\alpha = 46°$), 3 ($\alpha = 51°$), and 6 ($\alpha = 53°$), as shown in table 8 and the spin time histories in figures 18 to 20. With ailerons neutral, left spins were steeper (about 2° to 5° lower angle of attack) than right spins for tails 2 and 4; right spins were steeper than left spins for tail 6. Changes in TDR, URVC, and TDPF did not produce consistent changes in spin angle of attack or in spin rate. Angle of attack increased with increased yaw rate of the fully developed spin.

For tail 4 the moderate spin mode was predominant. Specific sequencing of elevator motions during spin entry was required to accelerate the airplane in yaw and drive it into the flat spin, as shown in figure 21. At the stall, full rudder and trailing-edge-up elevator were applied with ailerons neutralized. After 3 turns of the spin, the elevator was moved to full trailing edge down for 1 turn, which increased the roll rate. At the 4-turn point, the elevator was moved to 15° trailing edge up for 1 turn to convert the increased rolling motion into yawing motion. After an additional turn, the elevator was neutralized and the airplane spun up to the flat-spin mode.

In general, deflecting the ailerons with the spin (rolling in the direction of the spin) tended to steepen the spin (reduce angle of attack), reduce the yaw rate, and increase the magnitude of the oscillations in roll rate and in pitch rate; deflecting the ailerons against the spin (rolling against the direction of the spin) tended to flatten the spin (increase angle of attack), increase the yaw rate, and reduce the oscillations in roll rate and in pitch rate. Deflecting the ailerons with the spin resulted in a slipping rotation (positive sideslip in a right spin); deflecting the ailerons against the spin resulted in a skidding rotation (negative sideslip in a right spin). These effects of aileron deflection are shown in figure 22.

Consistent with the roll-off and autorotative tendencies identified during the stall investigation, the airplane with tail 6 entered a left spin when full aft control wheel was applied and held at idle power with ailerons and rudder neutralized, as shown in figure 23. The spin was a slipping rotation at about $\alpha = 33°$, with $\beta = -7° \pm 7°$.

The steady spin of the airplane with tail 4 was not noticeably affected by entry conditions or power level. Figure 24 illustrates entry into a left spin from a maximum-power stall with 14° of left sideslip. Following the application of prospin controls, the angle of attack increased to the fully developed spin value more quickly than during idle-power entries from coordinated stalls. Once the airplane was in the spin, the engine lost power even though a maximum-power throttle setting

was maintained throughout the spin. In flat spins, the engine stopped and the propeller stopped turning, as shown in figure 21.

Figure 16 presents the airplane angle of attack and turn rate at the instant that recovery controls were applied for all the spins at the baseline loading conditions of table 4 (IYMP = -50×10^{-4} and c.g. at $0.26\bar{c}$). At the 1-turn point, the angle of attack was 40° or less and typically was between 25° to 35°. At the 6-turn point of the spin and beyond, angle of attack was usually above 40°. The ranges of angles of attack and turn rates in the fully developed spins reflect the effects of varying aileron and elevator deflections.

Recovery Characteristics With Baseline Loading

The airplane spin-recovery characteristics were investigated for five different antispin control inputs:

1. Normal recovery controls, defined as full antispin rudder followed by full trailing-edge-down elevator with ailerons neutralized

2. Simultaneous recovery controls, defined as simultaneous application of full antispin rudder and full trailing-edge-down elevator with ailerons neutralized

3. Rudder only, defined as full antispin rudder alone

4. Neutral recovery controls, defined as neutralized rudder, elevator, and ailerons

5. Elevator only, defined as full trailing-edge-down elevator with prospin rudder and aileron deflections maintained

If the antispin control input did not stop the spin, the controls were returned to the prospin position and then normal recovery controls were applied.

Recovery controls were evaluated for their ability to stop spins at idle power with flaps retracted and ailerons neutral, with the spin, and against the spin. Recovery control inputs were applied in left and right spins at the 1-, 3-, and 6-turn points. The spin was considered to have stopped when the yaw rate was reduced to zero. The number of turns required for recovery from idle-power spins with flaps retracted is presented in table 9 for the four tail configurations.

For the moderate spin modes, tail 4 generally produced consistently faster recoveries than the other tail configurations. All four tail configurations produced recoveries from 1-turn spins that would meet the current spin-recovery requirements for normal and utility category airplanes as defined in the Federal Aviation Regulations (ref. 19). That is, using normal recovery controls, the pilot could terminate 1-turn spins within 1 turn following the application of recovery controls.

For all four tails, normal recovery controls provided the quickest recovery. The steeper spins generated by ailerons held with the spin tended to quicken the recovery. The flatter spins generated by ailerons held against the spin tended to slow the recovery. Figure 25 presents the recovery time as a function of the number of turns required to recover from idle-power spins through use of normal recovery controls for the four tails. Because a linear relationship appears to exist between

time required for recovery and number of turns required for recovery for this airplane, either can be used as a gauge of recovery characteristics. This is consistent with results of tests of the T-tail light airplane of reference 5.

Simultaneous recovery controls were practically as effective as normal recovery controls.

For tails 2, 3, and 6, when spin recovery was attempted by reversing the rudder alone, the airplane would recover from left spins but not from right spins. Following the application of antispin rudder alone in a right spin, the airplane transitioned to a steep spin at about $\alpha = 20°$ (fig. 26 for $\delta_e = -27°$). In cases where a rudder-only recovery control input was ineffective in terminating the spin, reducing the elevator deflection to about -19° resulted in recovery (fig. 26). The airframe was checked for asymmetries, but no significant difference between the left side and the right side was found. To check for propeller slipstream effects, a 6-turn spin was performed with the propeller stopped. No changes were noted in the spin or recovery characteristics. A check of rudder travel indicated that maximum trailing-edge-left deflection was 22° and maximum trailing-edge-right deflection was 26°.

In general, neutral recovery controls produced slower recoveries than either normal or simultaneous recovery controls.

Elevator-only control input did not recover the airplane from fully developed spins. For tail 4, attempting an elevator-only recovery from a fully developed spin (fig. 27) resulted in a momentary reduction in angle of attack and an increase in roll rate, followed by transition to a higher angle-of-attack spin at an increased yaw rate. For tail 6, attempting an elevator-only recovery from a fully developed spin reduced the spin angle of attack about 11 percent, increased the roll rate about 28 percent, and increased the yaw rate about 5 percent. For tail 2, attempting an elevator-only recovery reduced the spin angle of attack about 8 percent, increased the roll rate about 40 percent, and increased the yaw rate about 20 percent. For tail 3, attempting an elevator-only recovery reduced the spin angle of attack about 4 percent, increased the roll rate about 27 percent, and increased the yaw rate about 21 percent.

Releasing the controls as a means of spin recovery was briefly investigated for the baseline configuration. The controls were released at the completion of the third turn of idle-power spins to the right with ailerons neutral. Releasing the controls did not stop the spin. The controls floated to 16° trailing edge up elevator, 4° right rudder, and -4° right aileron. The angle of attack of the spin initially decreased when the controls were released and then increased again as the airplane spun back up toward the moderate spin mode.

Effect of Changing Mass Distribution

For the tail configurations tested, making the airplane more wing heavy (changing from $IYMP = -50 \times 10^{-4}$ to $IYMP = 50 \times 10^{-4}$) did not appreciably change the spin mode, as shown in figure 28. However, spin recovery was affected.

Table 9 presents the turns required for recovery for the tail configurations and mass loadings tested. Table 10 highlights the effect of IYMP on the airplane spin and recovery characteristics for tails 2, 3, and 4 for ailerons neutral, with the spin, and against the spin. In general, as mass was added to the wings, the airplane

recovered more slowly from the spin; however, recoveries using normal recovery controls were affected very little by the mass changes. For tails 2 and 3, neutral and rudder-only control inputs became ineffective for recovery as the airplane was made wing heavy. For tail 4, rudder-only control input became ineffective for recovering the airplane from right spins, as was the case for tails 2, 3, and 6 at IYMP = -50×10^{-4}.

A slight asymmetry in mass distribution made a marked difference in the spin and recovery characteristics, as evidenced by tests with tail 3 at IYMP = 0. Removing 20 lb from the left wing tip and adding it to the right wing tip (right wing 40 lb heavy) did not change the IYMP, but it produced a flatter, faster spin toward the light wing (α = 59° and Ω = 170 deg/sec) than toward the heavy wing (α = 42° and Ω = 150 deg/sec) and significantly increased the turns required for recovery (3 1/8 turns versus 1 1/8 turns), as shown in figure 29.

A similar test was performed with tail 4 at IYMP = 0 and left wing 33 lb heavy. Spinning toward the light wing increased the angle of attack in the flat spin from 61° to greater than 66° (the spin angle of attack exceeded the instrumentation measurement capability) and markedly increased the airplane turn rate from 211 to 250 deg/sec. With symmetric mass distribution, the airplane recovered from the 61° angle-of-attack spin 8 7/8 turns after application of normal recovery controls. With asymmetric mass distribution, the spin-recovery parachute was needed to stop the α > 66° spin.

Effect of Center-of-Gravity Position

Moving the center of gravity from 26 to 35 percent mean aerodynamic chord ($0.26\bar{c}$ to $0.35\bar{c}$) had little effect on the moderate spin mode ($\alpha \approx 43°$) of the baseline configuration, as shown in table 11. As the center of gravity was moved aft, the turn rate of the fully developed spin decreased.

Following the application of prospin controls, the airplane typically experienced two or three transient increases and decreases in angle of attack as it progressed to the fully developed spin. Moving the airplane center of gravity aft increased the magnitude of the initial angle-of-attack transient generated by prospin control input, as shown in figure 30. Recovery from a 1-turn spin by use of normal recovery controls was not significantly changed for the range of center-of-gravity positions tested.

Comparison of Airplane and Model Spin Characteristics

Table 12 shows characteristics of fully developed spins and recoveries of the airplane and of spin-tunnel model test results from reference 7. The spin-tunnel model exhibited all the spin modes obtained on the airplane. The moderate spin modes of the airplane and of the model agreed quite well. The model tests indicated that both tails 3 and 4 would have flat spin modes; however, a flat spin mode was not encountered during flight tests with tail 3. The flat spin mode of the airplane with tail 4 (ailerons neutral) was at a lower angle of attack and a slower turn rate than indicated by the model tests. In general, rudder-only control input was not as effective at recovering the airplane from spins (particularly right spins) as it was at recovering the model.

For rudder-only recoveries from fully developed spins with ailerons neutral, the flight-test results in table 9 indicate the same effect of varying mass distribution (IYMP) as that of the tail design criterion presented in figure 6; that is, changing from fuselage-heavy (IYMP < 0) loading to wing-heavy (IYMP > 0) loading reduced the effectiveness of the rudder for stopping the spin. Simultaneous control reversal also became less effective for stopping spins as the airplane loading changed from fuselage heavy to wing heavy. This appears to be counter to the trend expected from the tail design criterion of figure 6. With tail 4, the airplane had an unrecoverable flat spin for all three loadings tested; this is not consistent with the tail design criterion of figure 6. Thus, as concluded from the model tests, the tail design criterion cannot be used alone to predict spin-recovery characteristics. However, certain principles implicit in the criterion, as noted in the introduction, are still valid and should be considered when designing a tail configuration for spin recovery.

SUMMARY OF RESULTS

Flight tests were conducted to investigate the stall, spin, and recovery characteristics of a low-wing, single-engine, light airplane with four interchangeable tail configurations. The four tail configurations were evaluated for the effects of varying mass distribution, center-of-gravity position, and control inputs. The following results were indicated:

1. Stall departures were characteristized by roll-off tendencies.

2. At idle power with ailerons neutral and flaps retracted, the baseline configuration (tail 4 at inertia yawing-moment parameter IYMP = -50×10^{-4}) had two spin modes, one at angle of attack $\alpha = 43°$ and one at $\alpha = 60°$. When fitted with tail 2 the airplane spun at $\alpha = 46°$, with tail 3 it spun at $\alpha = 51°$, and with tail 6 it spun at $\alpha = 53°$.

3. In general, normal recovery controls (antispin rudder followed by full trailing-edge-down elevator with ailerons neutralized) provided the quickest recovery from 1-turn through fully developed moderate spins for all tail configurations and loadings tested.

4. For the baseline loading tested (IYMP = -50×10^{-4}), the simultaneous recovery control input was practically as effective as the normal recovery control input. The rudder-only recovery control input did not always stop the spin. The neutral recovery control input produced slower recoveries than either normal or simultaneous recovery controls. The elevator-only recovery control input did not recover the airplane from fully developed spins.

5. Through use of normal recovery controls for all tail configurations and loadings tested, 1-turn spins could be terminated within 1 additional turn following application of recovery controls.

6. Making the airplane more wing heavy (increasing the rolling moment of inertia relative to the pitching moment of inertia) did not appreciably change the spin mode, but it did degrade spin recovery. Recoveries using normal recovery controls were affected less by the mass changes than recoveries using the other control inputs tested.

7. As there was ample elevator deflection to fully stall the airplane at all center-of-gravity positions tested, moving the center of gravity rearward nine percent of the mean aerodynamic chord had little effect on spin characteristics of the baseline configuration.

8. For all four tail configurations, the moderate spin modes of the airplane agreed very well with those predicted from spin-tunnel model tests. The flat spin encountered with tail 4 was at a lower angle of attack and at a slower turn rate than those predicted from spin-tunnel model tests.

9. The 1947 NACA tail design criterion for light airplanes, which uses the tail damping power factor (TDPF) as a parameter, cannot be used alone to predict airplane spin recovery characteristics.

NASA Langley Research Center
Hampton, VA 23665-5225
October 20, 1986

REFERENCES

1. Chambers, Joseph R.: Overview of Stall/Spin Technology. AIAA-80-1580, Aug. 1980.

2. Stough, H. P., III; and Patton, J. M., Jr.: The Effects of Configuration Changes on Spin and Recovery Characteristics of a Low-Wing General Aviation Research Airplane. AIAA Paper 79-1786, Aug. 1979.

3. O'Bryan, Thomas C.; Edwards, Thomas E.; and Glover, Kenneth E.: Some Results From the Use of a Control Augmentation System To Study the Developed Spin of a Light Plane. AIAA Paper 79-1790, Aug. 1979.

4. Stewart, Eric C.; Suit, William T.; Moul, Thomas M.; and Brown, Philip W.: Spin Tests of a Single-Engine, High-Wing Light Airplane. NASA TP-1927, 1981.

5. Stough, H. Paul, III; DiCarlo, Daniel J.; and Patton, James M., Jr.: Flight Investigation of Stall, Spin, and Recovery Characteristics of a Low-Wing, Single-Engine, T-Tail Light Airplane. NASA TP-2427, 1985.

6. Stough, H. Paul; DiCarlo, Daniel J.; and Stewart, Eric C.: Wing Modification for Increased Spin Resistance. SAE Paper No. 830720, Apr. 1983.

7. Burk, Sanger M., Jr.; Bowman, James S., Jr.; and White, William L.: Spin-Tunnel Investigation of the Spinning Characteristics of Typical Single-Engine General Aviation Airplane Designs. I - Low-Wing Model A: Effects of Tail Configurations. NASA TP-1009, 1977.

8. Bihrle, William, Jr.; Barnhart, Billy; and Pantason, Paul: Static Aerodynamic Characteristics of a Typical Single-Engine Low-Wing General Aviation Design for an Angle-of-Attack Range of -8° to 90°. NASA CR-2971, 1978.

9. Bihrle, William, Jr.; Hultberg, Randy S.; and Mulcay, William: Rotary Balance Data for a Typical Single-Engine Low-Wing General Aviation Design for an Angle-of-Attack Range of 30° to 90°. NASA CR-2972, 1978.

10. Bowman, James S., Jr.; Stough, Harry P.; Burk, Sanger M., Jr.; and Patton, James M., Jr.: Correlation of Model and Airplane Spin Characteristics for a Low-Wing General Aviation Research Airplane. AIAA Paper 78-1477, Aug. 1978.

11. Staff of Langley Research Center: Exploratory Study of the Effects of Wing-Leading-Edge Modifications on the Stall/Spin Behavior of a Light General Aviation Airplane. NASA TP-1589, 1979.

12. Bradshaw, Charles F.: A Spin-Recovery Parachute System for Light General-Aviation Airplanes. 14th Aerospace Mechanisms Symposium, NASA CP-2127, 1980, pp. 195-209.

13. Burk, Sanger M., Jr.; Bowman, James S., Jr.; and White, William L.: Spin-Tunnel Investigation of the Spinning Characteristics of Typical Single-Engine General Aviation Airplane Designs. II - Low-Wing Model A: Tail Parachute Diameter and Canopy Distance for Emergency Spin Recovery. NASA TP-1076, 1977.

14. Neihouse, A. I.: Tail-Design Requirements for Satisfactory Spin Recovery for Personal-Owner-Type Light Airplanes. NACA TN 1329, 1947.

15. Moul, Thomas M.; and Taylor, Lawrence W., Jr.: Determination of an Angle of Attack Sensor Correction for a General Aviation Airplane at Large Angles of Attack as Determined From Wind Tunnel and Flight Tests. AIAA-80-1845, Aug. 1980.

16. Sliwa, Steven M.: Some Flight Data Extraction Techniques Used on a General Aviation Spin Research Aircraft. AIAA Paper 79-1802, Aug. 1979.

17. Sliwa, Steven Mark: A Study of Data Extraction Techniques for Use in General Aviation Aircraft Spin Research. M.S. Thesis, George Washington Univ., Sept. 1978.

18. Newsom, William A., Jr.; Satran, Dale R.; and Johnson, Joseph L., Jr.: Effects of Wing-Leading-Edge Modifications on a Full-Scale, Low-Wing General Aviation Airplane - Wind-Tunnel Investigation of High-Angle-of-Attack Aerodynamic Characteristics. NASA TP-2011, 1982.

19. Airworthiness Standards: Normal, Utility, and Acrobatic Category Airplanes. Federal Aviation Regulations, vol. III, pt. 23, FAA, June 1974.

TABLE 1.- BASELINE AIRPLANE CHARACTERISTICS

Overall dimensions:	
Span, ft	24.46
Length, ft	18.95
Height, ft	6.73
Engine:	
Type	Reciprocating, 4-cylinder, horizontally opposed
Rated continuous power, hp	108
Rated continuous speed, rpm	2600
Propeller:	
Type	2 blades, fixed pitch
Diameter, in.	71
Pitch, in.	46
Wing:	
Area, ft^2	98.11
Root chord, ft	4.00
Tip chord, ft	4.00
Mean aerodynamic chord, ft	4.00
Aspect ratio	6.10
Dihedral, deg	5.0
Incidence:	
Root, deg	3.5
Tip, deg	3.5
Airfoil section	NACA 64_2-415 modified
Aileron (each):	
Area, ft^2	2.60
Span, ft	3.82
Chord, ft	0.68
Hinge line, percent $\bar{c}$ aft of wing leading edge	85.4
Hinge line, percent $\bar{c}$ aft of aileron leading edge	14.2
Flap (each):	
Area, ft^2	2.68
Span, ft	4.01
Chord, ft	0.68
Hinge line, percent $\bar{c}$ aft of wing leading edge	85.4
Hinge line, percent $\bar{c}$ aft of flap leading edge	14.2
Horizontal tail:	
Area (excluding elevator), ft^2	9.52
Span, ft	7.69
Root chord, ft	3.60
Tip chord, ft	1.67
Aspect ratio	3.51
Incidence, deg	-3.0
Airfoil section	NACA 65_1-012
Vertical tail:	
Area (excluding rudder), ft^2	4.76
Span, ft	4.09
Root chord, ft	3.60
Tip chord, ft	1.67
Aspect ratio	1.46
Tail offset, deg	0.0
Airfoil section	NACA 65_1-012
Control surface deflections:	
Elevator, deg	25 up, 15 down
Aileron, deg	25 up, 20 down
Rudder, deg	25 left, 25 right
Flap, deg	0, 30 down

TABLE 2.- GEOMETRIC CHARACTERISTICS OF TAIL CONFIGURATIONS

Characteristic	Tail configuration			
	2	3	4	6
Rudder:				
Hinge line, in.	FS 218.92	FS 218.92	FS 218.92	FS 218.92
Area, ft^2	3.61	4.79	3.61	4.79
Elevator:				
Hinge line, in.	FS 218.92 WL 54.08	FS 218.92 WL 54.08	FS 233.05 WL 45.0	FS 218.92 WL 60.68
Area, ft^2	7.34	7.34	8.26	7.34
Stick-fixed neutral point (calculated for gliding flight, no propeller)	$0.327\bar{c}$	$0.327\bar{c}$	$0.352\bar{c}$	$0.330\bar{c}$
Stick-fixed neutral point (from flight tests, power on)			$0.333\bar{c}$	

TABLE 3.- DAMPING CHARACTERISTICS OF TAIL CONFIGURATIONS

Tail configuration	TDR	URVC	TDPF
2	0.028	0.012	336×10^{-6}
3	.018	.016	288
4	.0045	.018	81
6	.025	.021	525

TABLE 4.- AIRPLANE MASS CHARACTERISTICS AND INERTIA PARAMETERS FOR LOADINGS TESTED

Parameter[a]	Tail 2			Tail 3			Tail 4				Tail 6		
Nominal IYMP, $\times 10^{-4}$	b_{-50}	0	50	b_{-50}	c_0	50	b_{-50}	0	d_0	50	b_{-50}	0	50
Weight, lb	1530	1569	1609	1533	1576	1612	1538	1582	1577	1621	1537		
Center-of-gravity positions:													
$x/\bar{c}$	0.256	0.259	0.261	0.260	0.258	0.264	0.264	0.264	0.268	0.267	0.262		
$y/\bar{c}$	-0.011	-0.010	-0.010	-0.011	0.060	-0.010	-0.010	-0.008	-0.068	-0.008	-0.011		
$z/\bar{c}$	0.238	0.234	0.229	0.238	0.232	0.228	0.239	0.235	0.232	0.227	0.237		
Relative densities:													
μ at 5000 ft	9.7	9.9	10.2	9.7	10.0	10.2	9.7	10.0	10.0	10.2	9.7		
μ at 10 000 ft	11.3	11.6	11.9	11.3	11.6	11.9	11.3	11.7	11.6	11.9	11.3		
Moments of inertia:													
I_X, slug-ft^2	582	727	884	589	734	891	596	748	746	899	597		
I_Y, slug-ft^2	724	726	727	732	739	734	746	748	746	748	739		
I_Z, slug-ft^2	1236	1380	1536	1249	1399	1551	1273	1425	1422	1574	1262		
Moment parameters:													
$(I_X - I_Y)/mb^2$, $\times 10^{-4}$	-50	0	52	-50	-2	52	-53	0	0	50	-50		
$(I_Y - I_Z)/mb^2$, $\times 10^{-4}$	-180	-224	-271	-181	-225	-273	-184	-230	-231	-274	-183		
$(I_Z - I_X)/mb^2$, $\times 10^{-4}$	230	224	218	231	227	220	237	230	231	224	233		

[a]Fuel burn-off to test altitude accounted for in values listed.
[b]Baseline loading.
[c]Asymmetric loading; 20 lb removed from left wing tip and added to right wing tip.
[d]Asymmetric loading; 16.5 lb removed from right wing tip and added to left wing tip.

TABLE 5.- AIRPLANE STALL CHARACTERISTICS WITH TAIL 6

[IYMP = -50×10^{-4}; c.g. at $0.26\bar{c}$]

Power	ϕ, deg	β, deg	Description of maneuver	Result
Idle	0	0	Wheel back to stall, then controls fixed	Roll-off to left
		1	Wheel full back, then controls fixed	Roll-off to left and autorotation
		0	Wheel back to stall, then ailerons used	Ailerons effective at first, then airplane spirals to right
		0	Wheel full back, then rudder used	Roll-off controllable with anticipatory use of rudder but pilot eventually loses control of airplane
		24 ± 6	Right sideslip	Roll-off to left uncontrollable
		-32 ± 3	Left sideslip	Roll-off to right and pitch forward violently with apparent loss of directional stability
	-30	0	Left turn	Very mild wing rock
	-30	12	Skidding left turn	Tendency to roll-off to left and spin
	-30	-12	Slipping left turn	Gentle stall; roll-off to right
	30	4	Right turn	Left wing drop
	30	-10 ± 1	Skidding right turn	Roll-off to right uncontrollable
	30	12	Slipping right turn	Tendency to roll-off to left; controllable with rudder and aileron
	-60	3	Left turn	Roll-off to left and autorotation
	-60	-15	Slipping left turn	Mild stall followed by roll-off to right
	60	0	Right turn	Tendency to roll-off to left; autorotation to right if abused
	60	-12	Skidding right turn	Roll-off to right uncontrollable
	60	12	Slipping right turn	Roll-off to left over top

TABLE 5.- CONCLUDED

Power	ϕ, deg	β, deg	Description of maneuver	Result
Maximum	0	-4	Wheel back to stall, then controls fixed	Roll-off to right
		0	Wheel full back, then controls fixed	Roll-off to right
		-4	Wheel back to stall, then ailerons used	Random aileron effectiveness; full aileron input effective
		0	Wheel full back, then rudder used	More rolling and yawing than at idle power, but can hold indefinitely
		20	Right sideslip	Roll-off to left
		-13	Left sideslip	Roll-off to right
	-30	0	Left turn	Roll-off to right slowly; full aileron ineffective at countering roll-off
	-30	8	Skidding left turn	Tendency to roll-off to left
	-30	-13	Slipping left turn	Tendency to roll-off to right
	30	-4	Right turn	Roll-off to right
	30	6	Slipping right turn	Controllable about all axes
	-60	-1	Left turn	Roll-off to right controllable with rudder and ailerons
	-60	11	Skidding left turn	Roll-off to left and autorotation in vertical roll
	-60	13	Slipping left turn	Roll-off to right over top
	60	-2	Right turn	Roll-off to right and autorotation, rudder and ailerons can keep wings level
	60	6	Slipping right turn	Sudden roll-off to left over top

TABLE 6.- STALL CHARACTERISTICS FOR THE FOUR TAIL CONFIGURATIONS

[IYMP = -50×10^{-4}; c.g. at $0.26\bar{c}$]

Tail	Power	ϕ, deg	β, deg	Description of maneuver	Result
2	Idle	0	0	Wheel back to stall, then controls fixed	Roll-off to right slowly
			0	Wheel full back, then controls fixed	Roll-off to left
			0	Wheel full back, then rudder used	Roll-off to right $-11° < \beta < 18°$ from rudder
			15	Right sideslip	Roll-off to left mildly
			-16	Left sideslip	Roll-off to right (not stall break)
	Max	-60	0	Left turn	Stays in stable stall
3	Idle	0	0	Wheel back to stall, then controls fixed	Tendency for autorotation to right
			0	Wheel full back, then controls fixed	Roll left, then right into vertical maneuver
			0	Wheel full back, then rudder used	$\alpha = 24°$ with full aft stick
			28	Right sideslip	Roll-off to left uncontrollable
			-32	Left sideslip	Roll-off to right uncontrollable
	Max	-60	0	Left turn	Development of left β; roll-off to right
4	Idle	0	3	Wheel back to stall, then controls fixed	Roll-off to left slowly
			3	Wheel full back, then controls fixed	Autorotation to left (left rudder was input)
			3	Wheel full back, then rudder used	Controllable with rudder
			18	Right sideslip	Roll-off to left
			-19	Left sideslip	Nothing
	Max	-60	0	Left turn	Heavy buffet with wing rock
6	Idle	0	0	Wheel back to stall, then controls fixed	Roll-off to left slowly
			1	Wheel full back, then controls fixed	Tendency for autorotation to left
			0	Wheel full back, then rudder used	Can control roll with judicious anticipatory use of rudder; pilot eventually loses control of airplane
			24 ± 6	Right sideslip	Roll-off to left uncontrollable
			-32 ± 3	Left sideslip	Roll-off to right and pitch forward violently; loss of directional stability
	Max	-60	-1	Left turn	Roll-off to right controllable with rudder and ailerons

TABLE 7.- NUMBER OF SPINS PERFORMED FOR EACH TAIL CONFIGURATION

[c.g. at $0.26\bar{c}$]

Tail	Number of spins for IYMP = -50×10^{-4} resulting in -			Number of spins for IYMP = 0 resulting in -			Number of spins for IYMP = 50×10^{-4} resulting in -			Total
	1 turn	⩾3, <6 turns	⩾6 turns	1 turn	⩾3, <6 turns	⩾6 turns	1 turn	⩾3, <6 turns	⩾6 turns	
2	17	13	14	10	8	9	10	7	10	98
3	11	8	21	1	1	8	10	3	13	76
4	18	12	58	12	5	11	10	6	17	149
6	13	8	12							33
[a]4	9	6	14							29
Total	68	47	119	23	14	28	30	16	40	385

[a]At various center-of-gravity positions ($0.30\bar{c}$ to $0.35\bar{c}$); IYMP ranged from -44×10^{-4} to -80×10^{-4} during these tests.

TABLE 8.- CHARACTERISTICS OF REPRESENTATIVE FULLY DEVELOPED SPINS

[IYMP = -50×10^{-4}; c.g. at $0.26\bar{c}$]

Quantity	Tail 2			Tail 3			Tail 4				Tail 6[a]	
	Ailerons with	Ailerons neutral	Ailerons against	Ailerons with	Ailerons neutral	Ailerons against	Ailerons with	Ailerons neutral[b]		Ailerons against	Ailerons neutral	Ailerons against
α, deg	43 ± 2	46 ± 1	52 ± 3	40 ± 2	51 ± 2	57 ± 2	40 ± 2	43 ± 1	60 ± 2	45 ± 2	53 ± 2	55 ± 3
β, deg	3 ± 11	1 ± 2	-5 ± 4	3 ± 9	-2 ± 1	-6 ± 4	4 ± 1	2 ± 2	-2 ± 2	-6 ± 2	-3 ± 4	-5 ± 3
p, deg/sec	105 ± 45	110 ± 10	100 ± 5	116 ± 54	98 ± 2	93 ± 7	110	105 ± 5	100	110	100 ± 10	97 ± 7
q, deg/sec	30 ± 34	13 ± 3	-3 ± 3	23 ± 30	6 ± 3	-2 ± 4	24 ± 2	16 ± 9	5 ± 5	2 ± 6	5 ± 5	-5 ± 5
r, deg/sec	101 ± 6	110	125	95 ± 5	123	145	100 ± 5	105 ± 7	180	108	127 ± 5	142
Ω, deg/sec	152 ± 32	154 ± 6	157 ± 7	155 ± 45	157 ± 5	170 ± 4	147 ± 5	151 ± 9	208 ± 2	155	161 ± 10	165 ± 5
T, sec	2.37	2.34	2.29	2.32	2.29	2.12	2.45	2.38	1.73	2.32	2.24	2.18
V, ft/sec	122	118	115	133	113	110	130	123	98	118	111	105
R/S, ft/sec	120	115	110	125	111	105	130	121	98	110	75	100
a_N, g units	1.5	1.4	1.3	1.6 ± 0.2	1.3	1.3	1.4	1.4	1.2	1.36	1.3	1.25
R, ft	4.9	4.3	3.3	5.2	3.5	2.4	5.8	5.0	1.4	4.4	3.1	2.7

[a]Fully developed spins not tested for ailerons-with condition.
[b]Two spin modes, moderate and flat.

TABLE 9.- TURNS REQUIRED FOR SPIN RECOVERY

[Idle power, flaps retracted, full prospin rudder and full trailing-edge-up elevator deflections during spin. A blank space indicates condition was not tested; ∞ indicates airplane stabilized in a spin with recovery controls applied; > indicates airplane had not stopped spinning at that point and pilot reverted to secondary recovery control input]

Prospin turns and direction	Aileron position	Recovery controls	Tail 2			Tail 3			Tail 4			Tail 6
			IYMP, $\times 10^{-4}$									
			-50	0	50	-50	0	50	-50	0	50	-50
1 Right	Neutral	Normal	$\frac{3}{8}$, $\frac{1}{2}$, $\frac{5}{8}$	$\frac{1}{2}$	$\frac{1}{2}$	$\frac{1}{4}$, $\frac{3}{8}$		$\frac{1}{4}$	$\frac{3}{8}$, $\frac{1}{2}$	1	$\frac{1}{2}$	$\frac{1}{3}$, $\frac{1}{2}$
3 Right	Neutral	Normal	$1\frac{1}{2}$, $1\frac{1}{2}$	$1\frac{5}{8}$		$1\frac{3}{8}$		$1\frac{7}{8}$	$1\frac{3}{8}$	[a] $\frac{7}{8}$	$1\frac{1}{2}$	$1\frac{1}{4}$, $1\frac{1}{2}$
6 Right	Neutral	Normal	2, $2\frac{1}{2}$	$2\frac{1}{4}$	$2\frac{1}{2}$, [b] $2\frac{3}{4}$	$1\frac{7}{8}$, 2		$2\frac{3}{4}$, [d] $3\frac{1}{2}$	$1\frac{1}{4}$, $1\frac{1}{4}$	$1\frac{1}{2}$	$1\frac{1}{2}$	$1\frac{1}{2}$, [c] $1\frac{1}{2}$
6 Left	Neutral	Normal	$1\frac{1}{4}$	$1\frac{7}{8}$	$2\frac{1}{4}$	$1\frac{1}{8}$		$1\frac{7}{8}$	$1\frac{1}{4}$	$1\frac{3}{8}$	$1\frac{3}{8}$	$1\frac{3}{4}$
6 Right	Neutral	Simulta-neous	$1\frac{7}{8}$	$2\frac{1}{4}$	$3\frac{3}{4}$	$1\frac{3}{4}$		$2\frac{5}{8}$	$1\frac{1}{8}$	$1\frac{1}{4}$	$1\frac{1}{2}$	$1\frac{7}{8}$
1 Right	Neutral	Neutral	$\frac{7}{8}$, $1\frac{3}{8}$	$\frac{3}{8}$	$\frac{1}{2}$	$\frac{3}{4}$		$1\frac{3}{4}$	$\frac{3}{8}$, $\frac{5}{8}$	$\frac{3}{4}$	$\frac{3}{4}$	$\frac{1}{2}$, $\frac{1}{2}$, $1\frac{1}{4}$
1 Left	Neutral	Neutral	$\frac{5}{8}$	$\frac{7}{8}$	$\frac{7}{8}$	$\frac{1}{4}$		$1\frac{1}{8}$	$\frac{1}{2}$, $\frac{1}{2}$	$\frac{1}{2}$	1	1
3 Right	Neutral	Neutral	$2\frac{7}{8}$	∞	∞	$4\frac{3}{4}$			$2\frac{1}{8}$		>3	$2\frac{3}{4}$
6 Right	Neutral	Neutral	$5\frac{1}{2}$	>5	>5	$4\frac{1}{4}$		∞	$1\frac{1}{4}$, 2	$2\frac{3}{4}$	$2\frac{3}{8}$	$3\frac{1}{2}$
6 Left	Neutral	Neutral	$2\frac{1}{4}$	$3\frac{3}{8}$	∞				$1\frac{3}{8}$		$1\frac{3}{4}$	$>4\frac{1}{4}$
1 Right	Neutral	Rudder	$2\frac{1}{4}$, $>4\frac{1}{4}$	1	∞	$\frac{5}{8}$		∞	$\frac{1}{4}$, $\frac{1}{2}$, $\frac{3}{4}$	$>2\frac{1}{2}$, ∞	$2\frac{1}{4}$	>3
1 Left	Neutral	Rudder	$\frac{5}{8}$	$1\frac{3}{8}$	∞	$\frac{1}{2}$		$1\frac{3}{4}$	$\frac{1}{2}$	$\frac{3}{4}$	$1\frac{1}{2}$	$\frac{3}{4}$
3 Right	Neutral	Rudder	>4, ∞	∞	∞	2		∞	$1\frac{1}{2}$	$2\frac{1}{4}$, $2\frac{1}{2}$	∞	$4\frac{1}{3}$
6 Right	Neutral	Rudder	$>5\frac{1}{2}$, $>6\frac{1}{4}$	∞	∞	>4, $>4\frac{1}{4}$, $4\frac{5}{8}$		∞	$1\frac{1}{4}$, [c] $1\frac{5}{8}$	$2\frac{1}{4}$	∞	$>3\frac{1}{2}$, $>5\frac{1}{2}$
6 Left	Neutral	Rudder	2	$4\frac{7}{8}$	∞	$1\frac{3}{4}$		∞	$1\frac{3}{8}$	2	$2\frac{5}{8}$	$2\frac{1}{4}$

Footnotes at end of table, p. 29.

TABLE 9.- CONCLUDED

Prospin turns and direction	Aileron position	Recovery controls	Tail 2			Tail 3			Tail 4			Tail 6
			IYMP, $\times 10^{-4}$									
			-50	0	50	-50	0	50	-50	0	50	-50
1 Right	Neutral	Elevator		Immediate	1			Immediate	$\frac{1}{4}$	$>4\frac{1}{2}$	$\frac{3}{4}$, >3	
3 Right	Neutral	Elevator		∞	∞				∞	e_∞	e_∞	
6 Right	Neutral	Elevator	b_∞			∞			∞	e_∞		∞
1 Right	With	Normal	$\frac{1}{4}$, $\frac{1}{2}$	$\frac{1}{4}$	$\frac{3}{4}$	$\frac{1}{4}$		$\frac{1}{2}$	$\frac{1}{2}$	$\frac{1}{2}$	$\frac{7}{8}$	$\frac{1}{2}$
1 Left	With	Normal	$\frac{1}{4}$			$\frac{1}{8}$			$\frac{1}{4}$			$\frac{1}{4}$
3 Right	With	Normal	$1\frac{1}{4}$	$1\frac{3}{4}$	$1\frac{3}{4}$	$1\frac{1}{4}$			$1\frac{1}{8}$	$1\frac{3}{8}$	$1\frac{3}{8}$	
6 Right	With	Normal	$1\frac{1}{2}$	$1\frac{1}{4}$	$2\frac{1}{4}$	$1\frac{1}{8}$		$1\frac{3}{4}$	$\frac{3}{4}$, 1	1	$1\frac{3}{4}$	
1 Right	Against	Normal	$\frac{5}{8}$	$\frac{1}{4}$	$\frac{1}{8}$	$\frac{1}{2}$		$\frac{1}{4}$	$\frac{3}{4}$	$\frac{1}{2}$	$\frac{5}{8}$	$\frac{1}{2}$
3 Right	Against	Normal	$2\frac{1}{8}$	$1\frac{7}{8}$	$2\frac{1}{2}$	$2\frac{1}{4}$			$1\frac{1}{2}$	$1\frac{1}{4}$	$1\frac{1}{4}$	$1\frac{7}{8}$
6 Right	Against	Normal		$2\frac{1}{4}$	$2\frac{1}{2}$	$2\frac{1}{2}$, $2\frac{3}{4}$		$3\frac{1}{4}$	$1\frac{5}{8}$	$1\frac{1}{8}$	$1\frac{1}{4}$	
1 Right	Against	Neutral	$1\frac{1}{8}$, $1\frac{3}{4}$	1	2	1		$\frac{7}{8}$	$\frac{3}{4}$, $\frac{7}{8}$	1	$\frac{3}{4}$	$1\frac{1}{2}$
1 Left	Against	Neutral	1	$1\frac{3}{4}$	>3	$1\frac{1}{8}$		$\frac{1}{2}$	1	$\frac{3}{4}$	$\frac{1}{2}$	
3 Right	Against	Rudder	$2\frac{1}{4}$			$3\frac{1}{4}$, $>3\frac{1}{2}$			$1\frac{3}{8}$			$\frac{3}{4}$
6 Right	Against	Rudder	$4\frac{1}{2}$, >6, ^{a}>8			^{c}>5			$1\frac{1}{2}$, $1\frac{5}{8}$			$2\frac{3}{4}$
6 Left	Against	Rudder	$3\frac{5}{8}$			$4\frac{3}{4}$			$1\frac{7}{8}$			$2\frac{1}{4}$

[a]Recovery controls applied after 4 turns.
[b]Recovery controls applied after 5 turns.
[c]Recovery controls applied after 7 turns.
[d]Recovery controls applied after 10 turns.
[e]Airplane transitioned to a higher angle-of-attack spin with faster turn rate.

TABLE 10.- EFFECT OF INERTIA YAWING-MOMENT PARAMETER ON AIRPLANE SPIN AND RECOVERY CHARACTERISTICS

(a) Ailerons neutral

Parameter	Tail 2			Tail 3		Tail 4					
IYMP, $\times 10^{-4}$	-50	0	50	-50	50	-50		0		50	
α, deg	46 ± 1	48	50 ± 2	51 ± 2	53 ± 1	43 ± 1	60 ± 2	44 ± 1	61 ± 1	44 ± 2	>60
Ω, deg/sec	154 ± 6	153	158 ± 2	157 ± 5	160 ± 5	151 ± 9	208 ± 2	150 ± 10	211	150 ± 10	210
Turns for recovery using normal recovery controls	$1\frac{1}{4}$, 2, $2\frac{1}{2}$	$1\frac{7}{8}$, $2\frac{1}{4}$	$2\frac{1}{4}$, $2\frac{1}{2}$, $2\frac{3}{4}$	$1\frac{1}{8}$, $1\frac{7}{8}$, 2	$1\frac{7}{8}$, $2\frac{3}{4}$, $3\frac{1}{2}$	$1\frac{1}{4}$, $1\frac{1}{4}$, $1\frac{1}{4}$	a_∞	$1\frac{3}{8}$, $1\frac{1}{2}$	$8\frac{7}{8}$	$1\frac{3}{8}$, $1\frac{1}{2}$	a_∞

[a]Airplane stabilized in a spin with recovery controls applied.

(b) Ailerons with the spin

Parameter	Tail 2			Tail 3		Tail 4		
IYMP, $\times 10^{-4}$	-50	0	50	-50	50	-50	0	50
α, deg	43 ± 2	41 ± 1	49 ± 2	40 ± 2	51 ± 2	40 ± 2	41 ± 2	46 ± 2
Ω, deg/sec	152 ± 32	150 ± 2	157 ± 5	155 ± 45	160 ± 5	147 ± 5	142 ± 5	154 ± 4
Turns for recovery using normal recovery controls	$1\frac{1}{2}$	$1\frac{1}{4}$	$2\frac{1}{4}$	$1\frac{1}{8}$	$1\frac{3}{4}$	$\frac{3}{4}$, 1	1	$1\frac{3}{4}$

(c) Ailerons against the spin

Parameter	Tail 2			Tail 3		Tail 4		
IYMP, $\times 10^{-4}$	-50	0	50	-50	50	-50	0	50
α, deg	52 ± 3	51 ± 2	50 ± 1	57 ± 2	55 ± 4	45 ± 2	43 ± 1	44 ± 2
Ω, deg/sec	157 ± 7	148 ± 5	151 ± 3	170 ± 4	165 ± 5	155	142 ± 10	150 ± 3
Turns for recovery using normal recovery controls		$2\frac{1}{4}$	$2\frac{1}{2}$	$2\frac{1}{2}$, $2\frac{3}{4}$	$3\frac{1}{4}$	$1\frac{5}{8}$	$1\frac{1}{8}$	$1\frac{1}{4}$

TABLE 11.- EFFECT OF CENTER-OF-GRAVITY POSITION ON MODERATE SPIN OF AIRPLANE WITH TAIL 4

Center-of-gravity position:												
$x/\bar{c}$	0.264			0.299			0.332			0.346		
$y/\bar{c}$	-.010			-.015			-.013			-.017		
$z/\bar{c}$	.239			.228			.227			.227		
Weight, lb	1538			1580			1580			1564		
Moments of inertia:												
I_X, slug-ft^2	596			625			624			623		
I_Y, slug-ft^2	746			783			795			800		
I_Z, slug-ft^2	1273			1329			1339			1343		
Moment parameters:												
$(I_X - I_Y)/mb^2$	-53×10^{-4}			-54×10^{-4}			-58×10^{-4}			-61×10^{-4}		
$(I_Y - I_Z)/mb^2$	-184×10^{-4}			-186×10^{-4}			-185×10^{-4}			-187×10^{-4}		
$(I_Z - I_X)/mb^2$	237×10^{-4}			240×10^{-4}			244×10^{-4}			248×10^{-4}		
Aileron position	With	Neutral	Against	With	Neutral	Against	With	Neutral	Against	With	Neutral	Against
Developed spin α, deg	40 ± 2	43	45	41	45	45	45 ± 5	43	44	47 ± 3	43	44
Developed spin Ω, deg/sec	145 ± 7	151 ± 9	155	140 ± 10	138	130	120 ± 20	122 ± 5	120 ± 10	130 ± 20	120 ± 10	120 ± 10
Recovery turns from developed spin[a]	$\frac{3}{4}$, 1	$1\frac{1}{4}$, $1\frac{1}{4}$	$1\frac{5}{8}$	$\frac{7}{8}$	1	1	$\frac{7}{8}$	1	$1\frac{1}{8}$	$1\frac{1}{8}$	$1\frac{1}{8}$	$1\frac{1}{8}$
Recovery turns from 1-turn spin[a]	$\frac{1}{2}$	$\frac{3}{8}$, $\frac{1}{2}$	$\frac{3}{4}$	$\frac{3}{8}$	$\frac{3}{8}$	$\frac{3}{8}$	$\frac{5}{8}$	$\frac{5}{8}$	$\frac{3}{8}$	$\frac{3}{8}$	$\frac{5}{8}$	$\frac{3}{4}$

[a]Number of turns for spin recovery using normal recovery controls.

TABLE 12.- COMPARISON OF AIRPLANE AND MODEL SPIN AND RECOVERY CHARACTERISTICS

[Recovery attempted from and developed spin data presented for rudder full with the spin and elevator full trailing edge up; IYMP = -50×10^{-4}; c.g. at $0.26\bar{c}$; model data from reference 7]

	Tail 2				Tail 3					
	Ailerons neutral		Ailerons against		Ailerons neutral			Ailerons against		
	Airplane	Model	Airplane	Model	Airplane	Model[a]		Airplane	Model	
α, deg	46 ± 1	45	52 ± 3	50	51 ± 2	52	80	57 ± 2	55	83
Ω, deg/sec	154 ± 6	166	157 ± 7	148	157 ± 5	180	270	170 ± 4	180	302
Turns for recovery using rudder only	2, $^{b}>5\frac{1}{2}$, $^{b}>6\frac{1}{4}$	1, 1, 2	$3\frac{5}{8}$, $4\frac{1}{2}$, $^{b}>6$, $^{b}>8$	$2\frac{1}{2}$, $3\frac{1}{2}$, $4\frac{1}{4}$	$1\frac{3}{4}$, $^{b}>4$, $^{b}>4\frac{1}{4}$, $4\frac{5}{8}$	1, 1, $1\frac{1}{4}$	$5\frac{1}{2}$, $7\frac{1}{2}$	$4\frac{3}{4}$, $^{b}>5$	2, $2\frac{1}{4}$, $2\frac{1}{2}$	$^{c}\infty$

	Tail 4							Tail 6			
	Ailerons neutral				Ailerons against			Ailerons neutral		Ailerons against	
	Airplane		Model		Airplane	Model		Airplane	Model	Airplane	Model
α, deg	43 ± 1	60 ± 2	38	77	45 ± 2	42	78	53 ± 2	53	55 ± 3	55
Ω, deg/sec	151 ± 9	208 ± 2	144	324	155	148	338	161 ± 10	173	165 ± 5	180
Turns for recovery using rudder only	$1\frac{1}{4}$, $1\frac{3}{8}$, $1\frac{5}{8}$	$^{c}\infty$	$\frac{1}{2}$, $\frac{1}{2}$, 1	$^{c}\infty$	$1\frac{1}{2}$, $1\frac{5}{8}$, $1\frac{7}{8}$	1, 1, $1\frac{1}{4}$	$^{c}\infty$	$2\frac{1}{4}$, $^{b}>3\frac{1}{2}$, $^{b}>5\frac{1}{2}$	1, $1\frac{1}{4}$, $1\frac{1}{2}$	$2\frac{1}{4}$, $2\frac{3}{4}$	2, 2, $2\frac{1}{4}$

[a] Two spin modes, moderate and flat.
[b] Airplane had not stopped spinning at that point and the pilot reverted to a secondary recovery control input.
[c] Airplane stabilized in a spin with recovery controls applied.

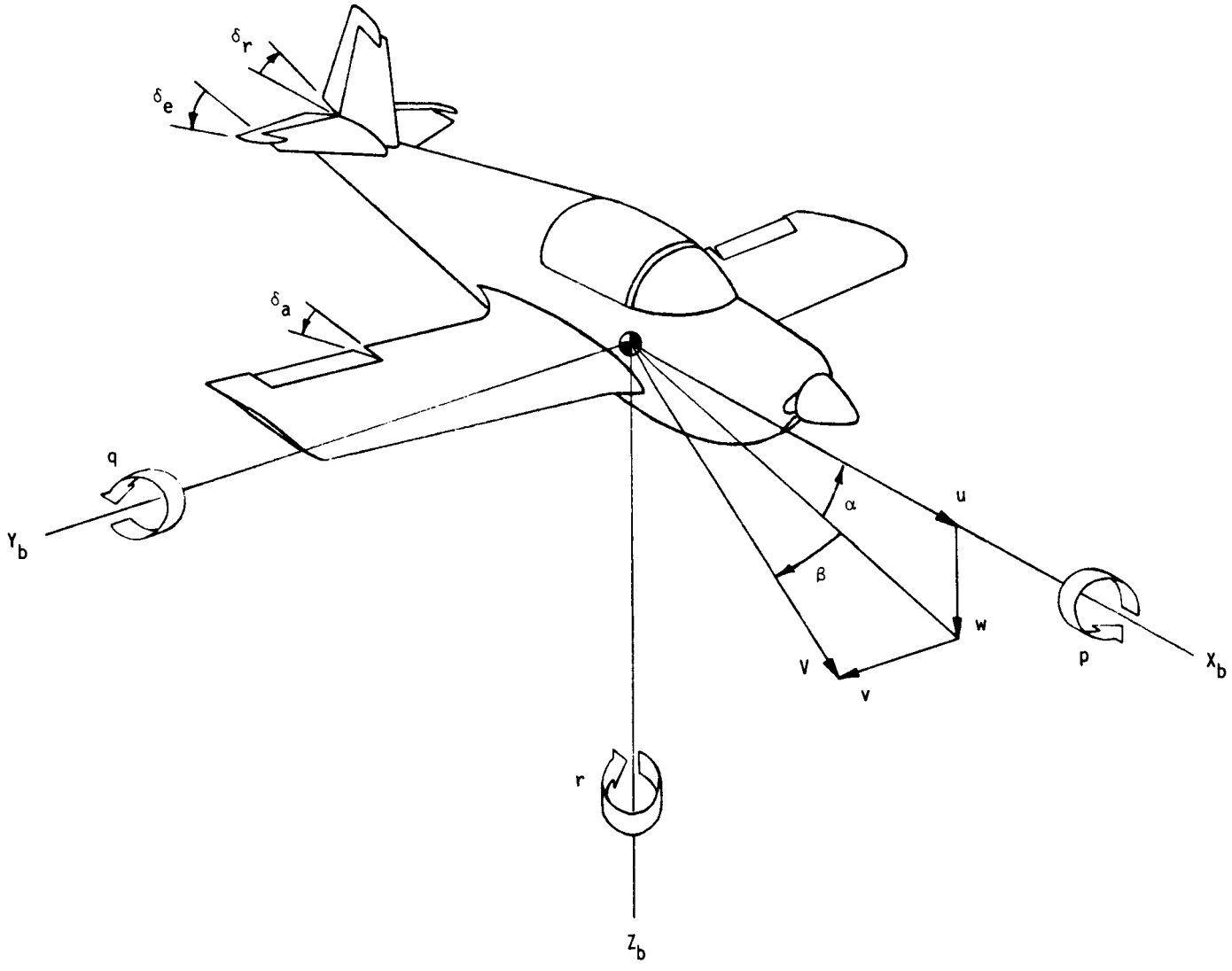

Figure 1.- Body system of axes. Arrows indicate positive direction of quantities.

L-86-408

Figure 2.- Baseline configuration of test airplane.

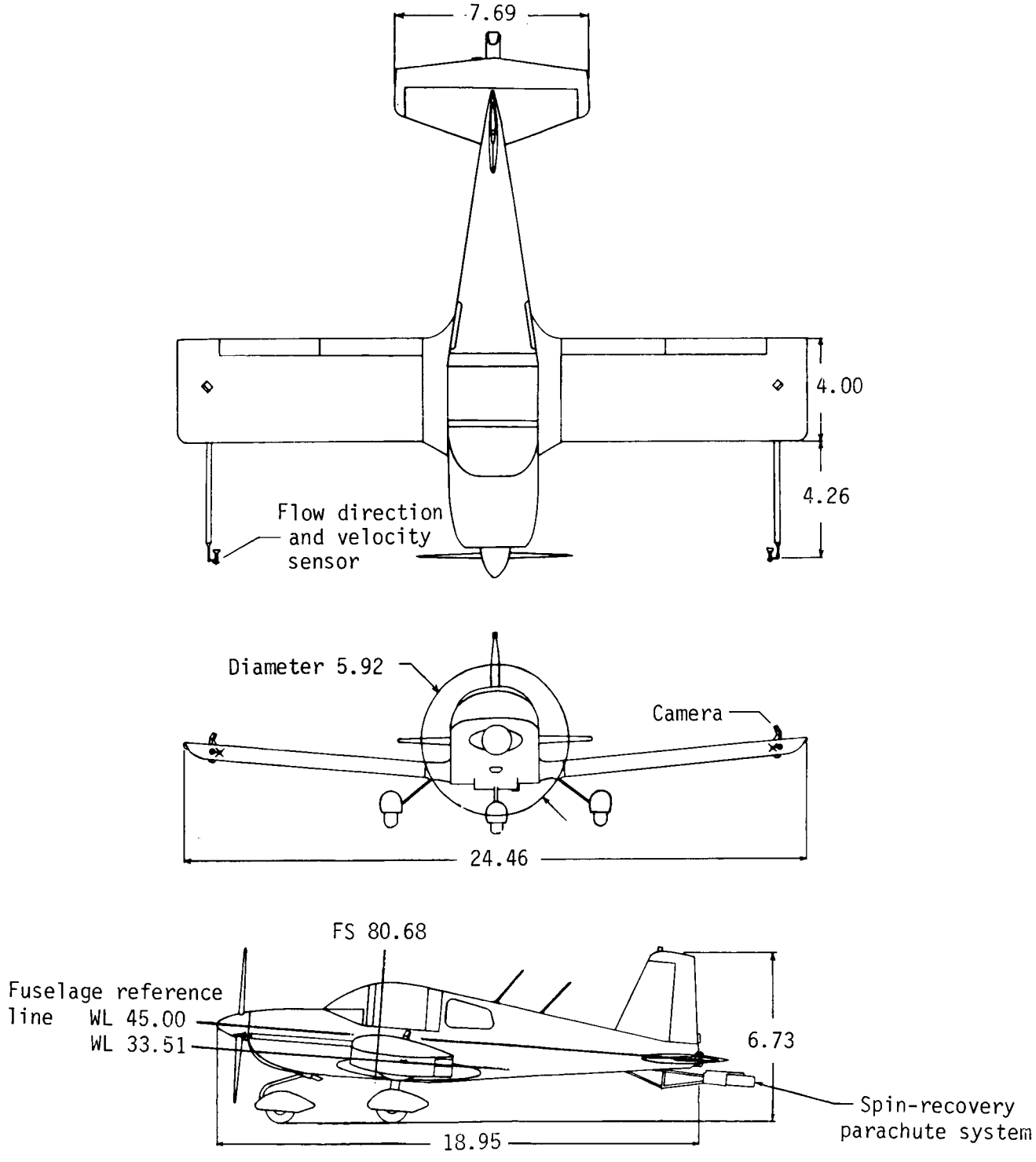

Figure 3.- Three-view drawing of test airplane baseline configuration. Dimensions are in feet.

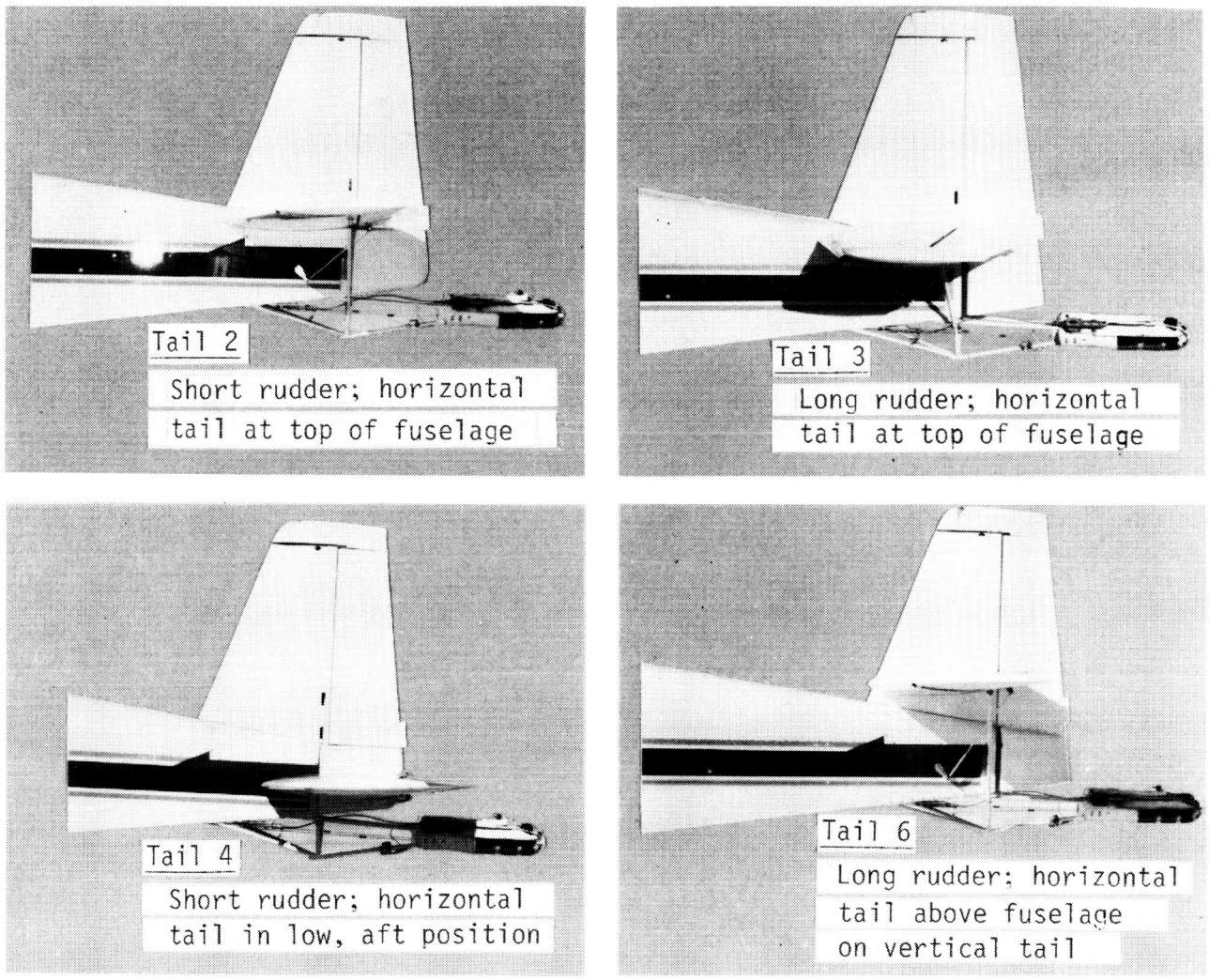

L-86-409

(a) Photographs of tails.

Figure 4.- Tail configurations tested.

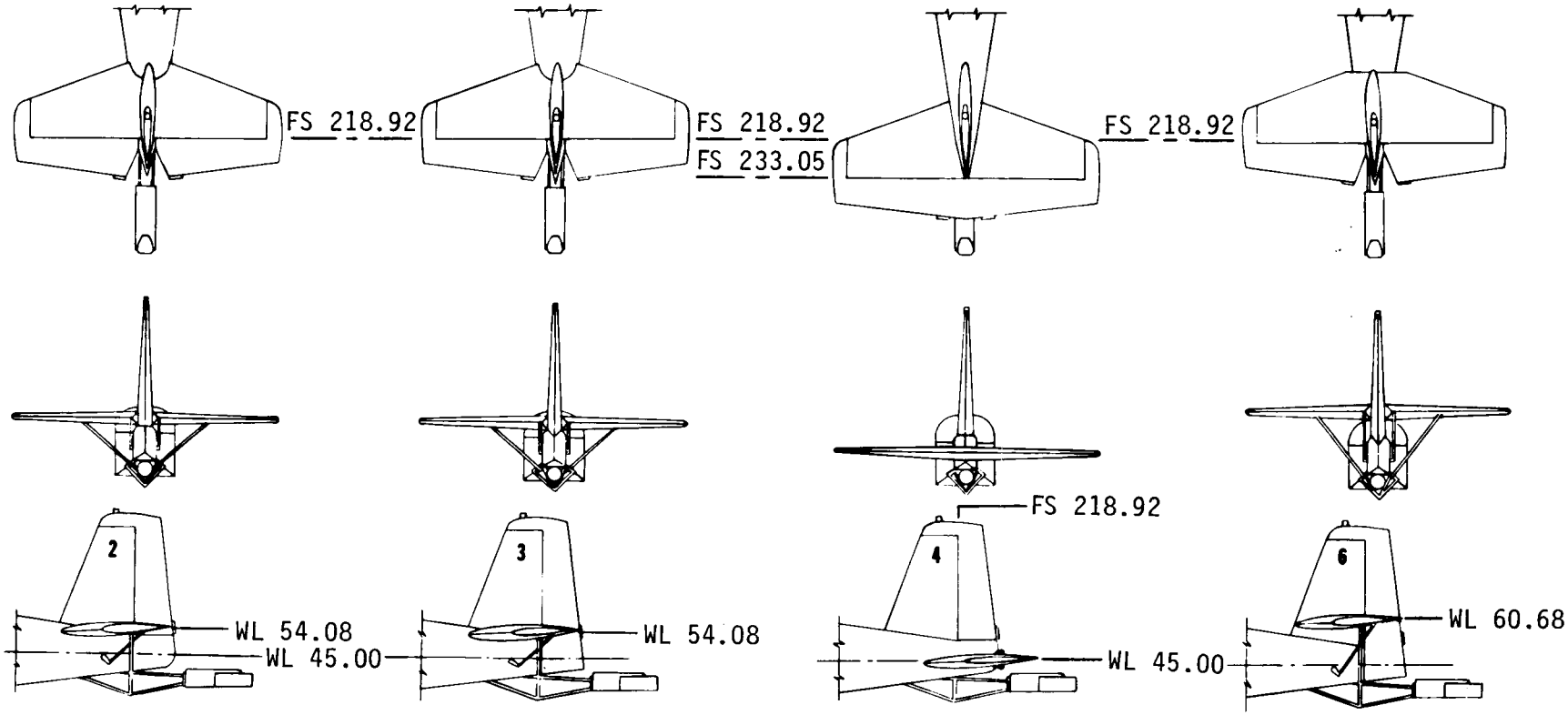

(b) Three-view drawings of tails. Locations of control surface hinge lines are in inches aft of fuselage reference datum. (Wing leading edge is at FS 68.03.)

Figure 4.- Concluded.

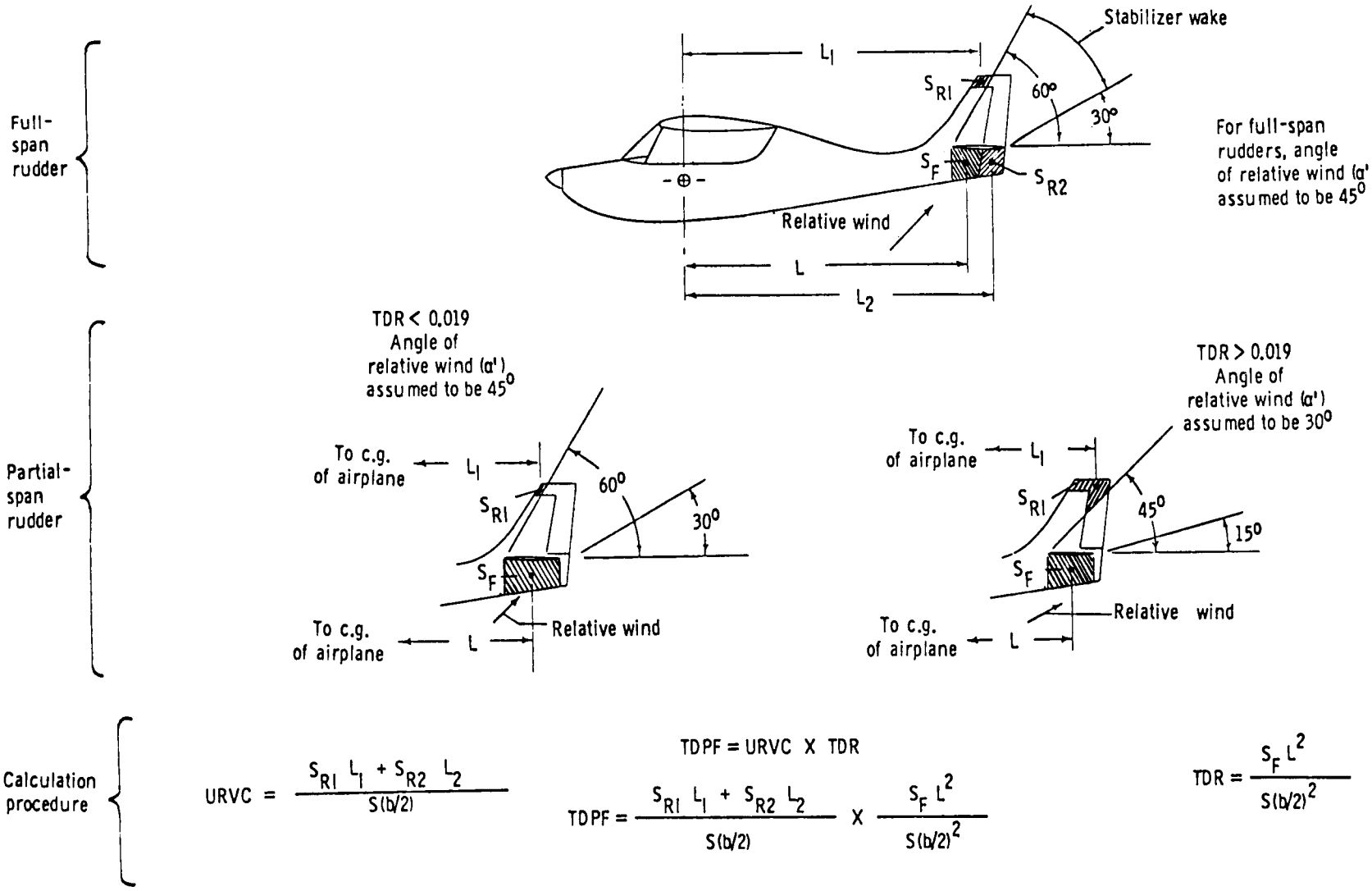

Figure 5.- Method of computing tail damping power factor. (From ref. 7.)

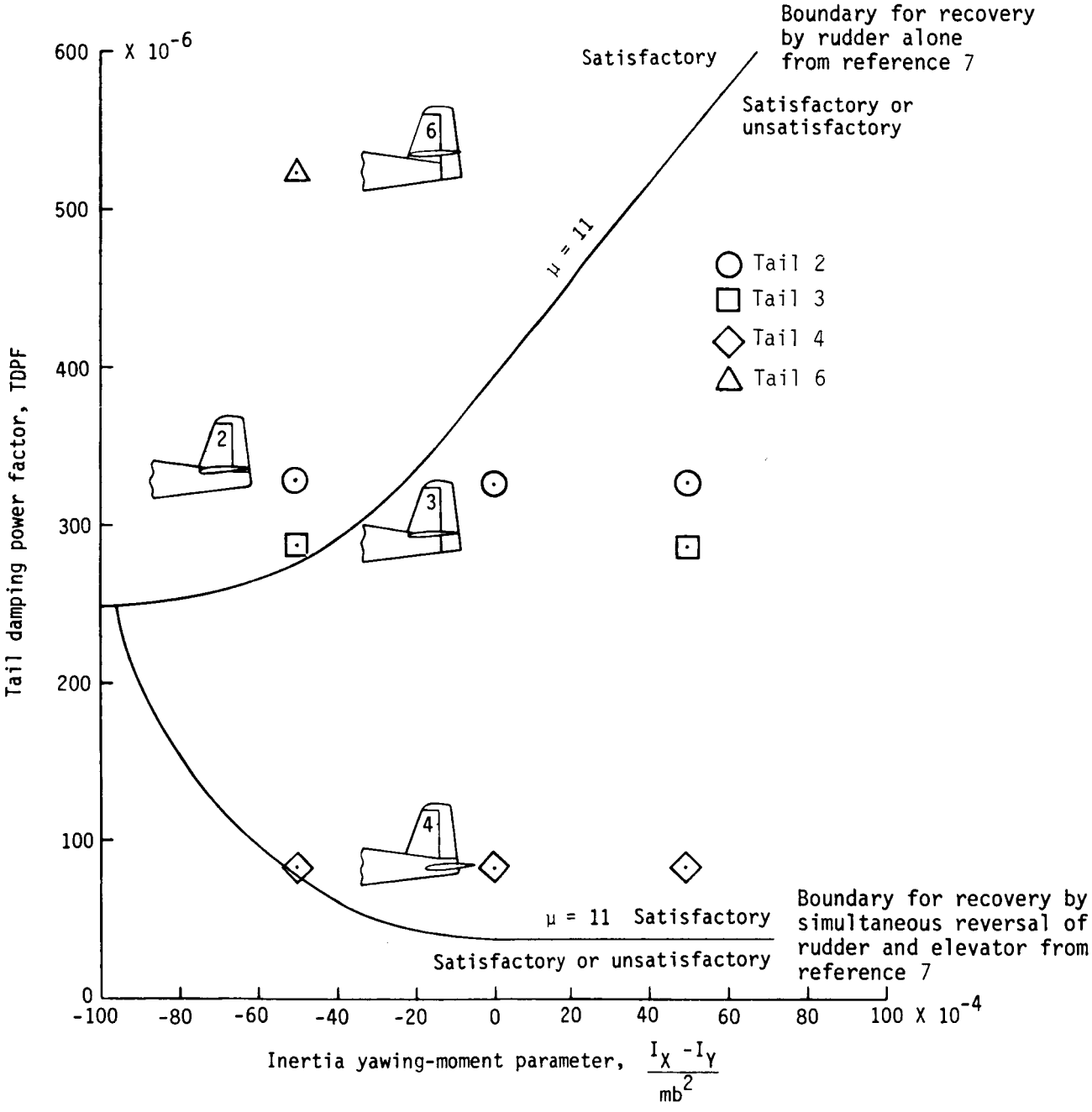

Figure 6.- Variation of tail damping power factor with inertia yawing-moment parameter for configurations tested showing 1947 NACA spin-recovery guideline.

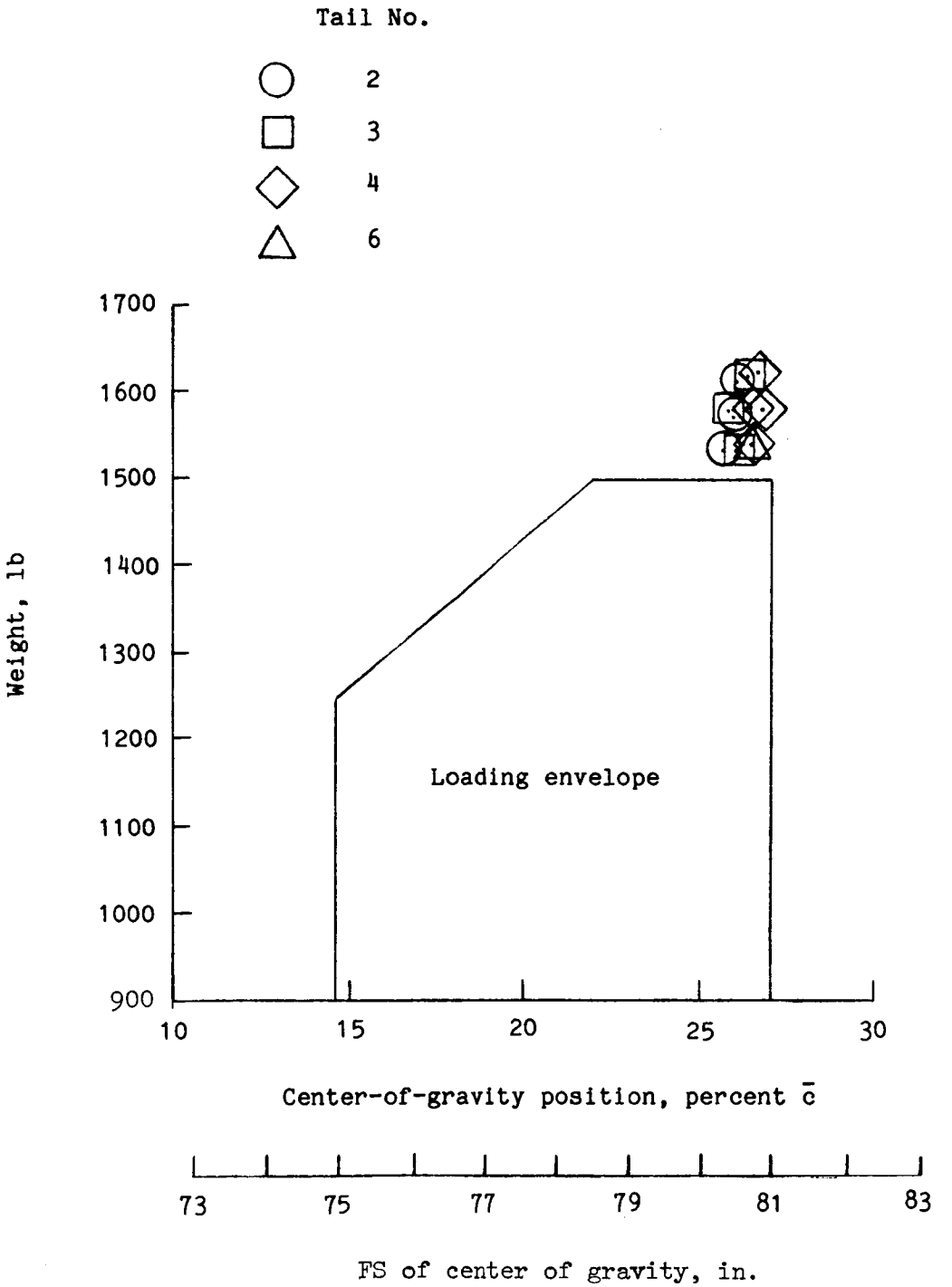

Figure 7.- Airplane design center-of-gravity envelope showing loading at test altitude.

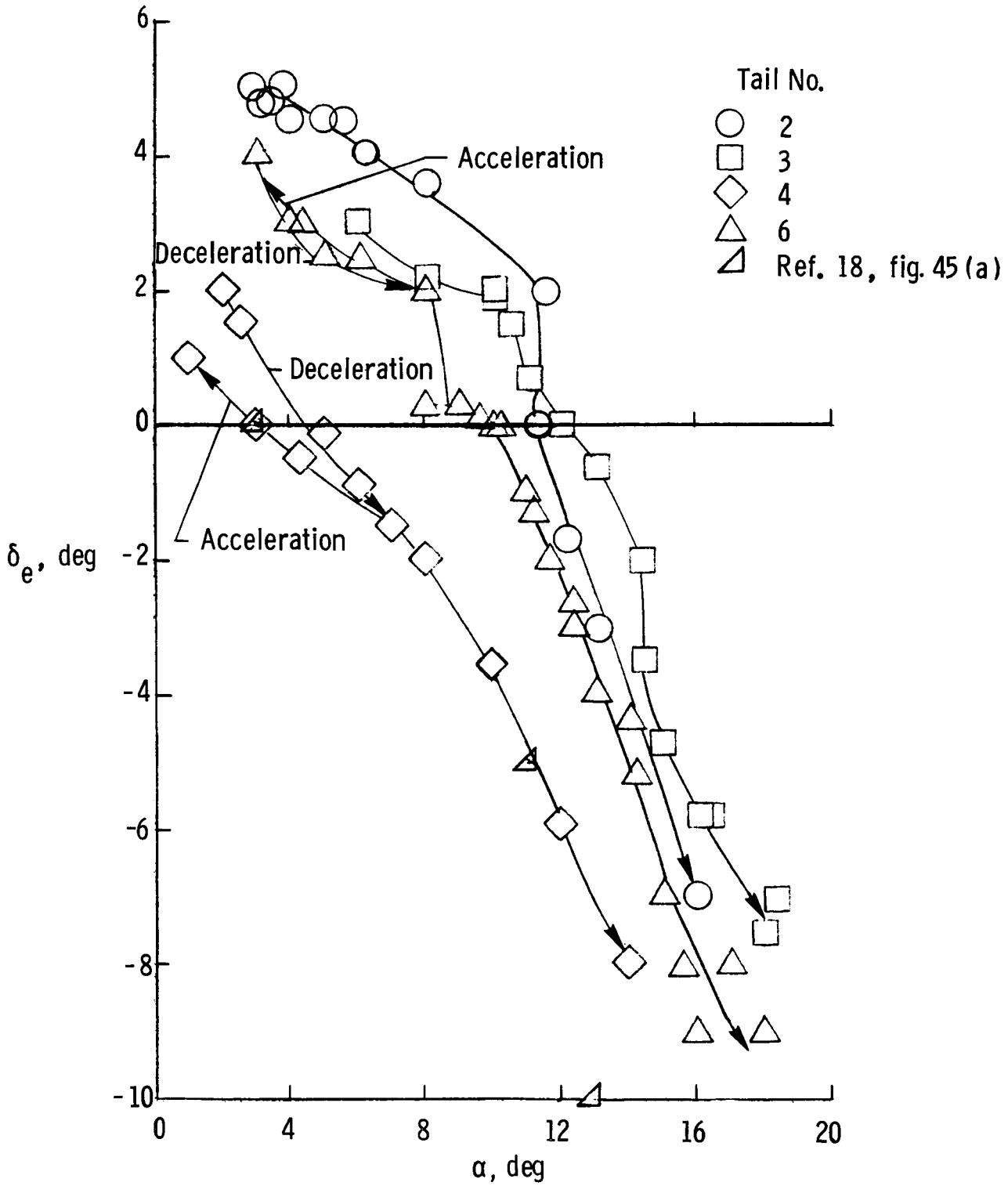

Figure 8.- Elevator deflection versus airplane angle of attack during idle-power acceleration-deceleration maneuvers. IYMP = -50×10^{-4}; c.g. at $0.26\bar{c}$.

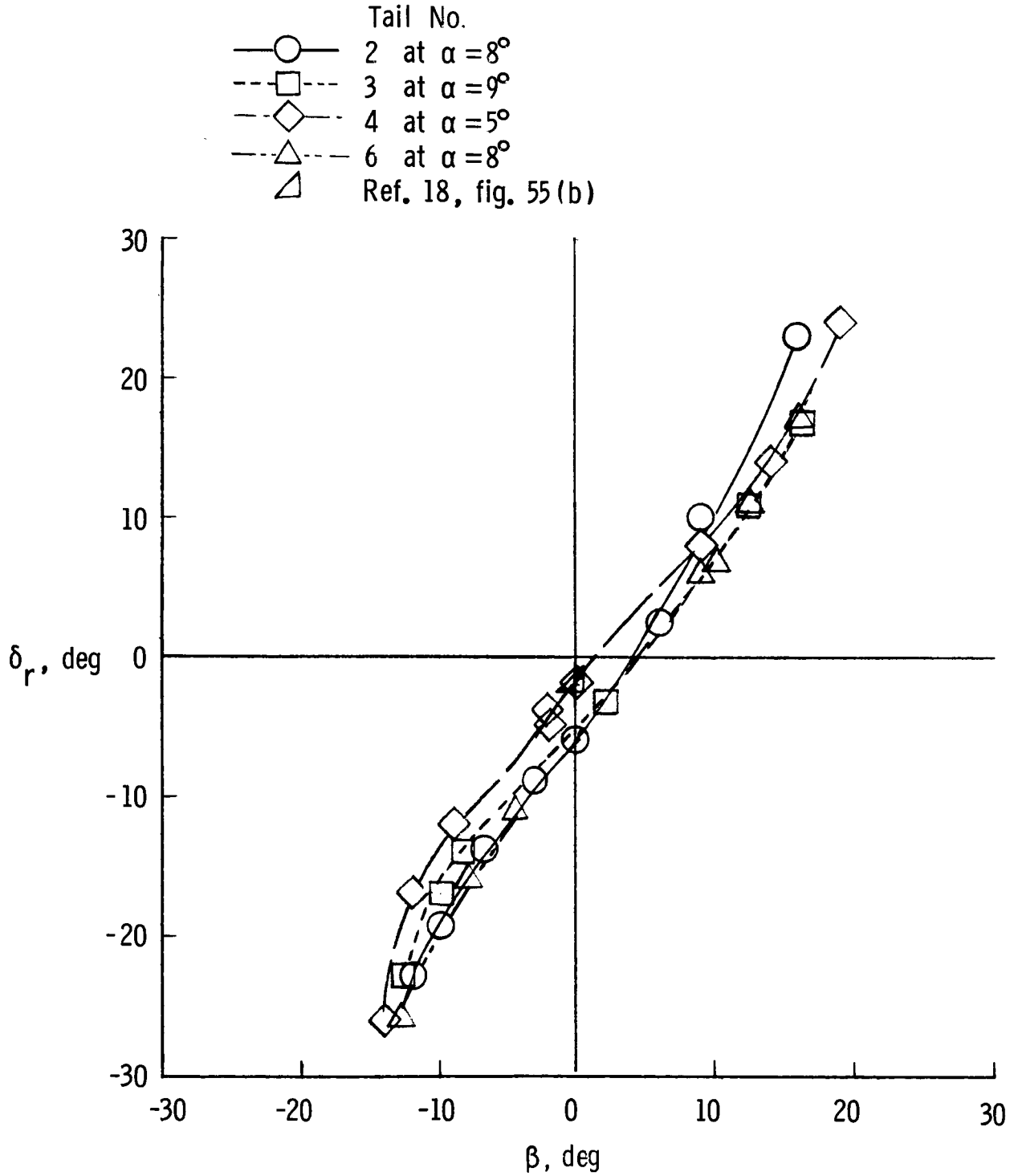

Figure 9.- Rudder deflection versus sideslip angle during steady-heading sideslips at constant indicated airspeed with power on. IYMP = -50×10^{-4}; c.g. at $0.26\bar{c}$.

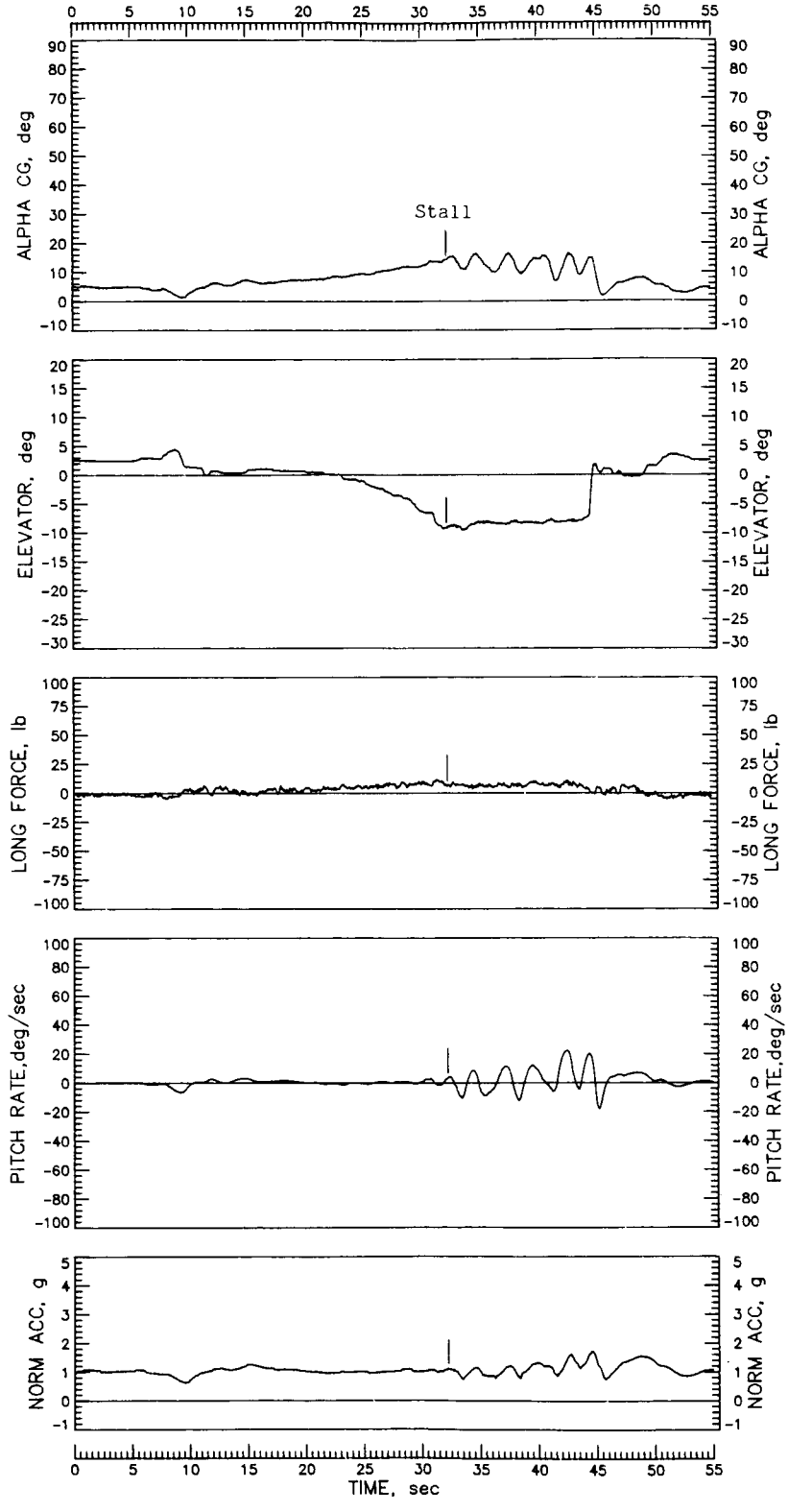

Figure 10.- Slow deceleration to idle-power, 1g, wings-level stall with tail 6. Controls held fixed at stall. IYMP = -50×10^{-4}; c.g. at $0.26\bar{c}$.

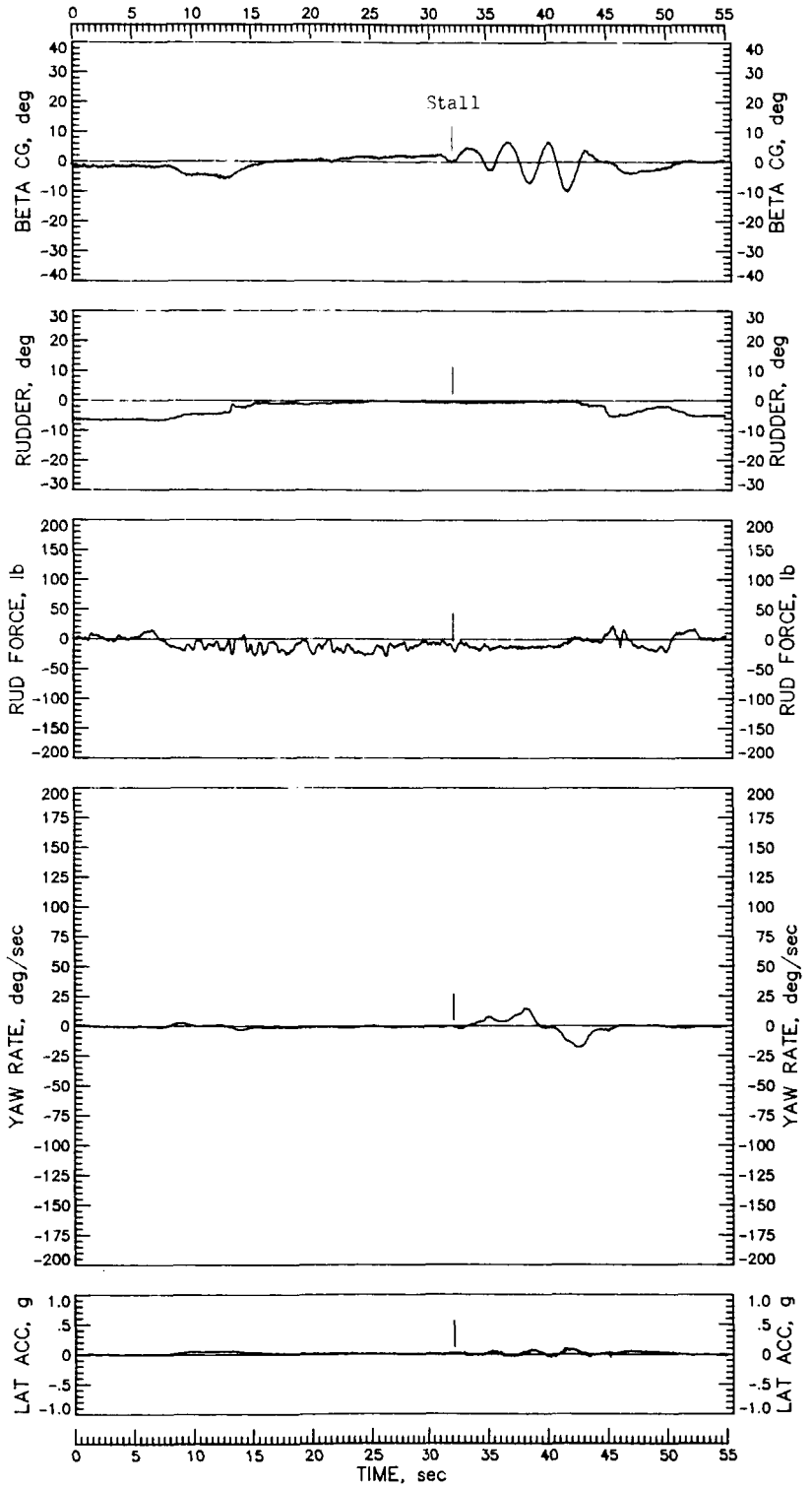

Figure 10.- Continued.

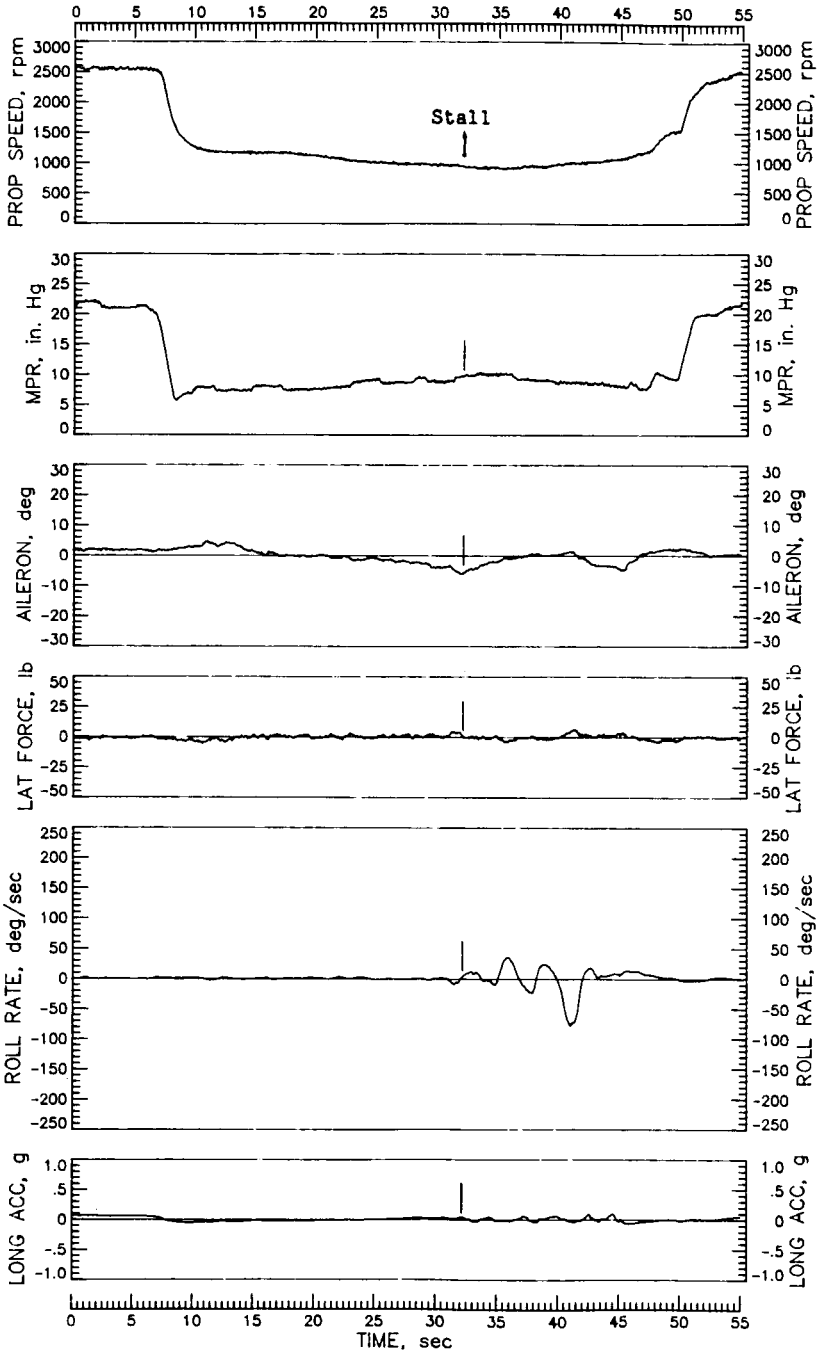

Figure 10.- Continued.

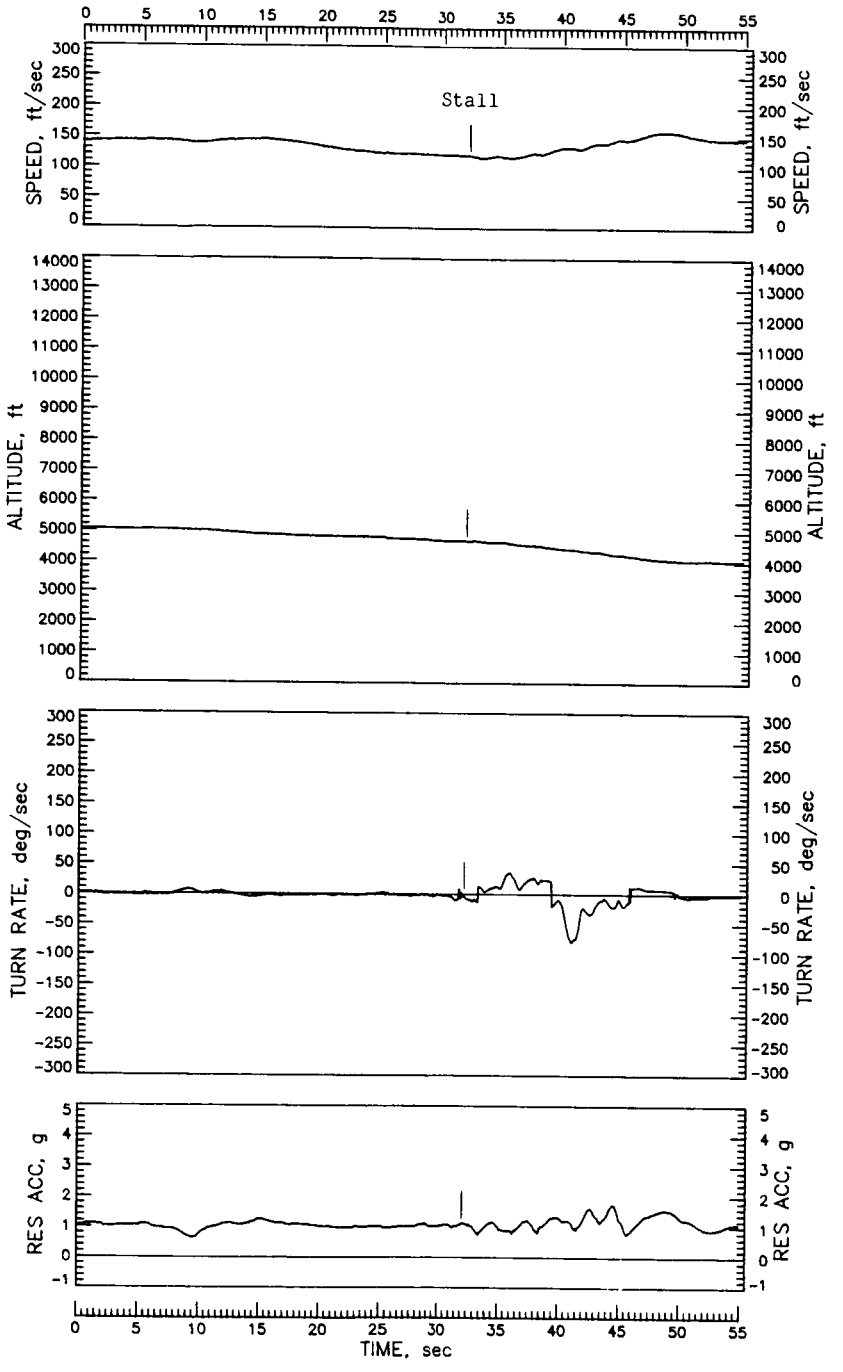

Figure 10.- Concluded.

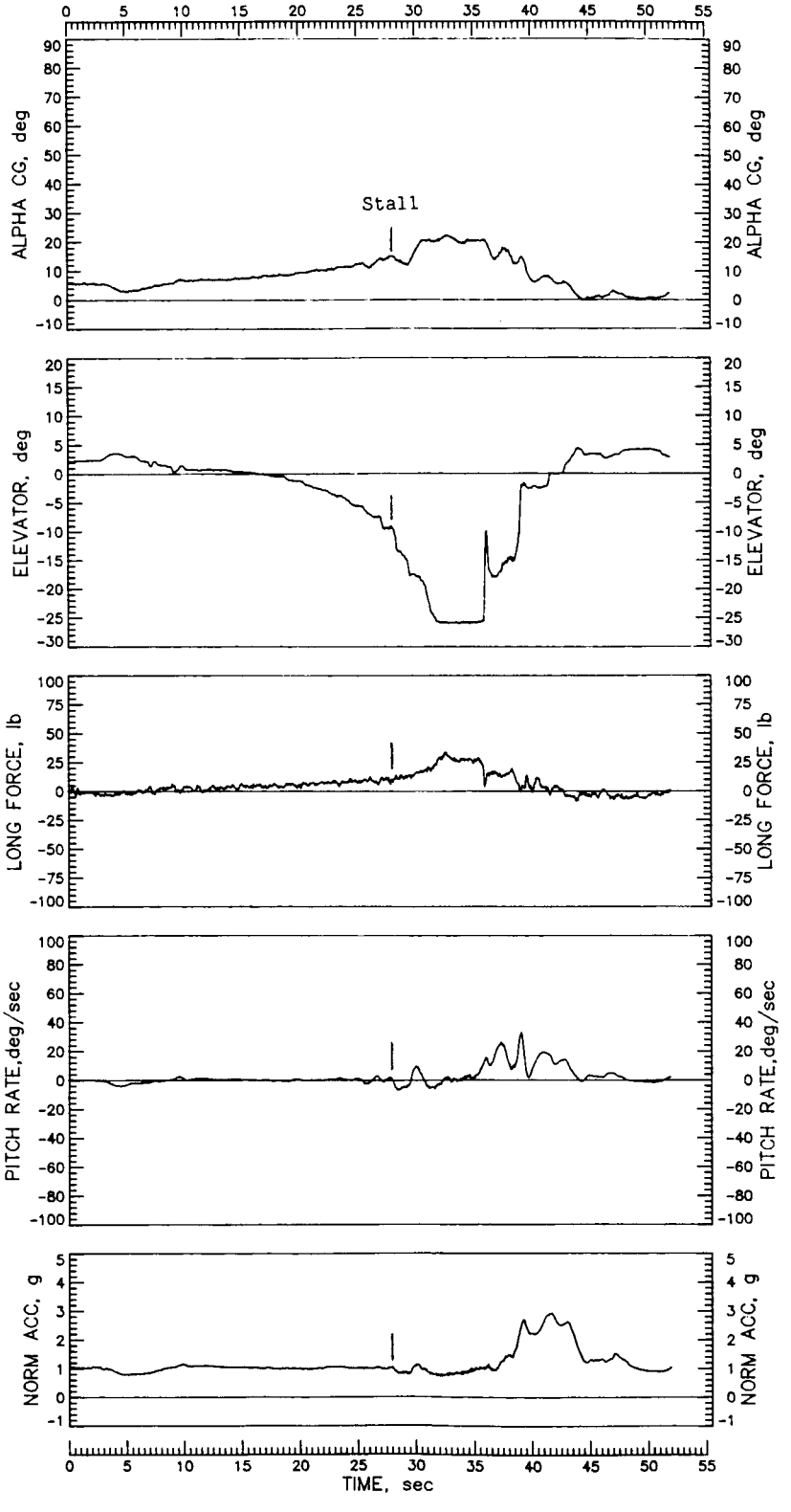

Figure 11.- Idle-power, 1g, wings-level stall with maximum elevator deflection with tail 6. Controls held fixed after stall. IYMP = -50×10^{-4}; c.g. at $0.26\bar{c}$.

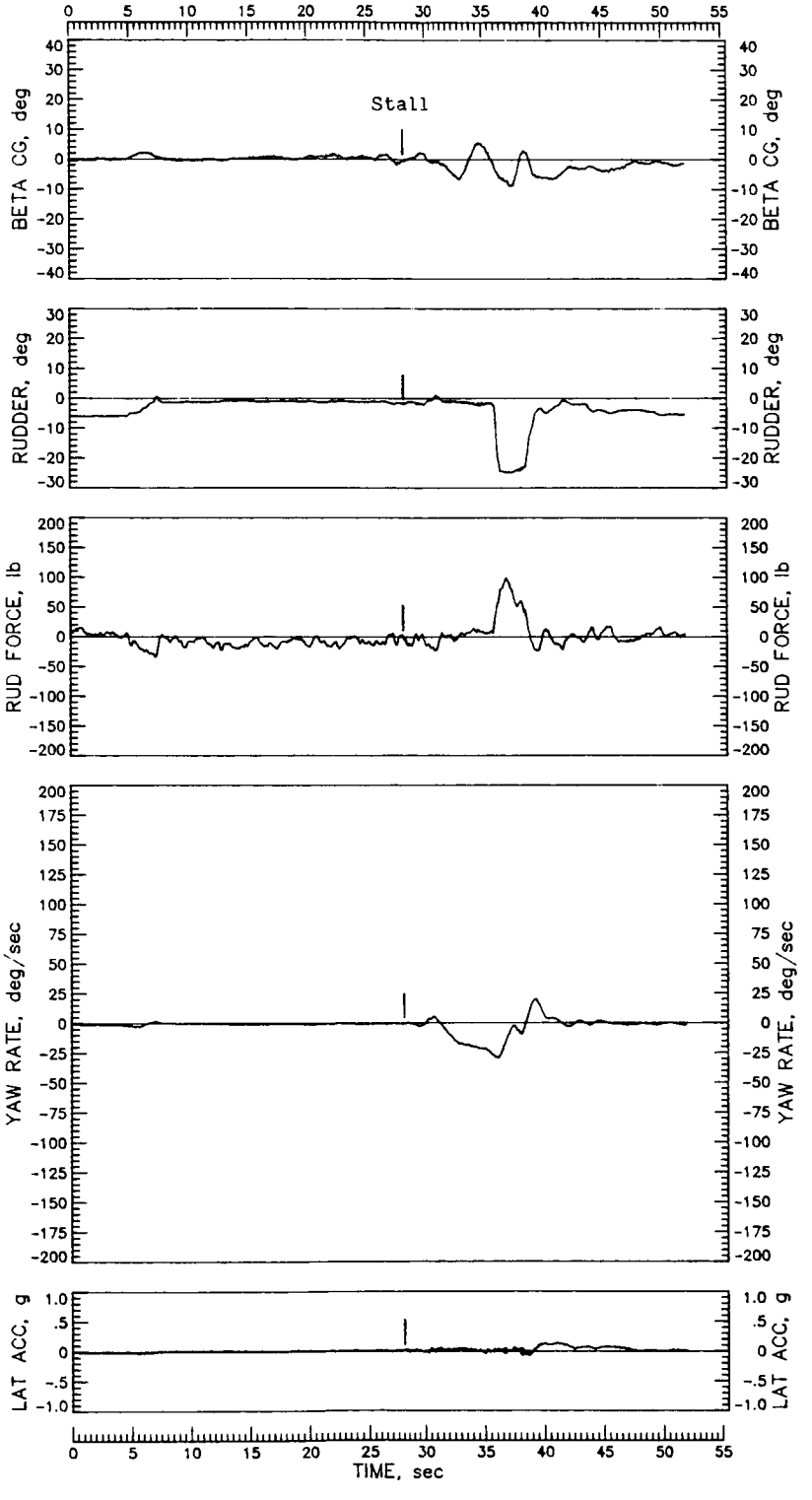

Figure 11.- Continued.

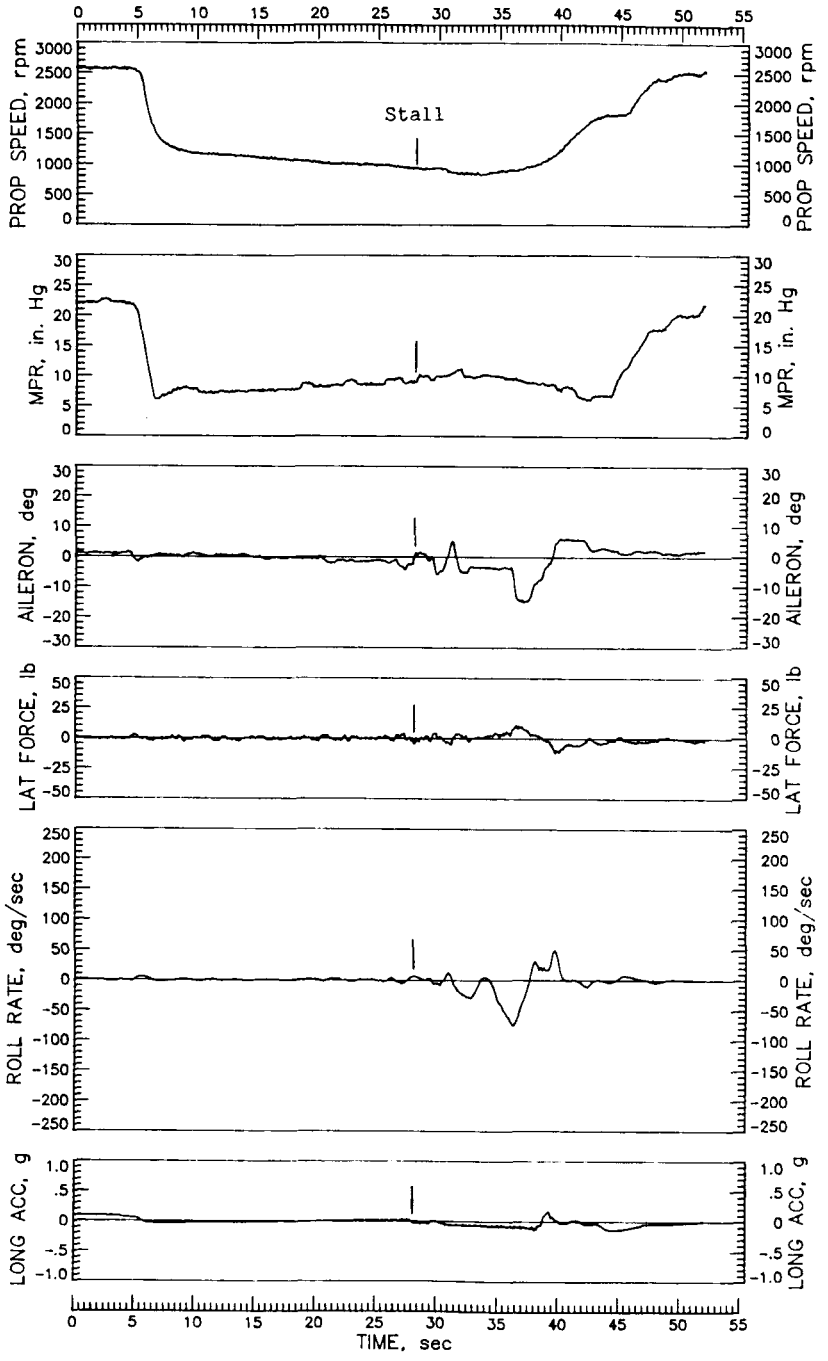

Figure 11.- Continued.

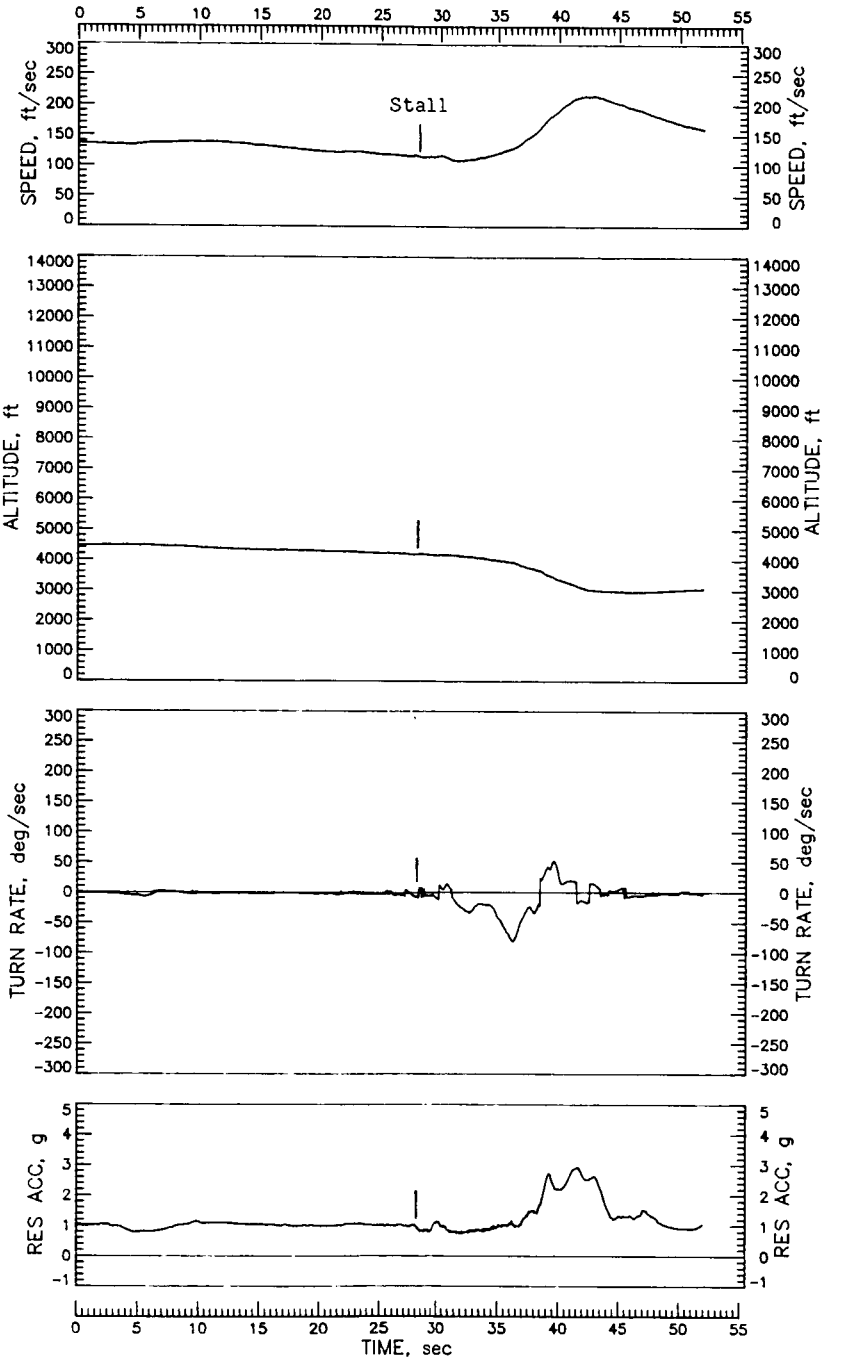

Figure 11.- Concluded.

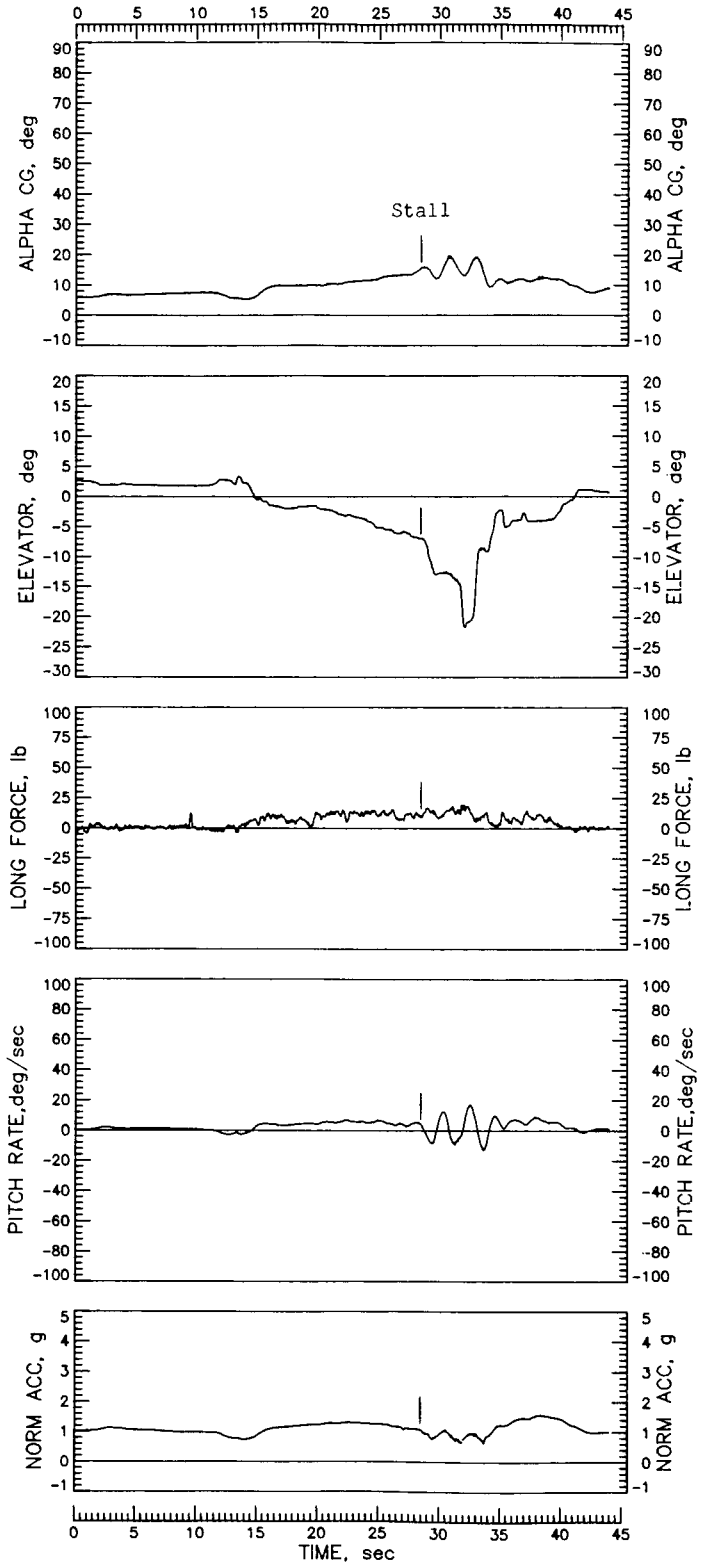

Figure 12.- Idle-power stall from 30° banked right turn with tail 6. IYMP = -50×10^{-4}; c.g. at $0.26\bar{c}$.

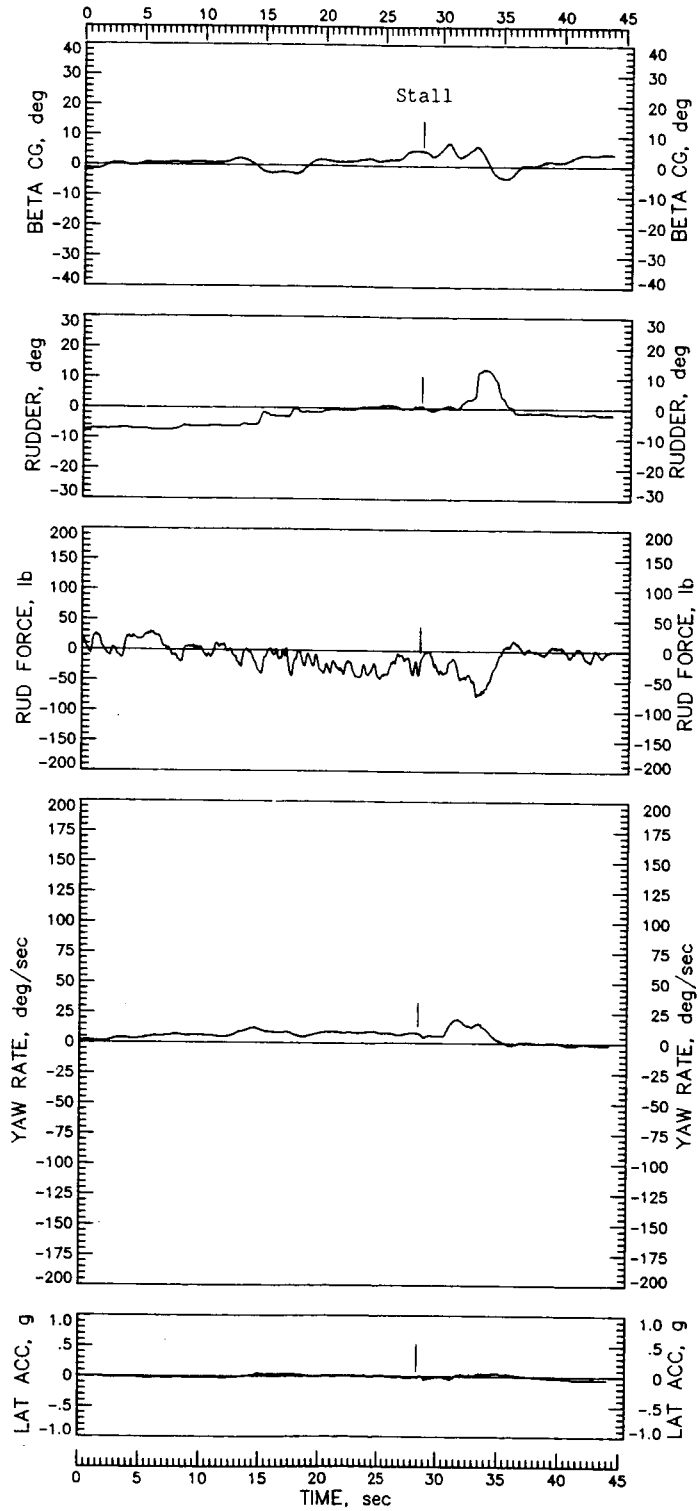

Figure 12.- Continued.

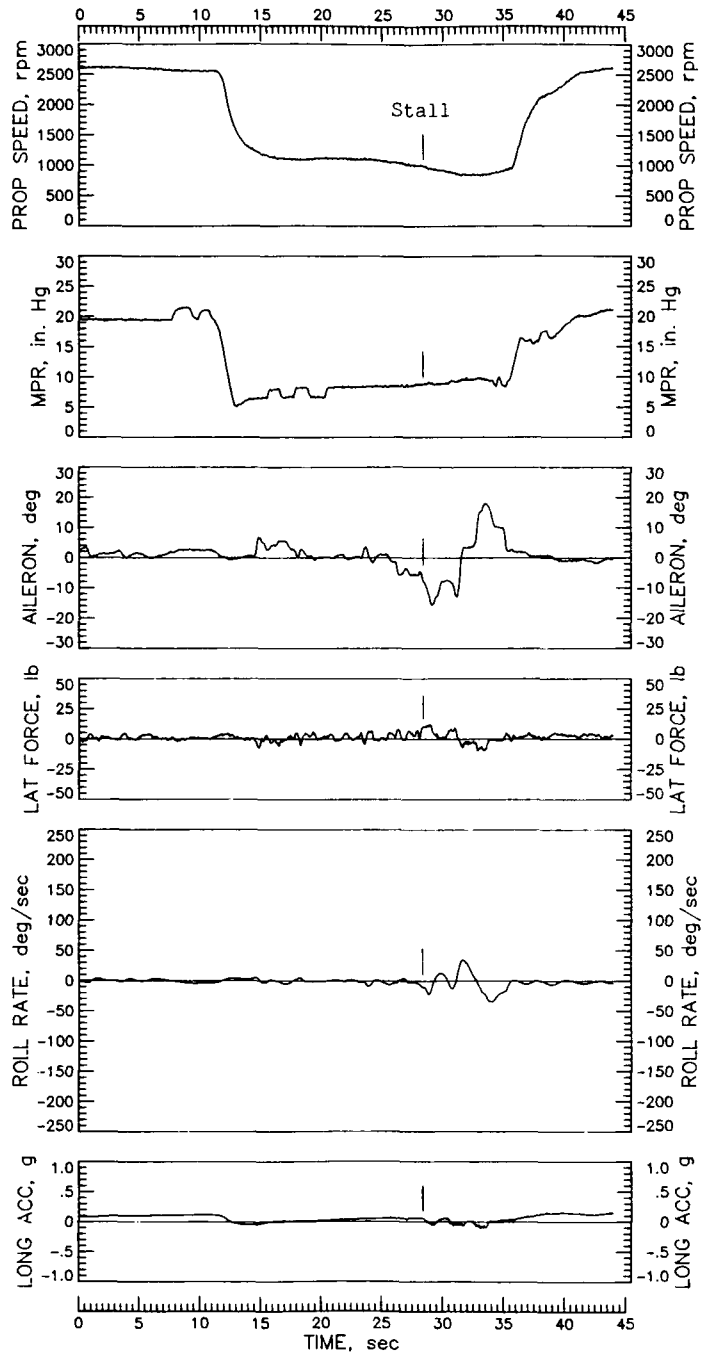

Figure 12.- Continued.

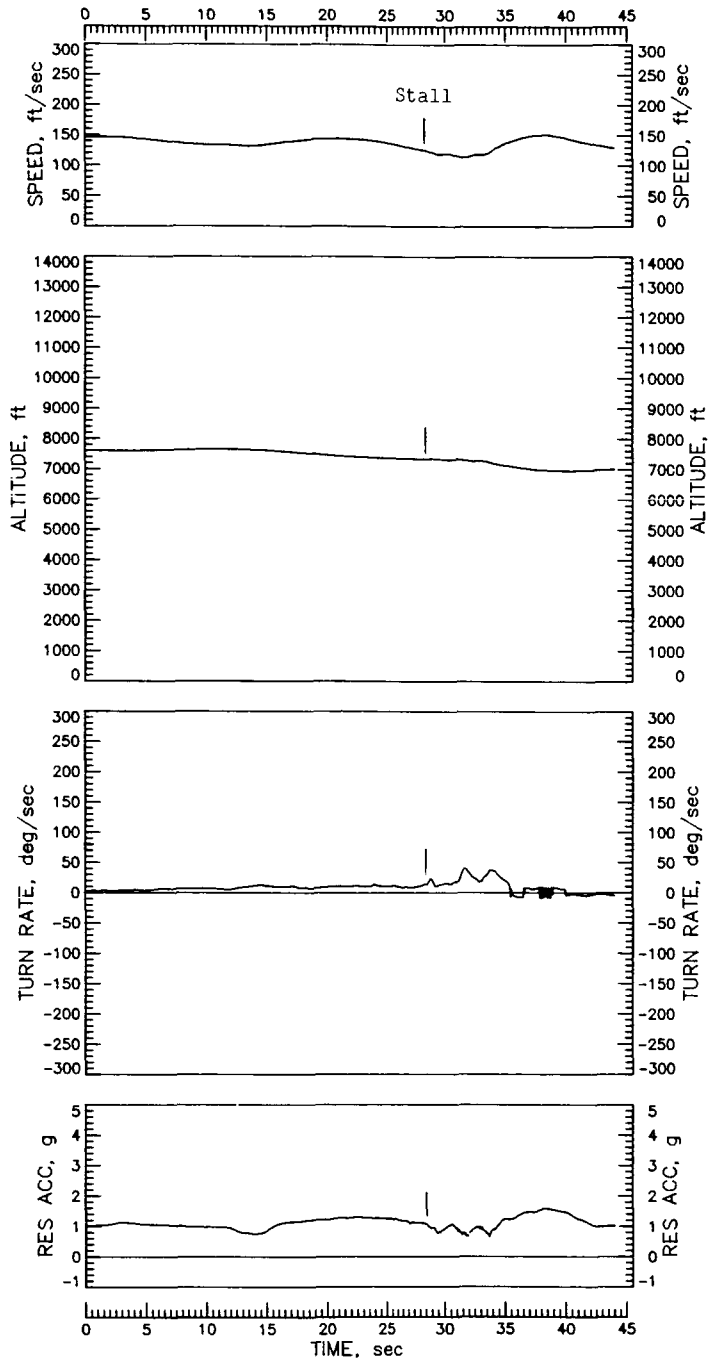

Figure 12.- Concluded.

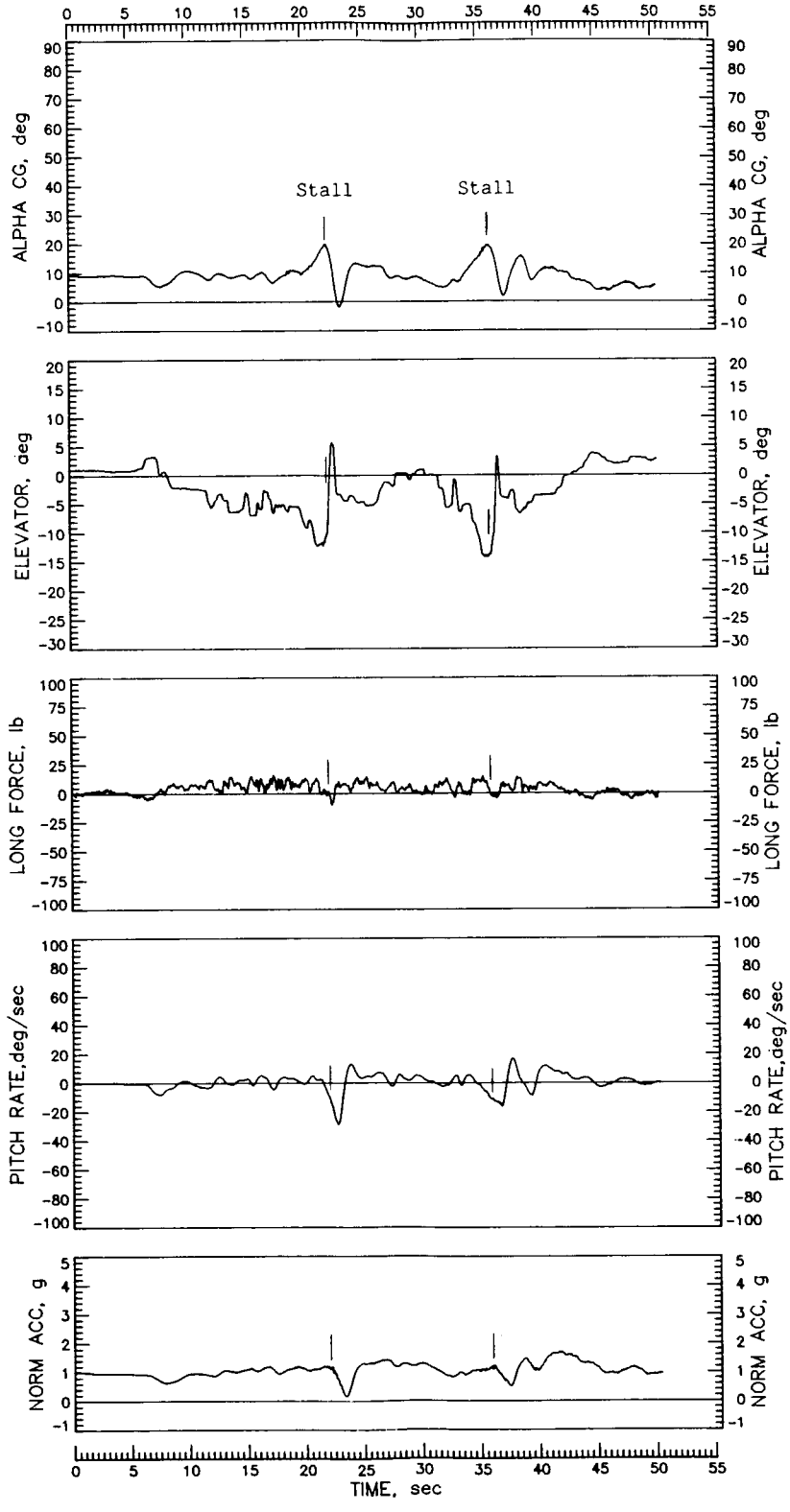

Figure 13.- Idle-power stalls with left and right sideslip with tail 6. IYMP = -50×10^{-4}; c.g. at $0.26\bar{c}$.

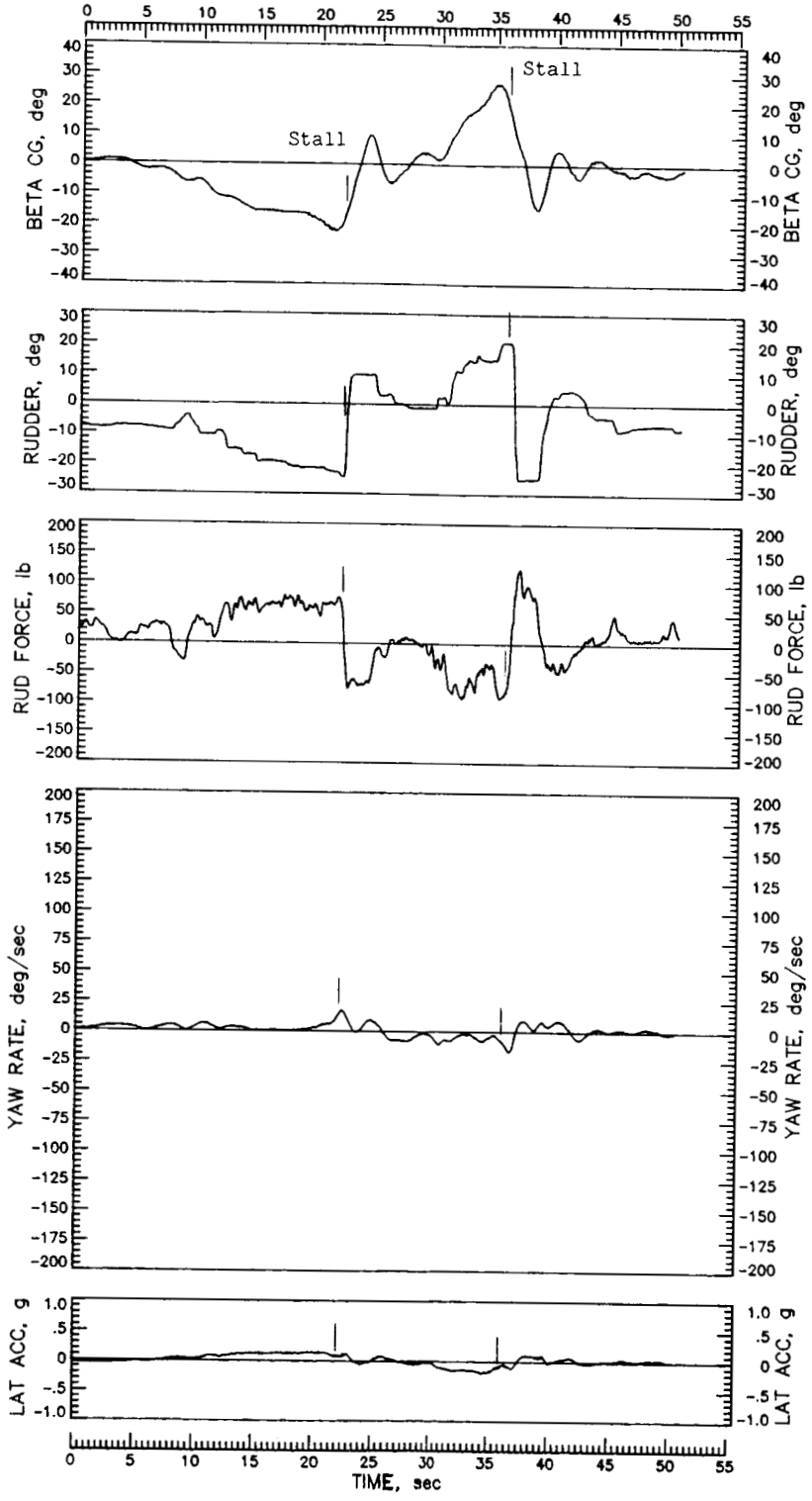

Figure 13.- Continued.

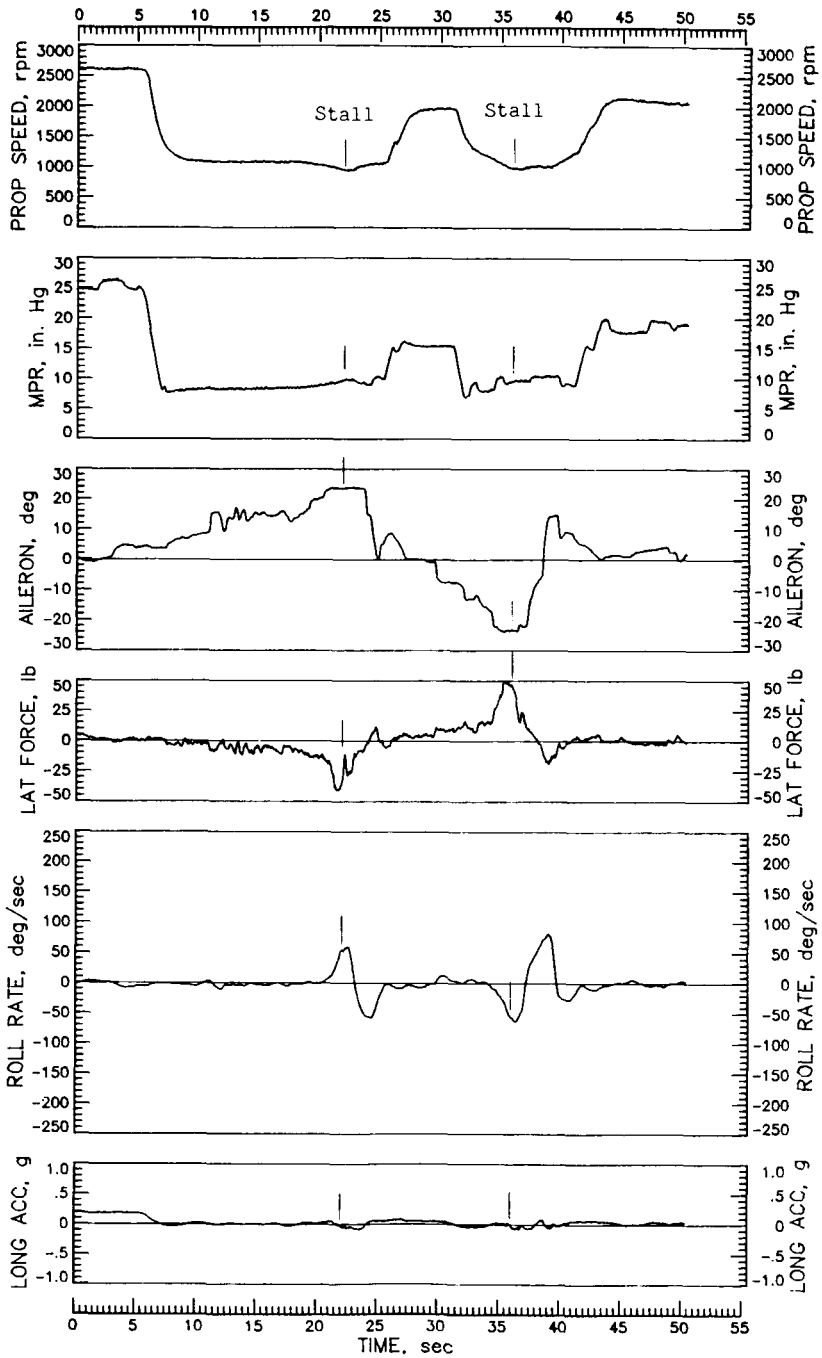

Figure 13.- Continued.

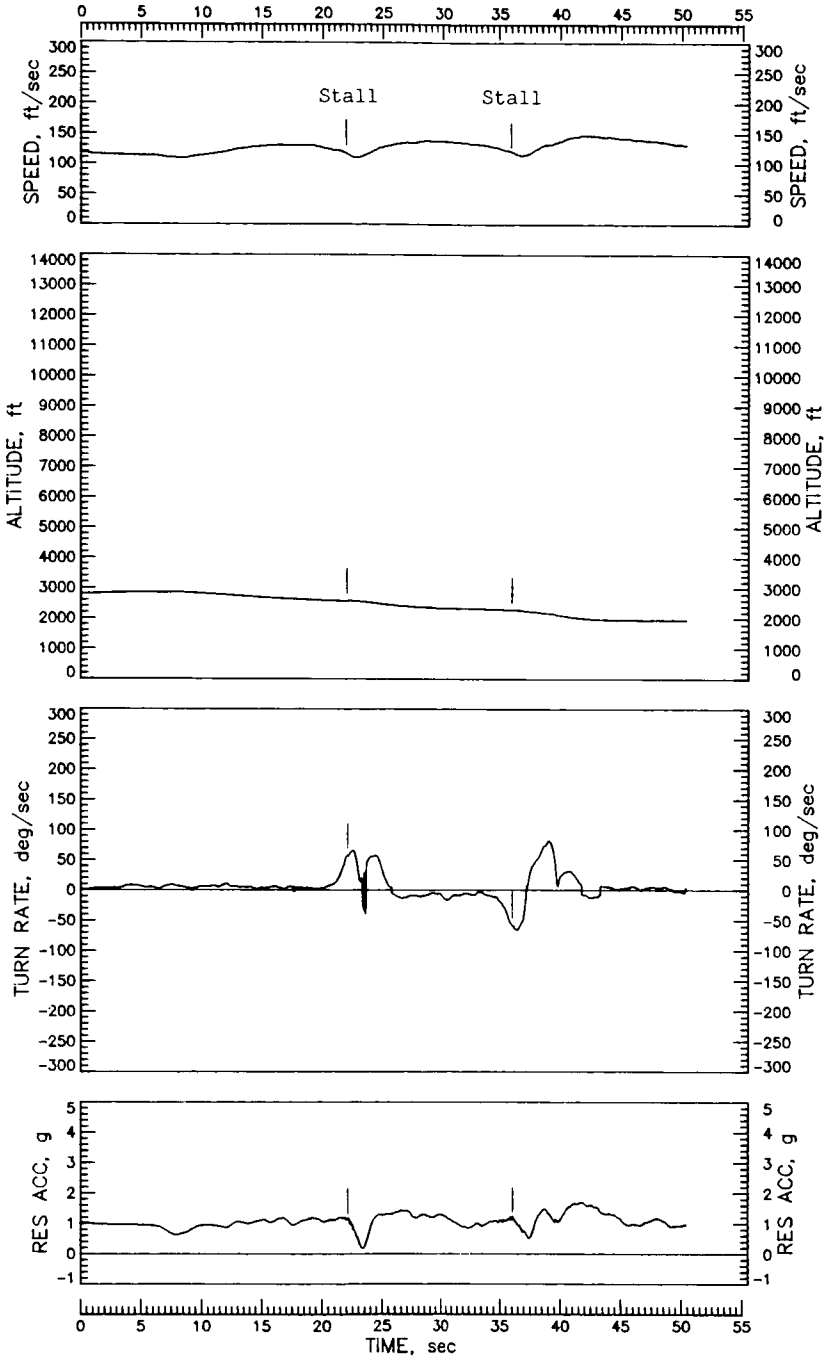

Figure 13.- Concluded.

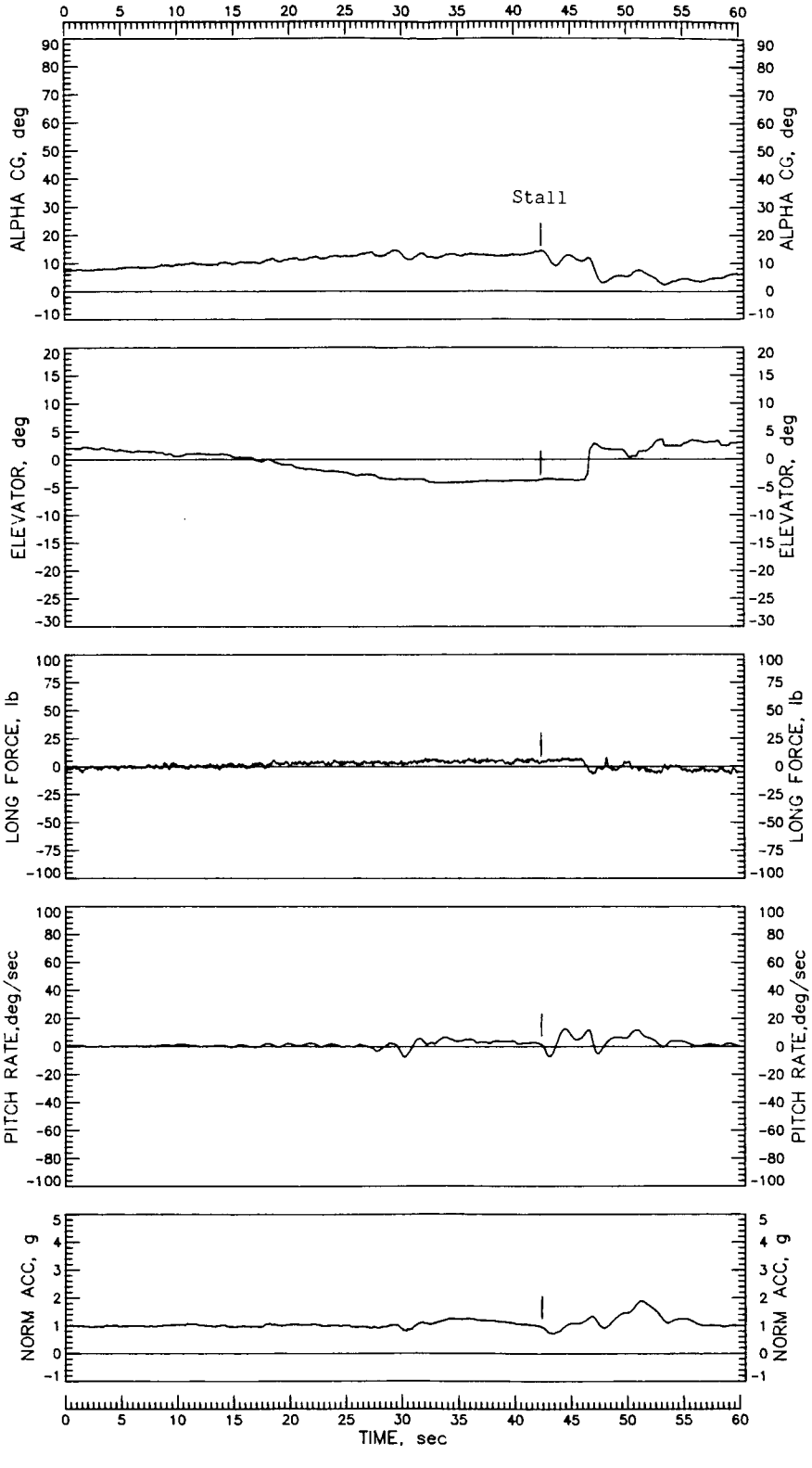

Figure 14.- Slow deceleration to maximum-power, 1g, wings-level stall with tail 6. Controls held fixed at stall. IYMP = -50×10^{-4}; c.g. at $0.26\bar{c}$.

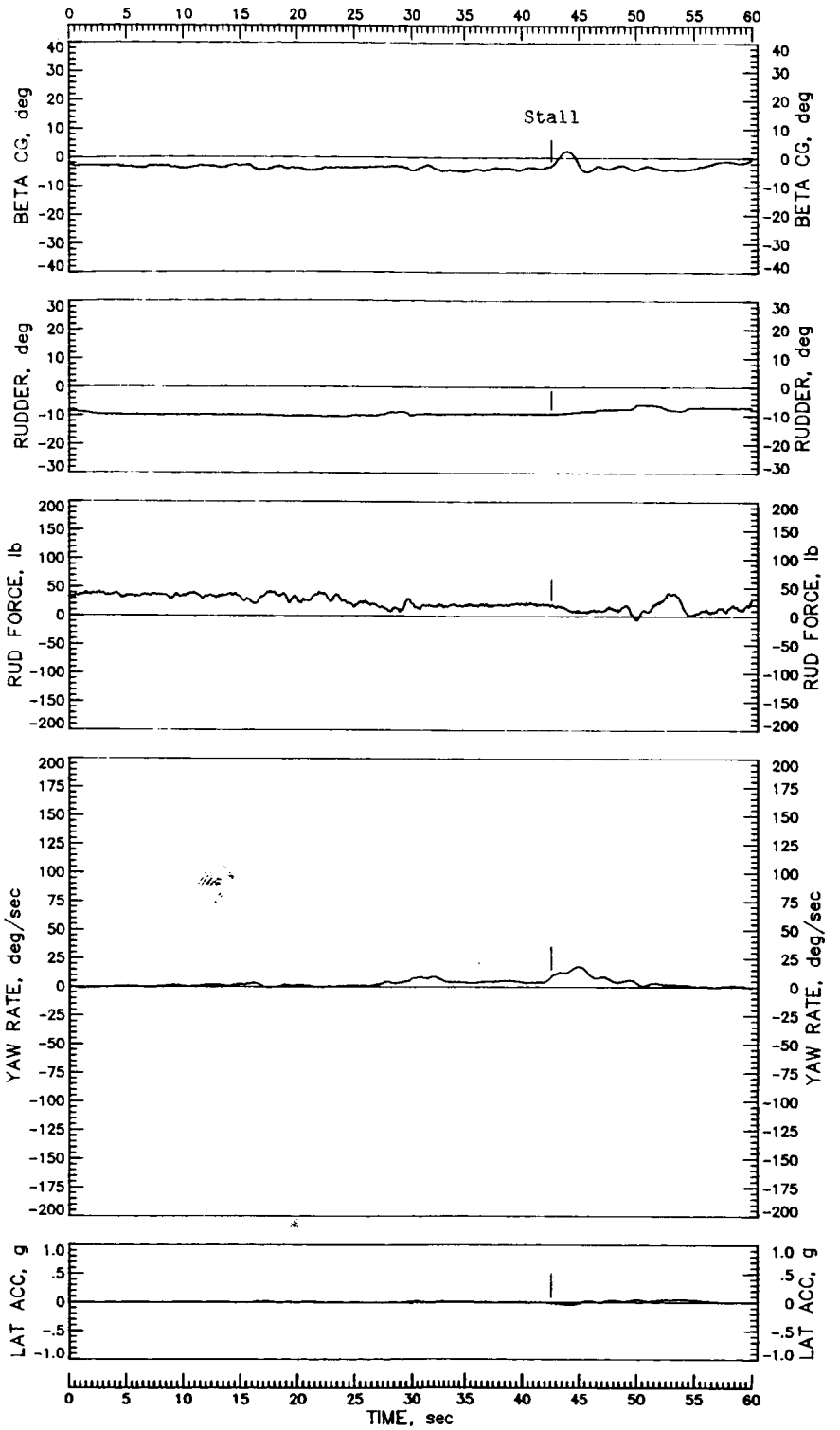

Figure 14.- Continued.

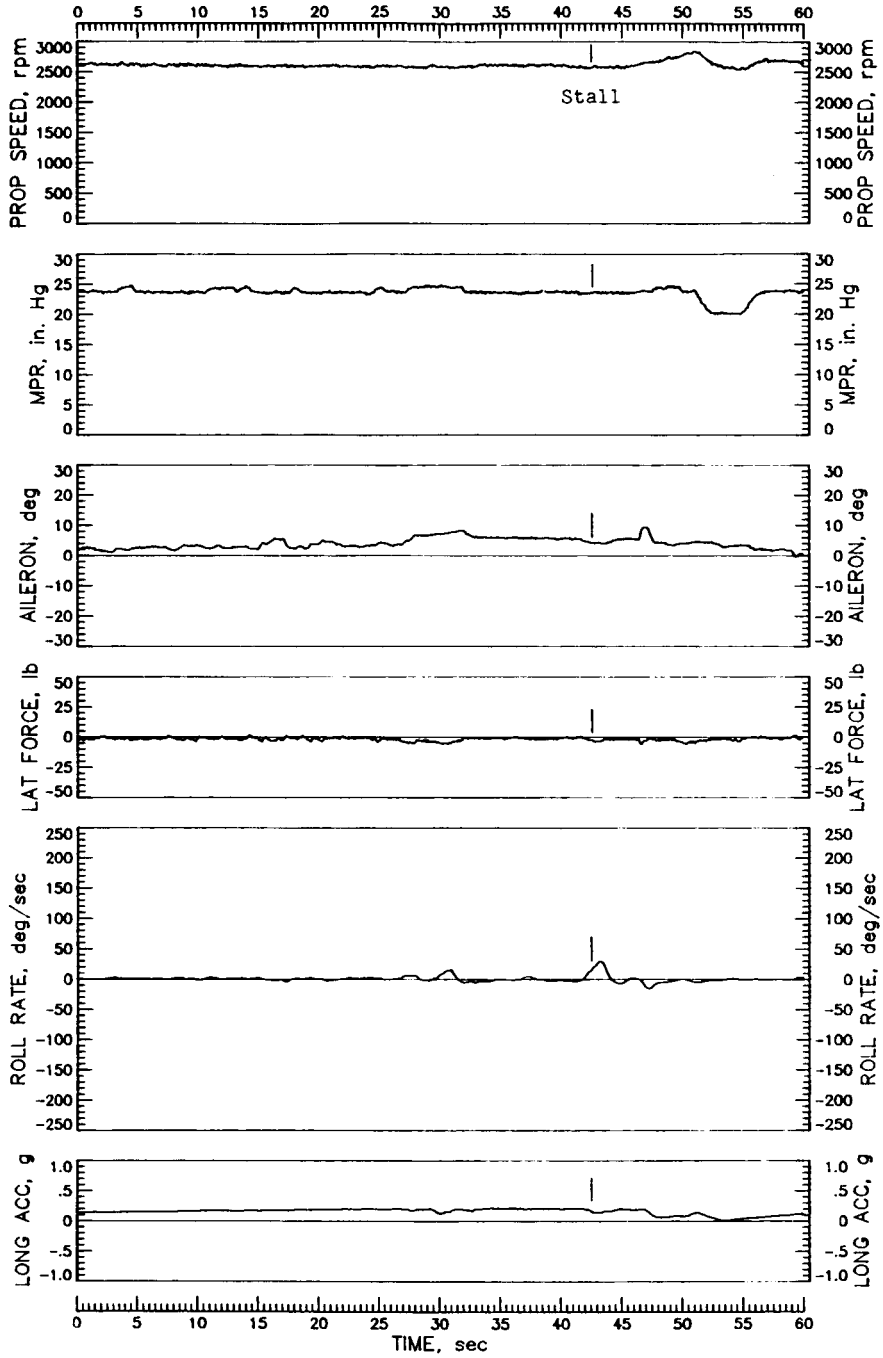

Figure 14.- Continued.

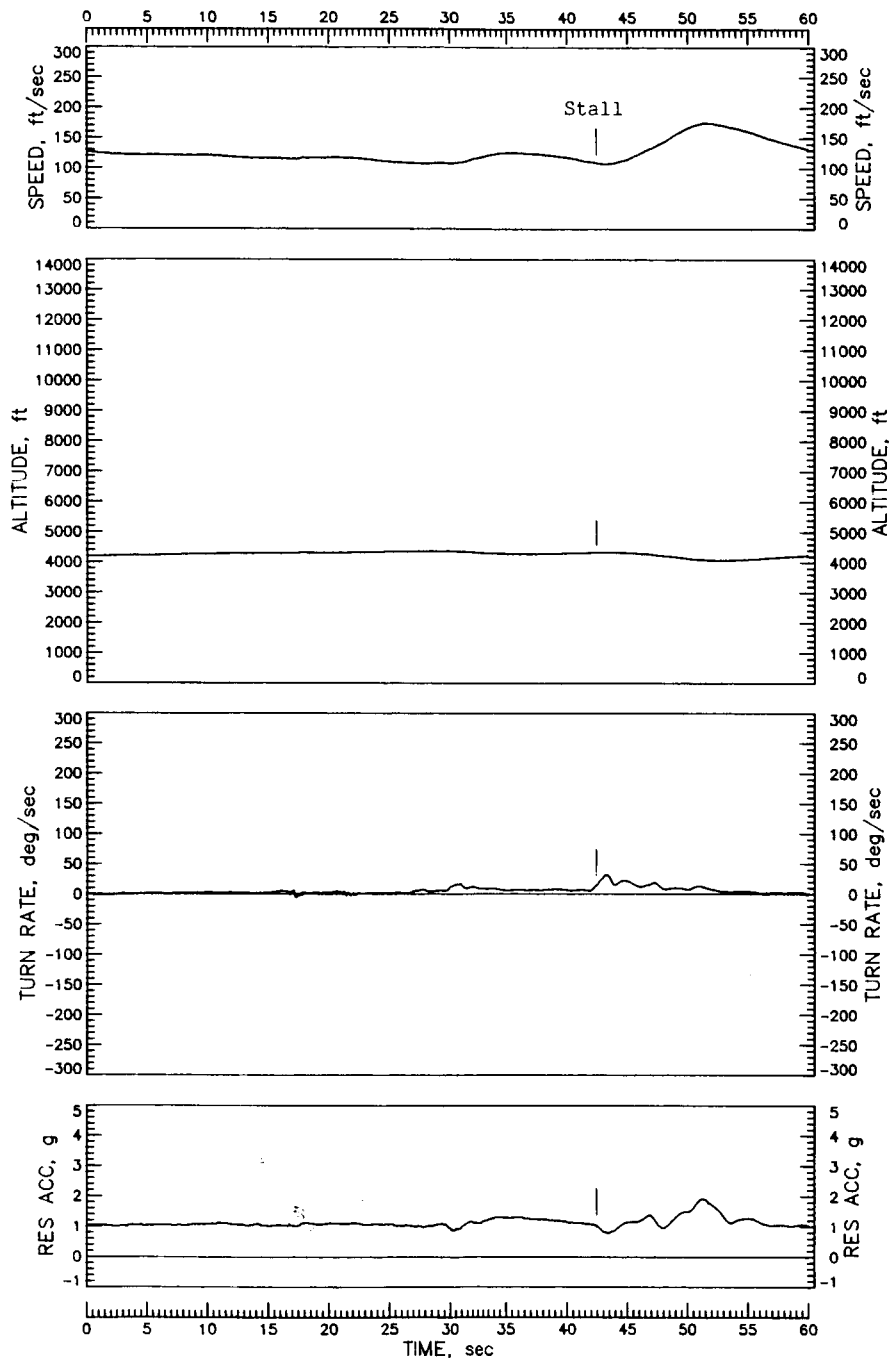

Figure 14.- Concluded.

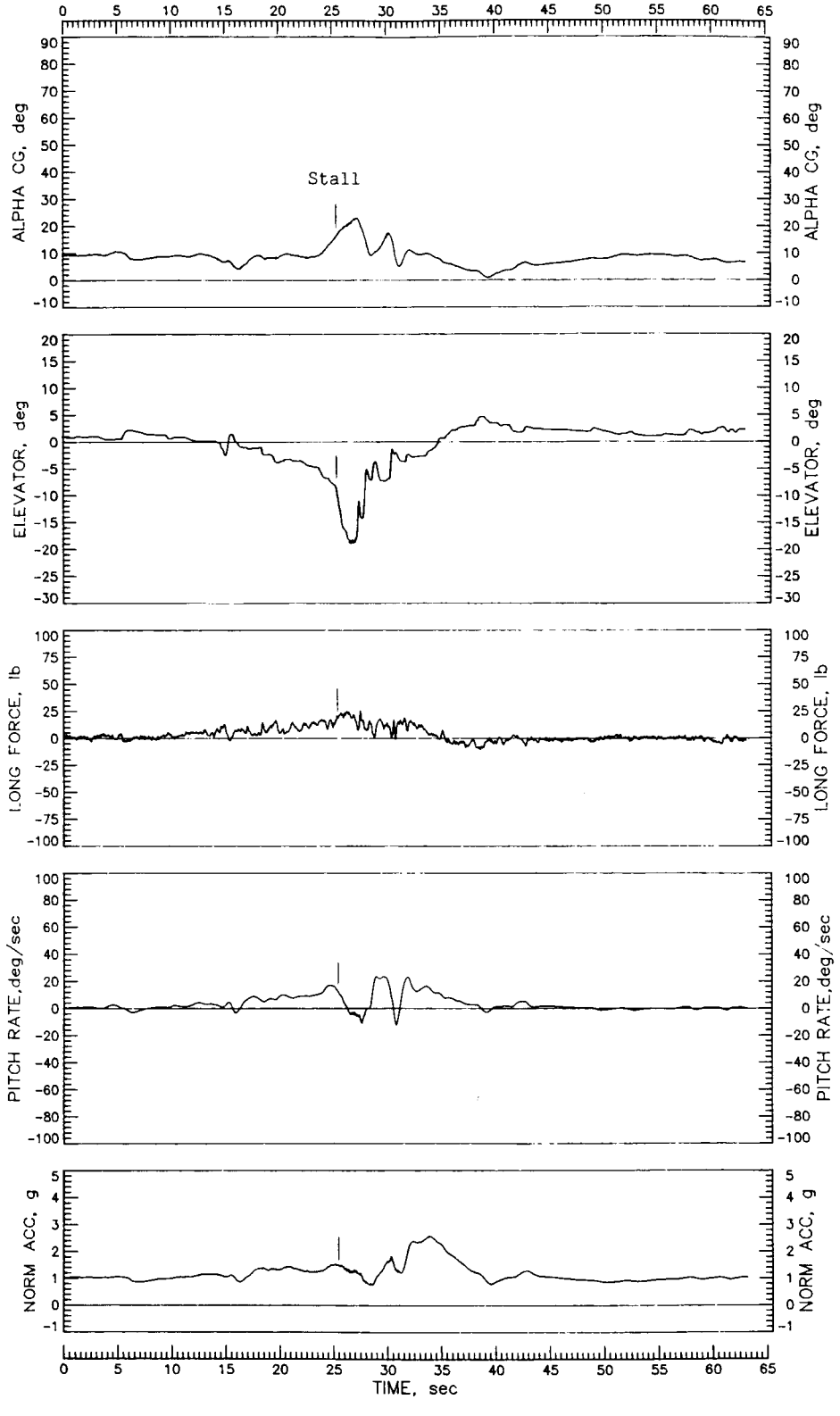

Figure 15.- Maximum-power stall in sideslipping 60° banked left turn with tail 6. IYMP = -50×10^{-4}; c.g. at $0.26\bar{c}$.

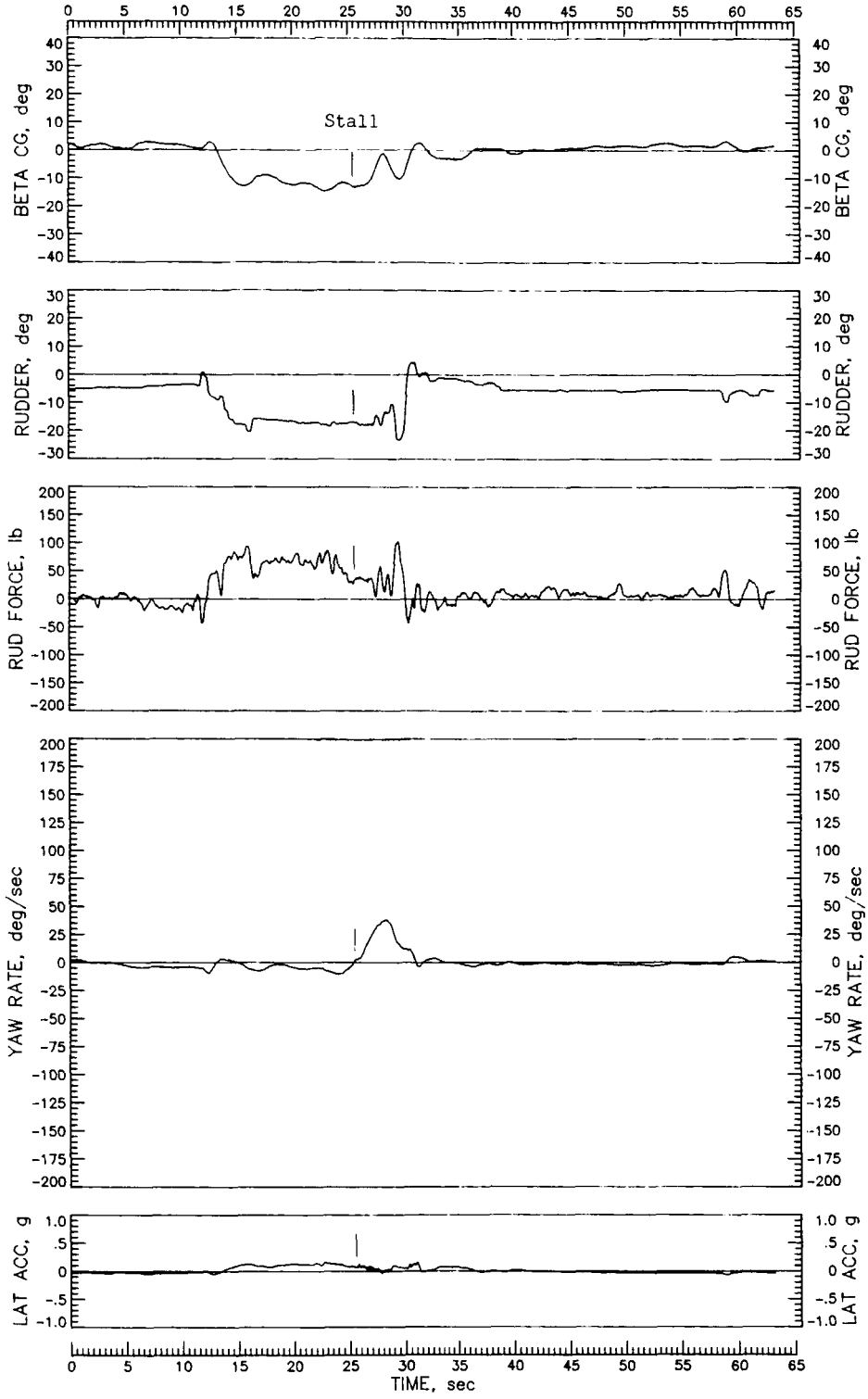

Figure 15.- Continued.

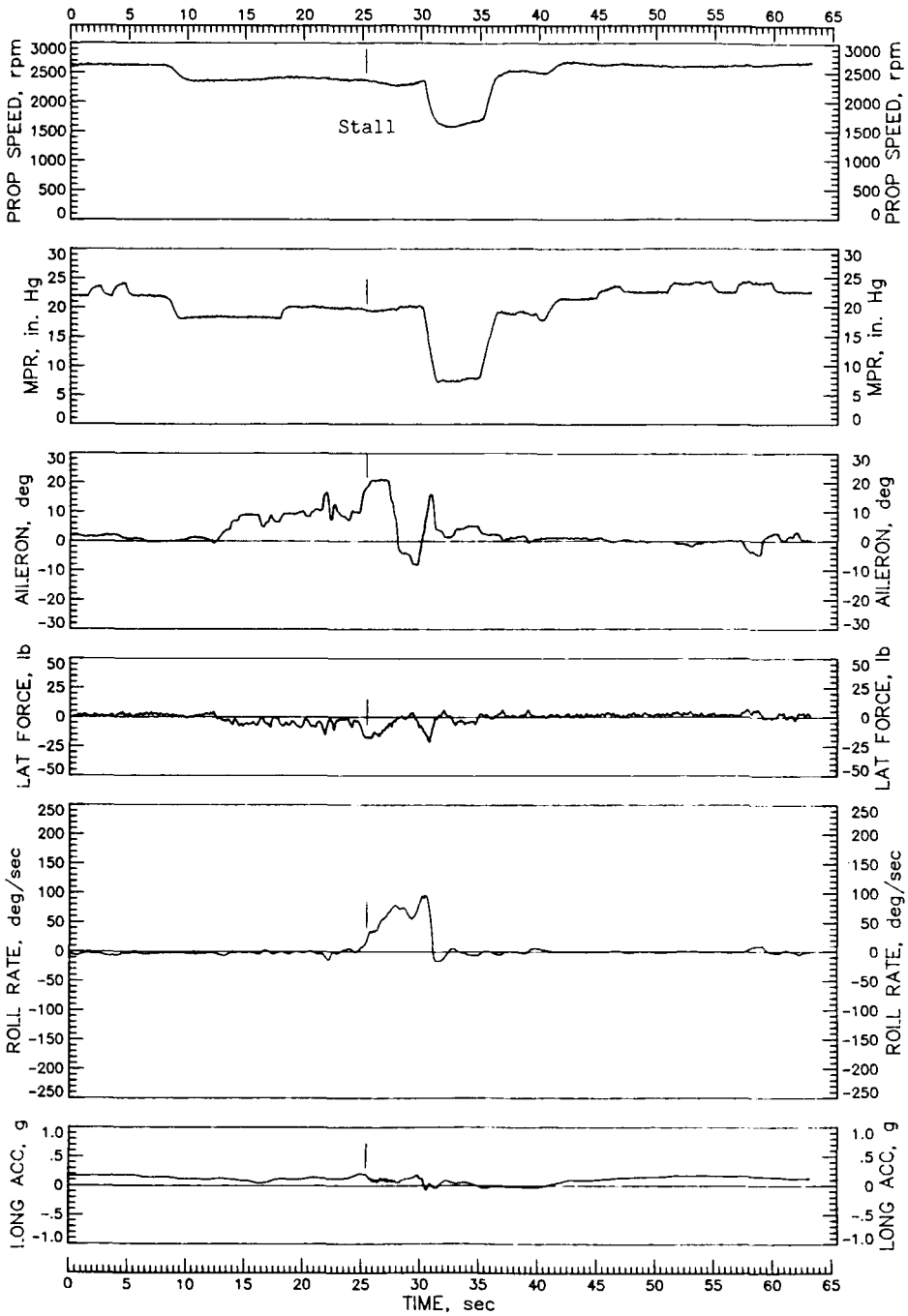

Figure 15.- Continued.

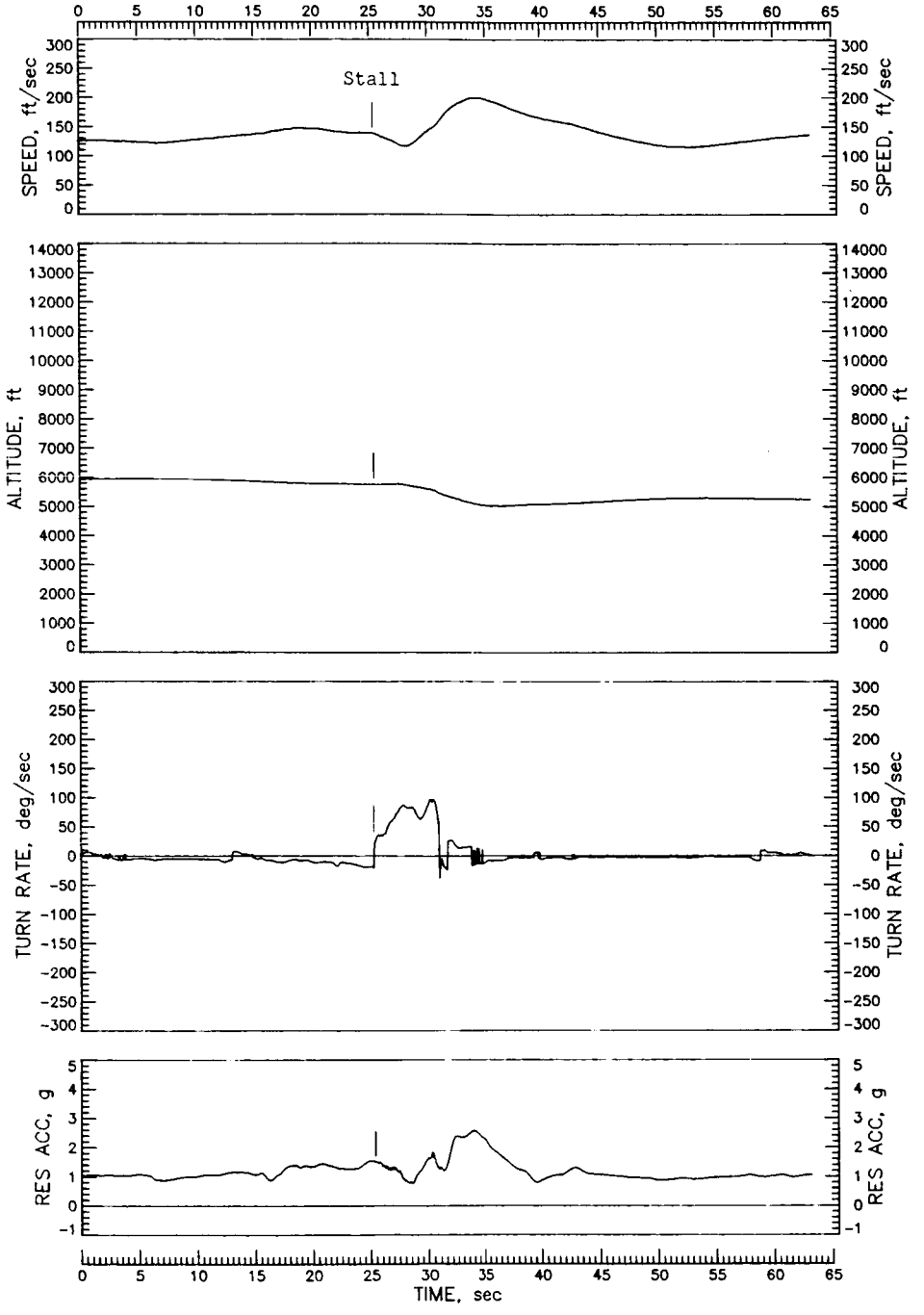

Figure 15.- Concluded.

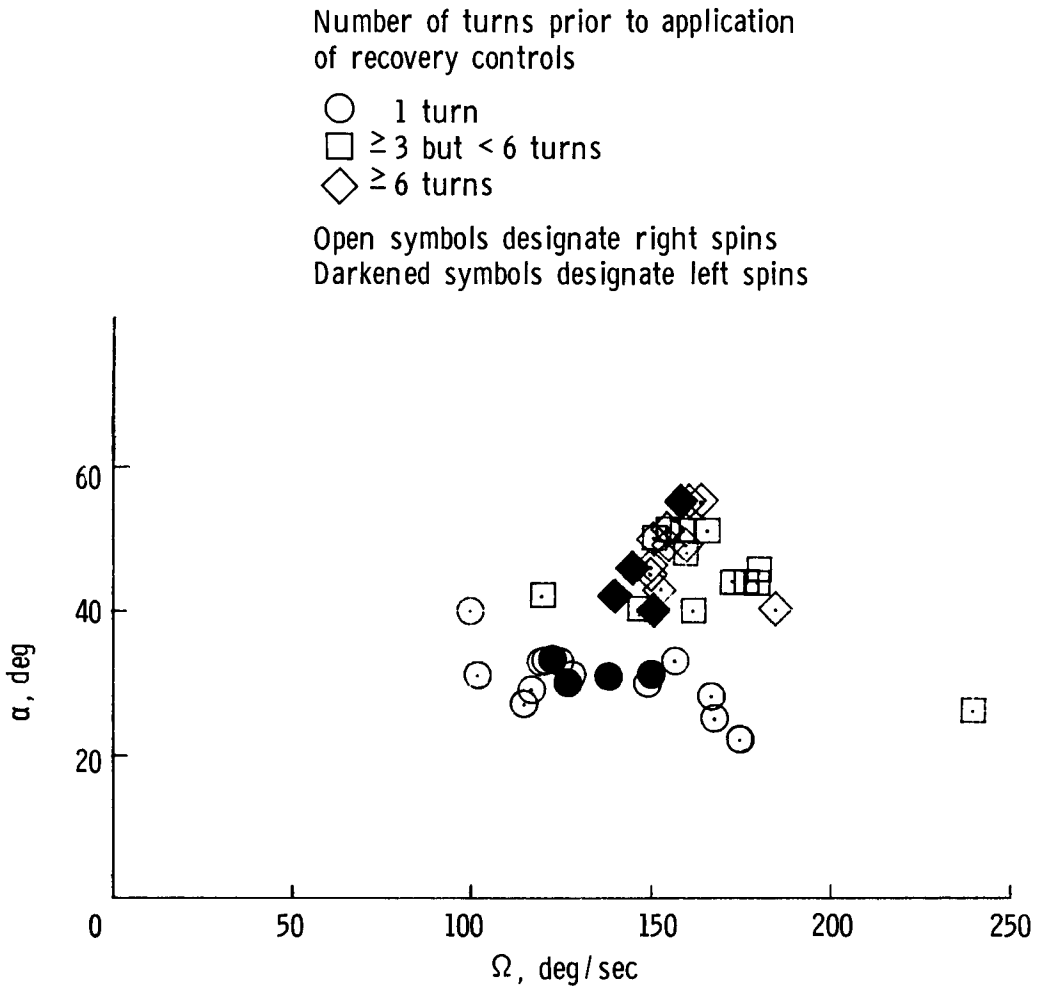

(a) Tail 2.

Figure 16.- Spin angle of attack and turn rate at time of application of recovery controls. Data include aileron deflections of neutral, with spin, and against spin. IYMP = -50×10^{-4}; c.g. at $0.26\bar{c}$.

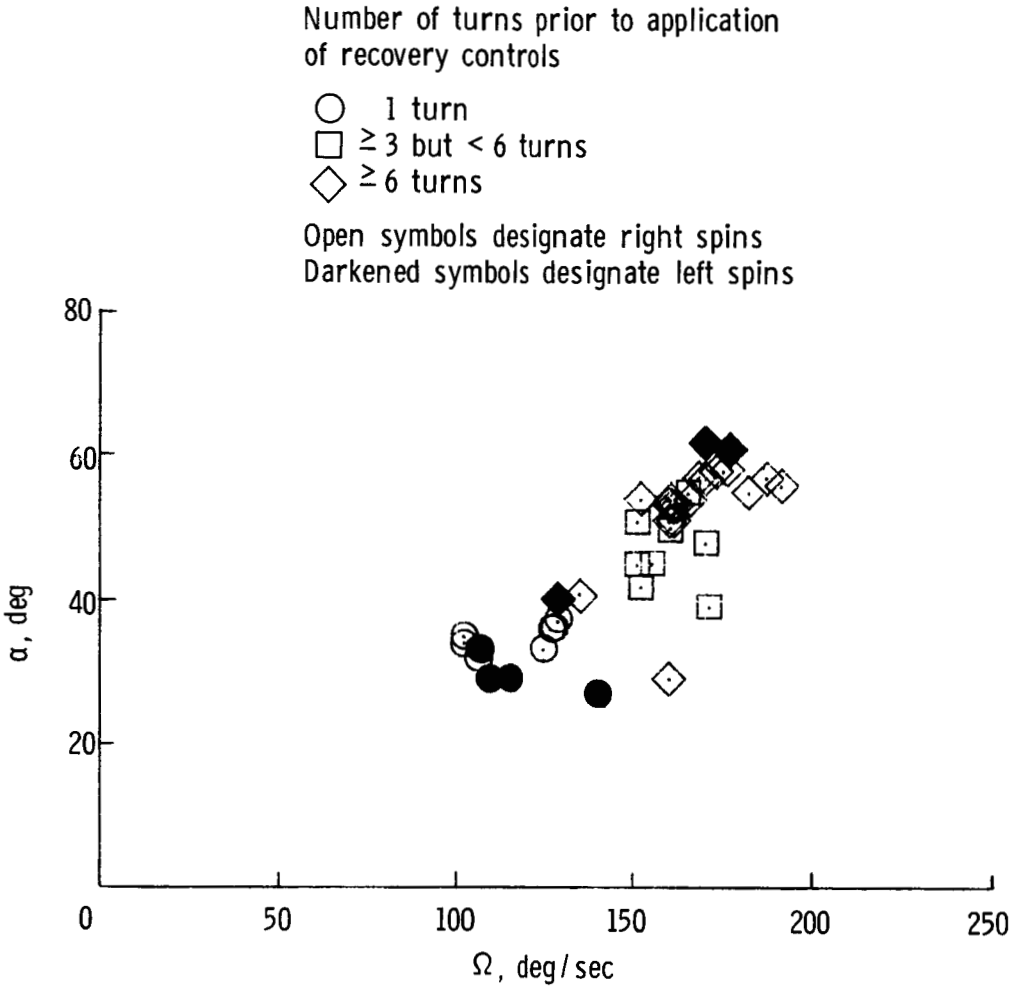

(b) Tail 3.

Figure 16.- Continued.

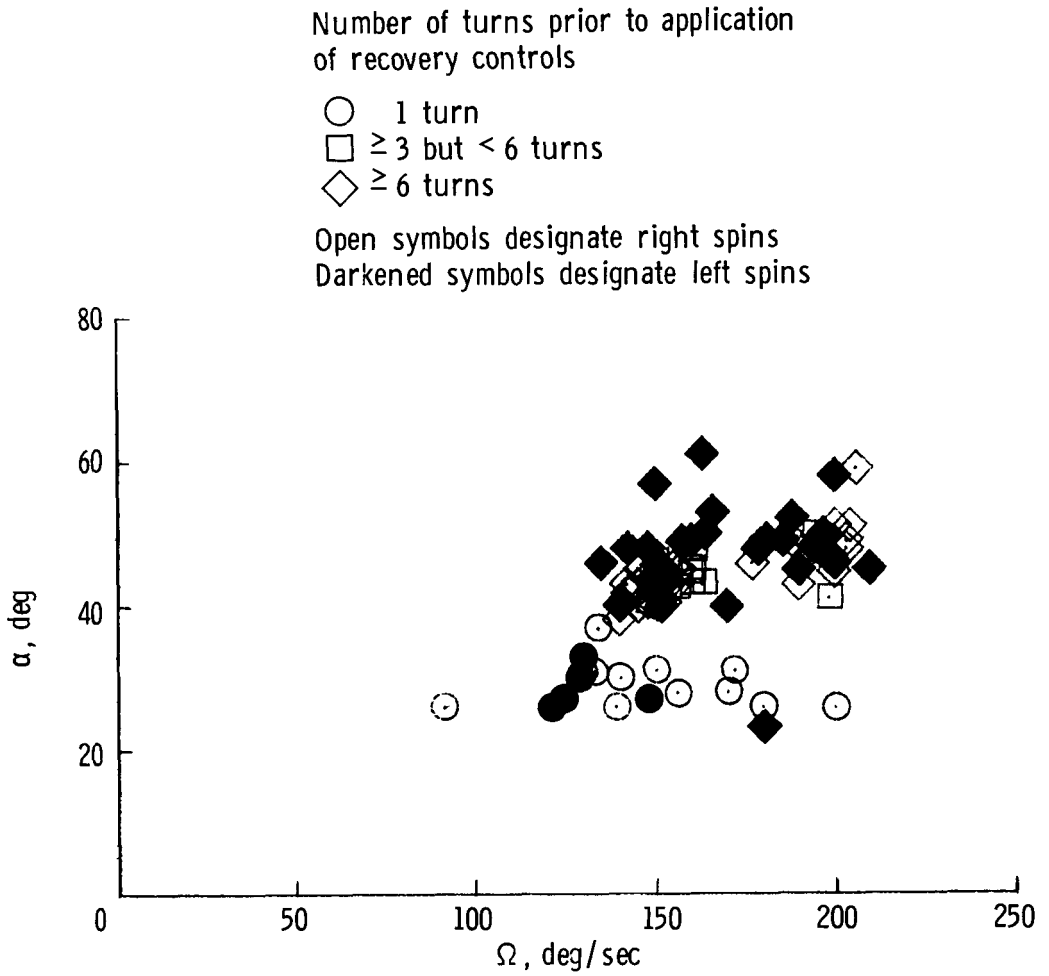

(c) Tail 4.

Figure 16.- Continued.

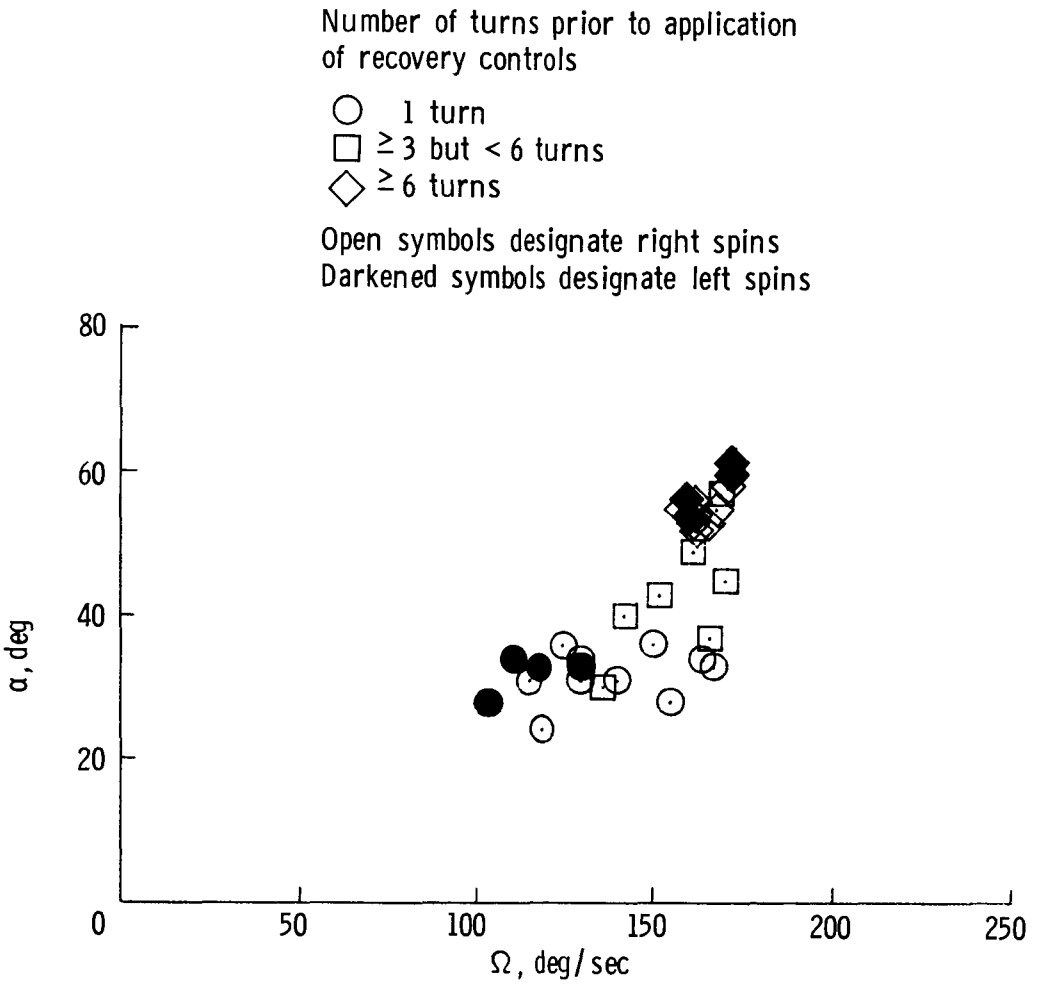

(d) Tail 6.

Figure 16.- Concluded.

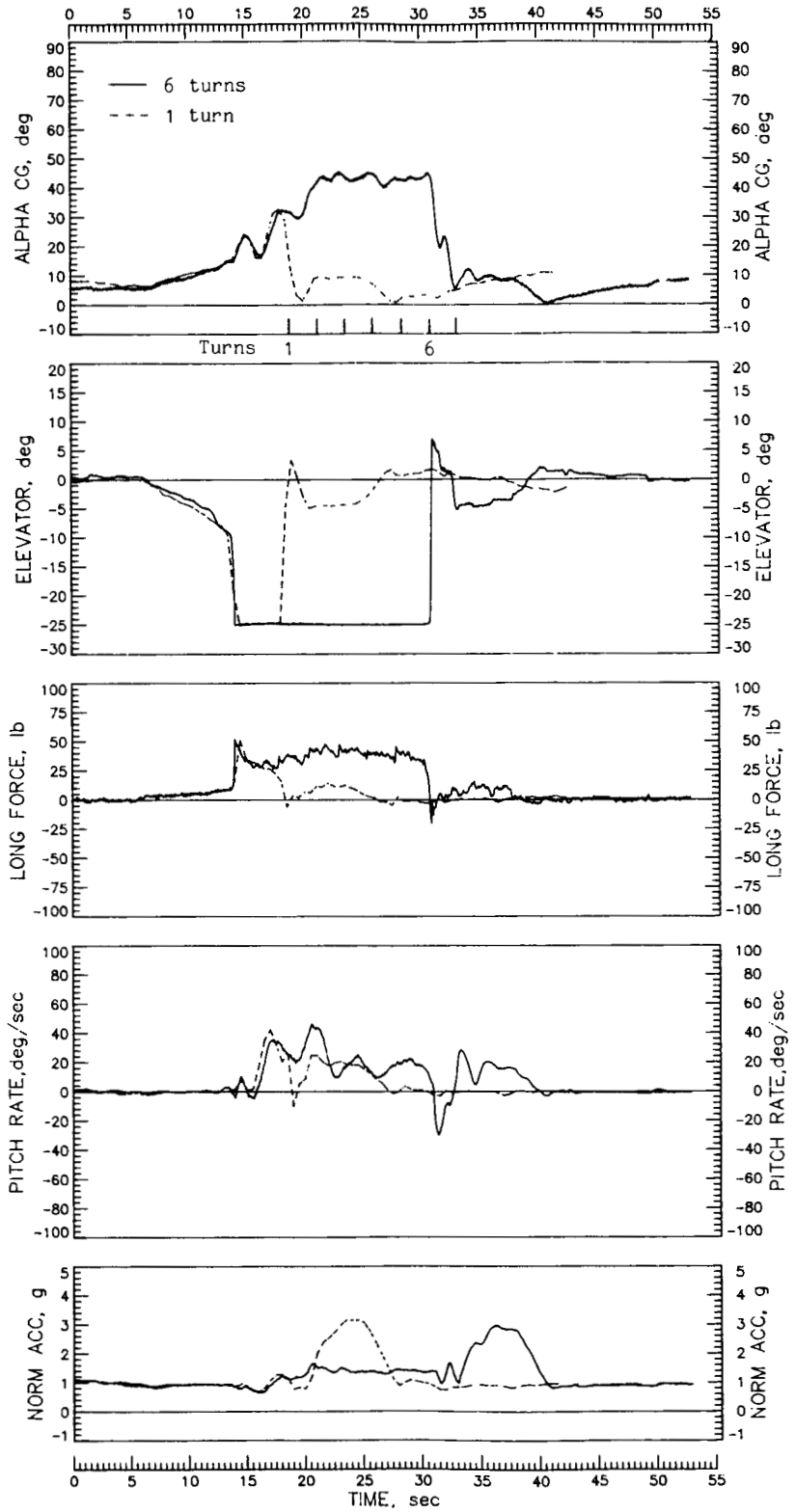

Figure 17.- Right spins of 1 and 6 turns with tail 4 at idle power with ailerons neutral. Normal recovery controls; IYMP = -53×10^{-4}; c.g. at $0.26\bar{c}$.

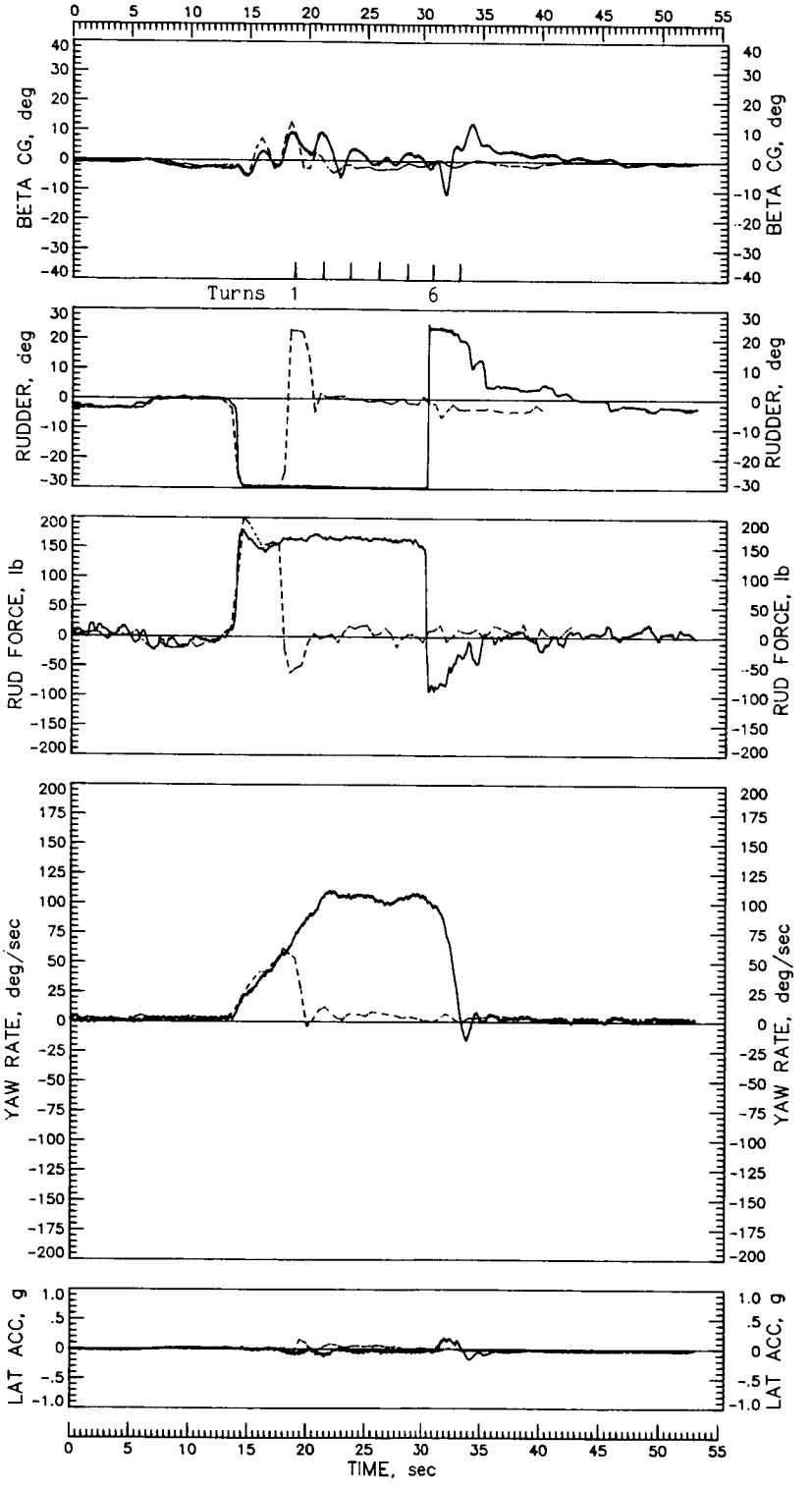

Figure 17.- Continued.

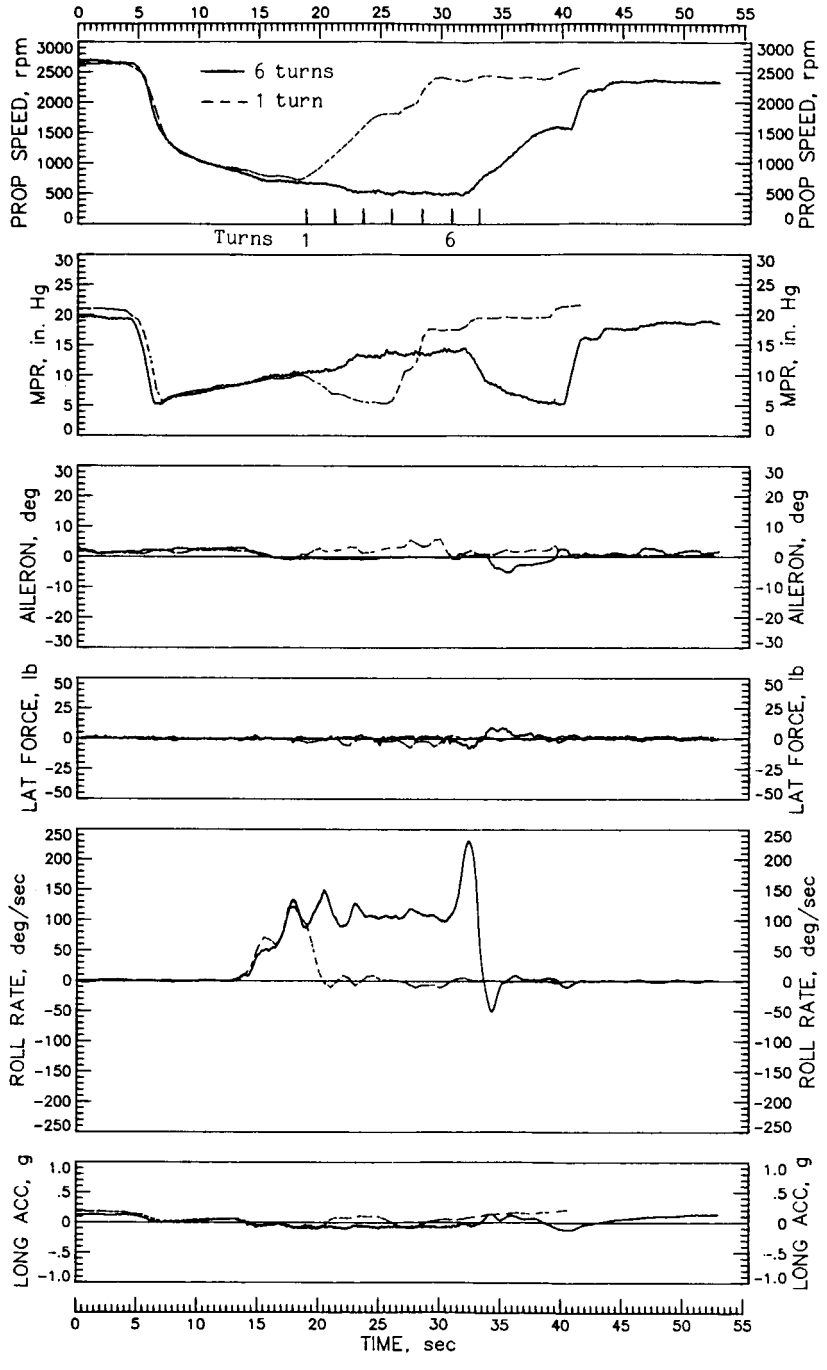

Figure 17.- Continued.

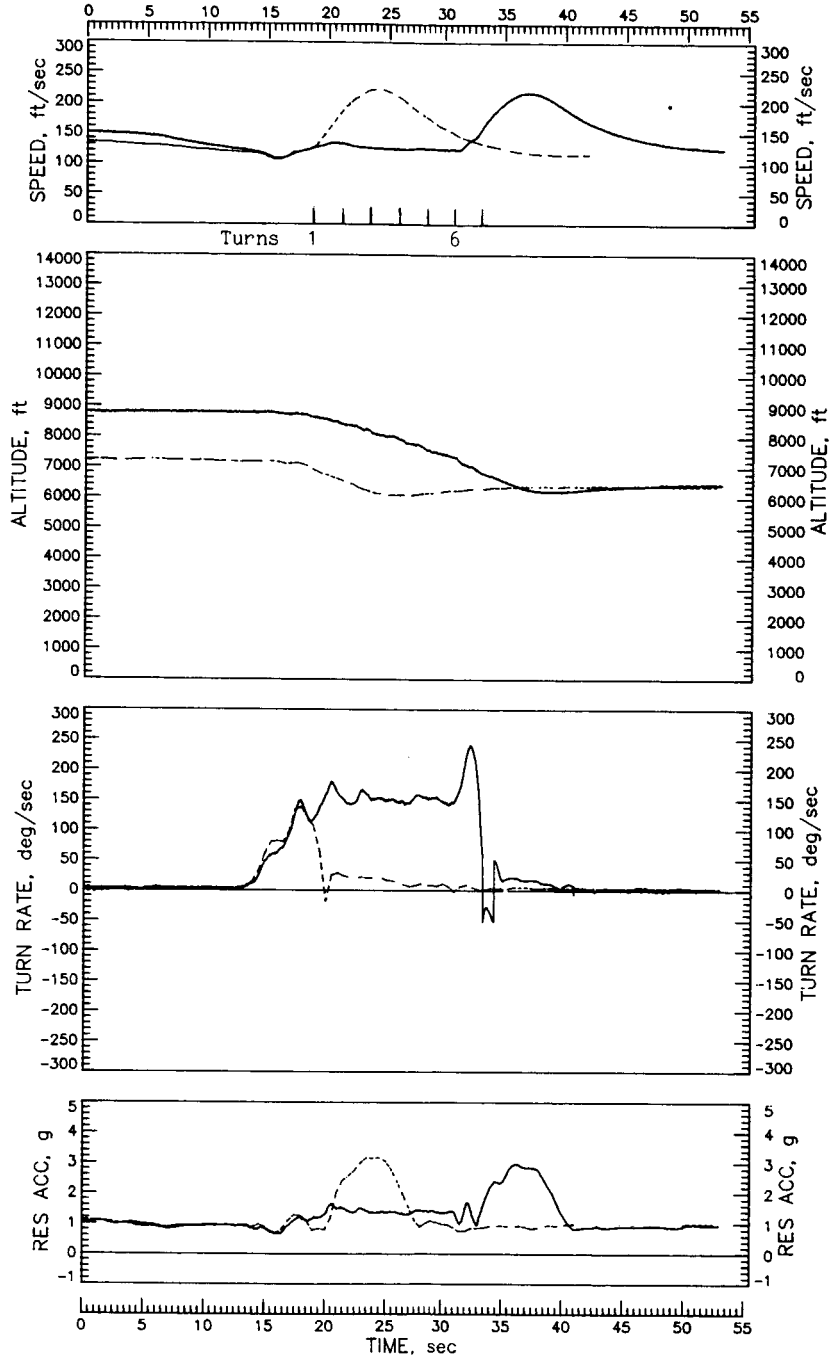

Figure 17.- Concluded.

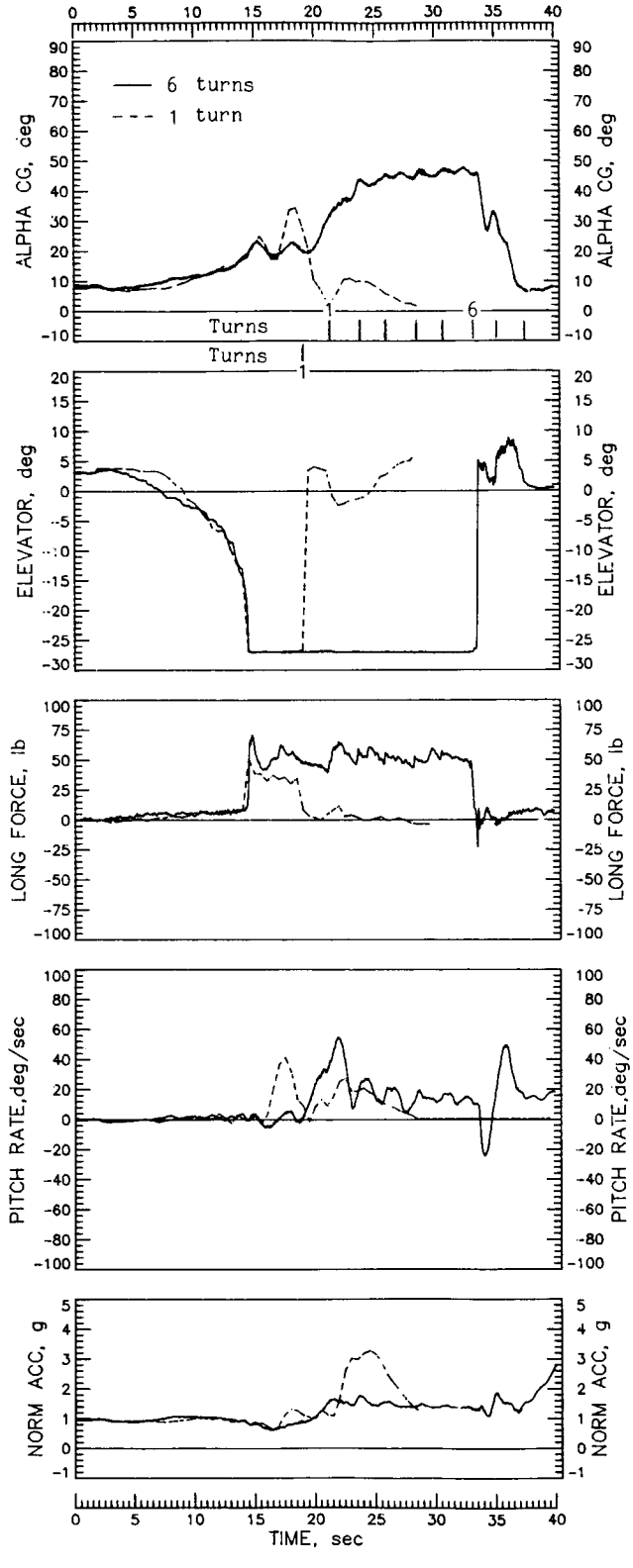

Figure 18.- Right spins of 1 and 6 turns with tail 2 at idle power with ailerons neutral. Normal recovery controls; IYMP = -50×10^{-4}; c.g. at $0.26\bar{c}$.

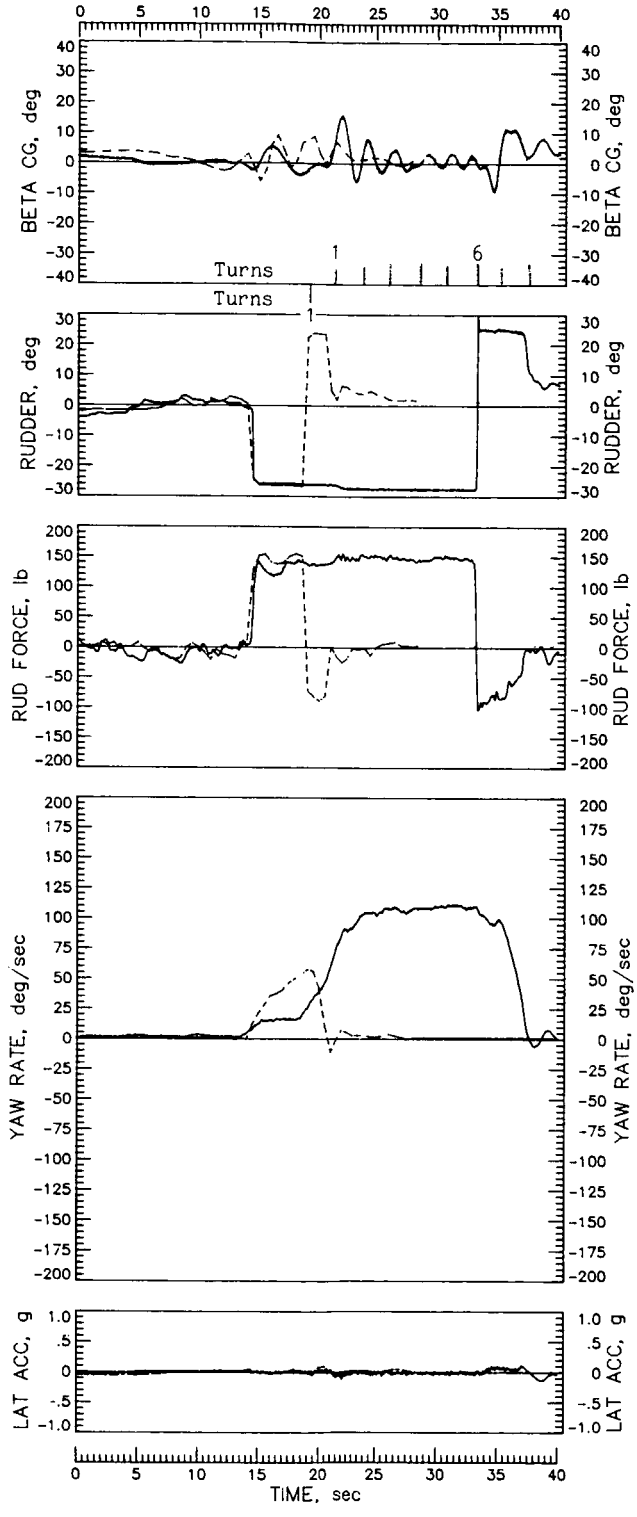

Figure 18.- Continued.

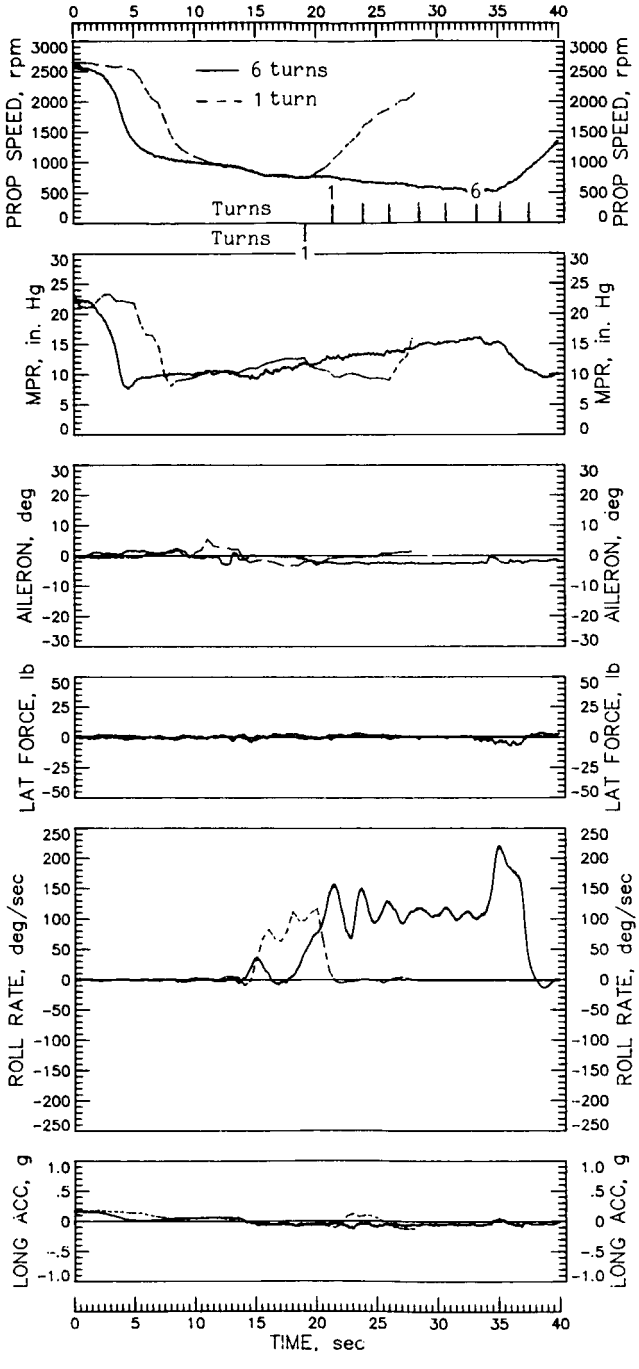

Figure 18.- Continued.

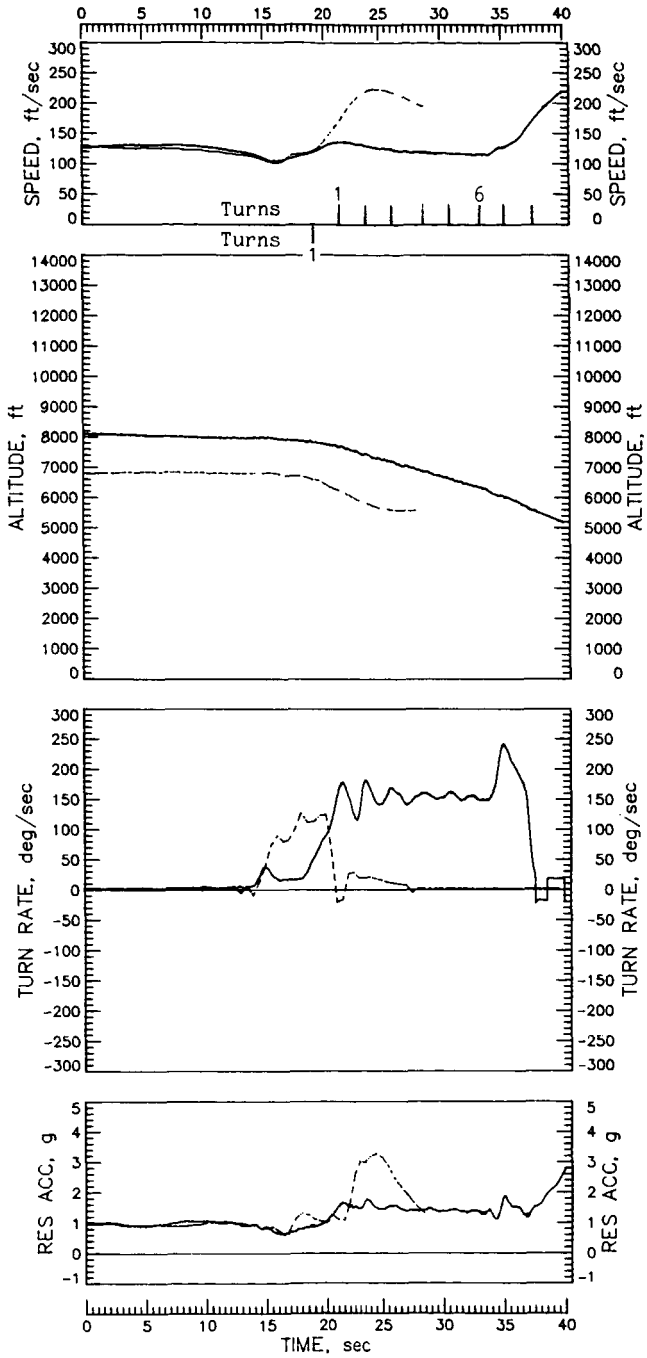

Figure 18.- Concluded.

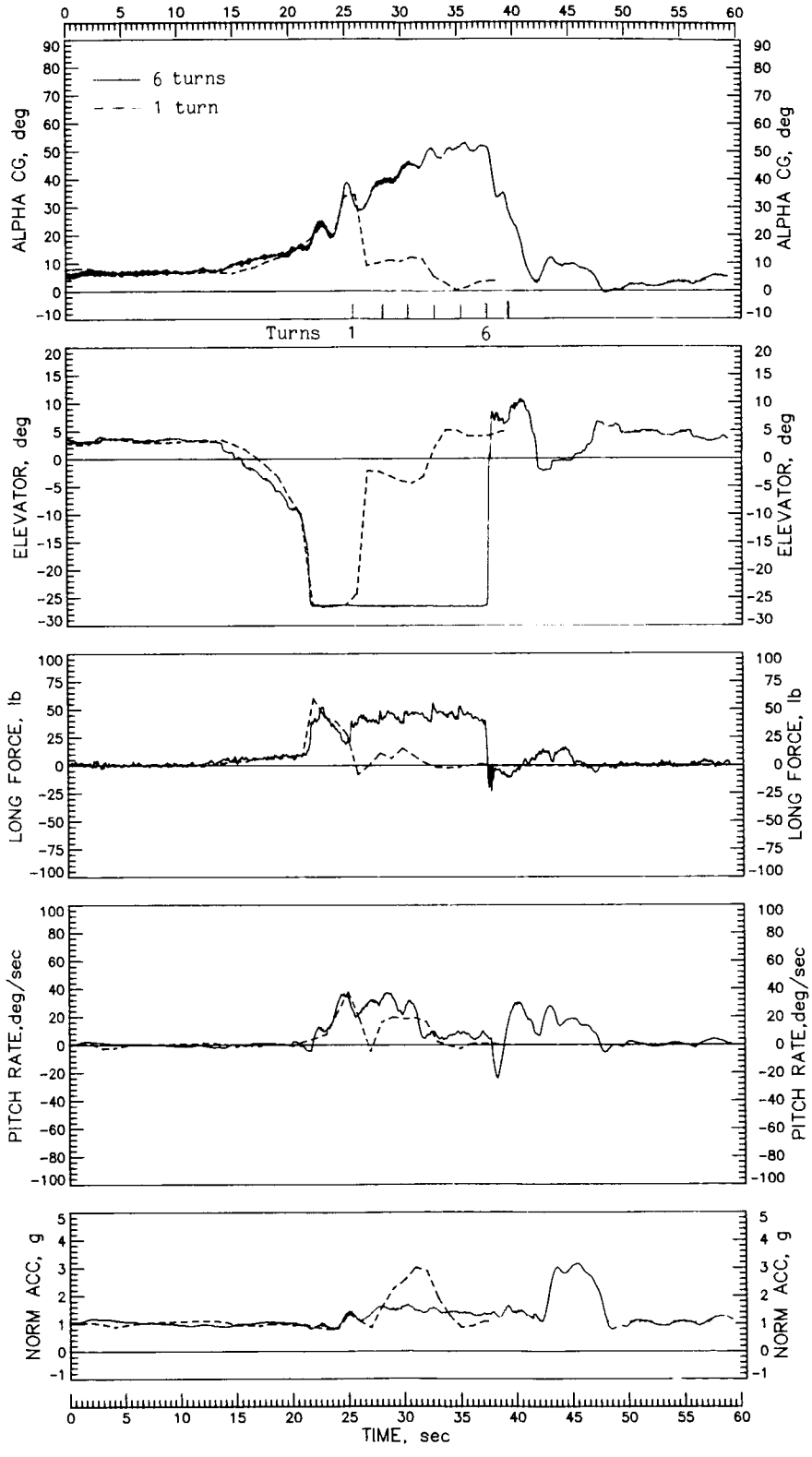

Figure 19.- Right spins of 1 and 6 turns with tail 3 at idle power with ailerons neutral. Normal recovery controls; IYMP = -50×10^{-4}; c.g. at $0.26\bar{c}$.

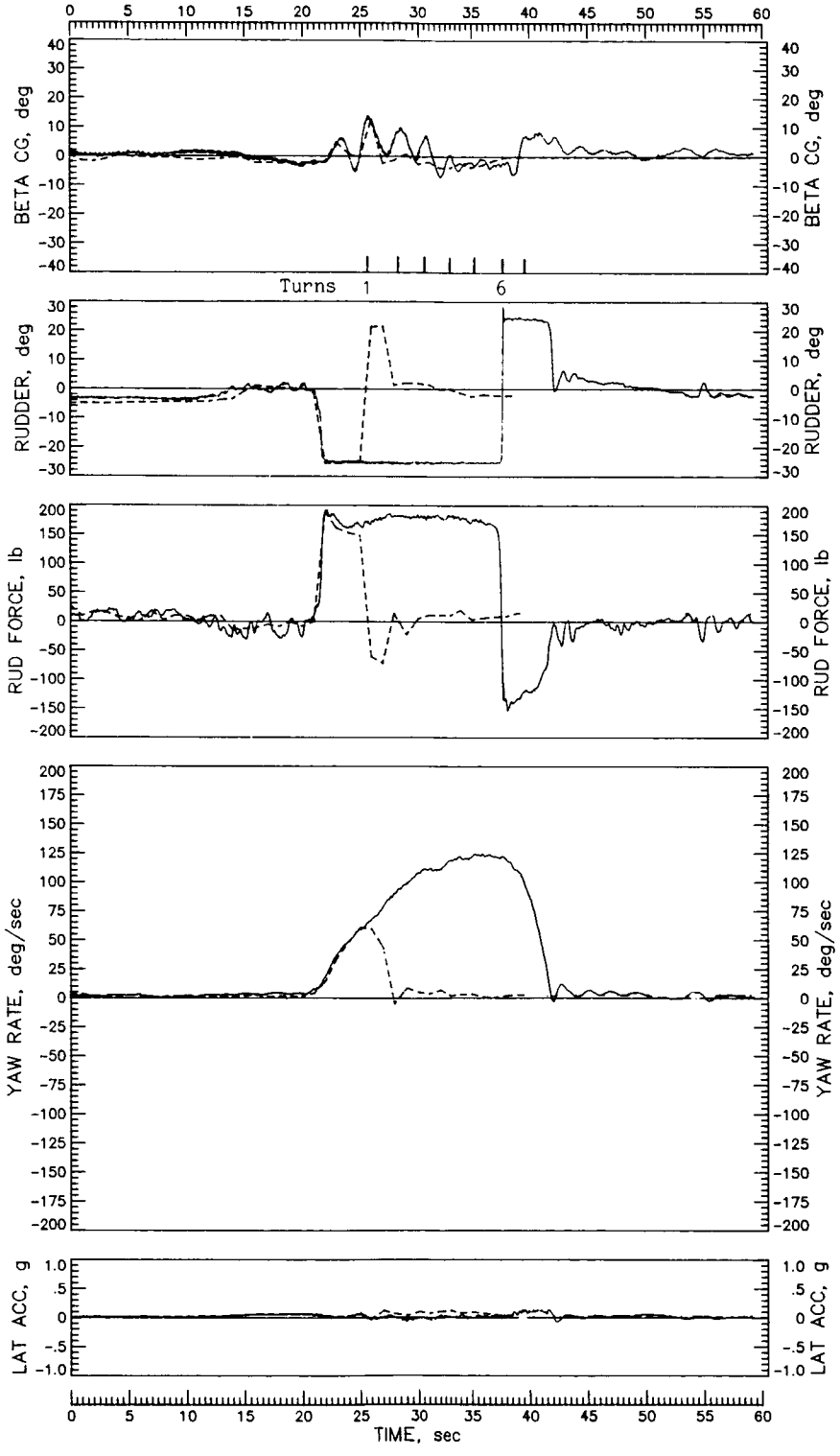

Figure 19.- Continued.

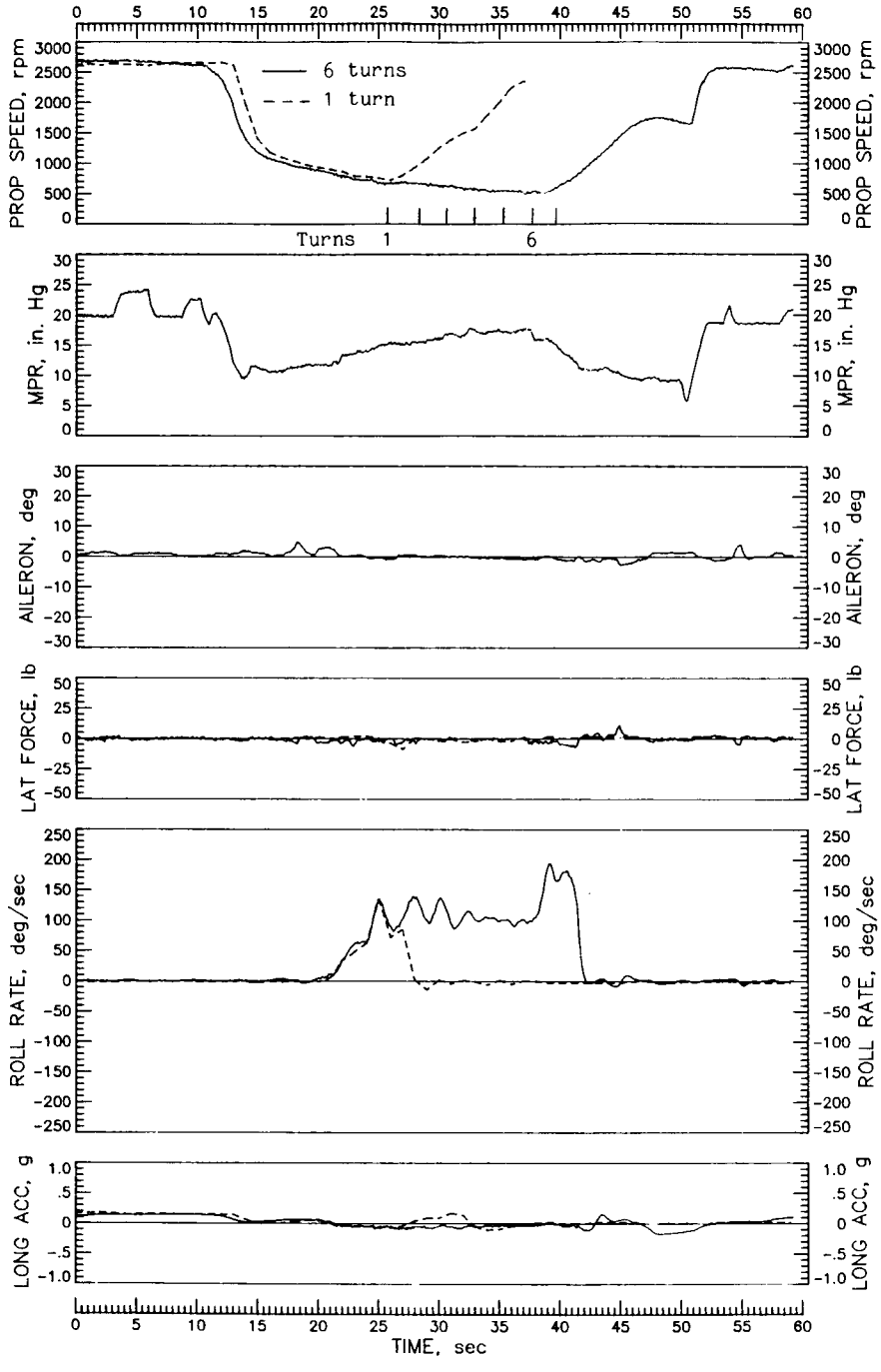

Figure 19.- Continued.

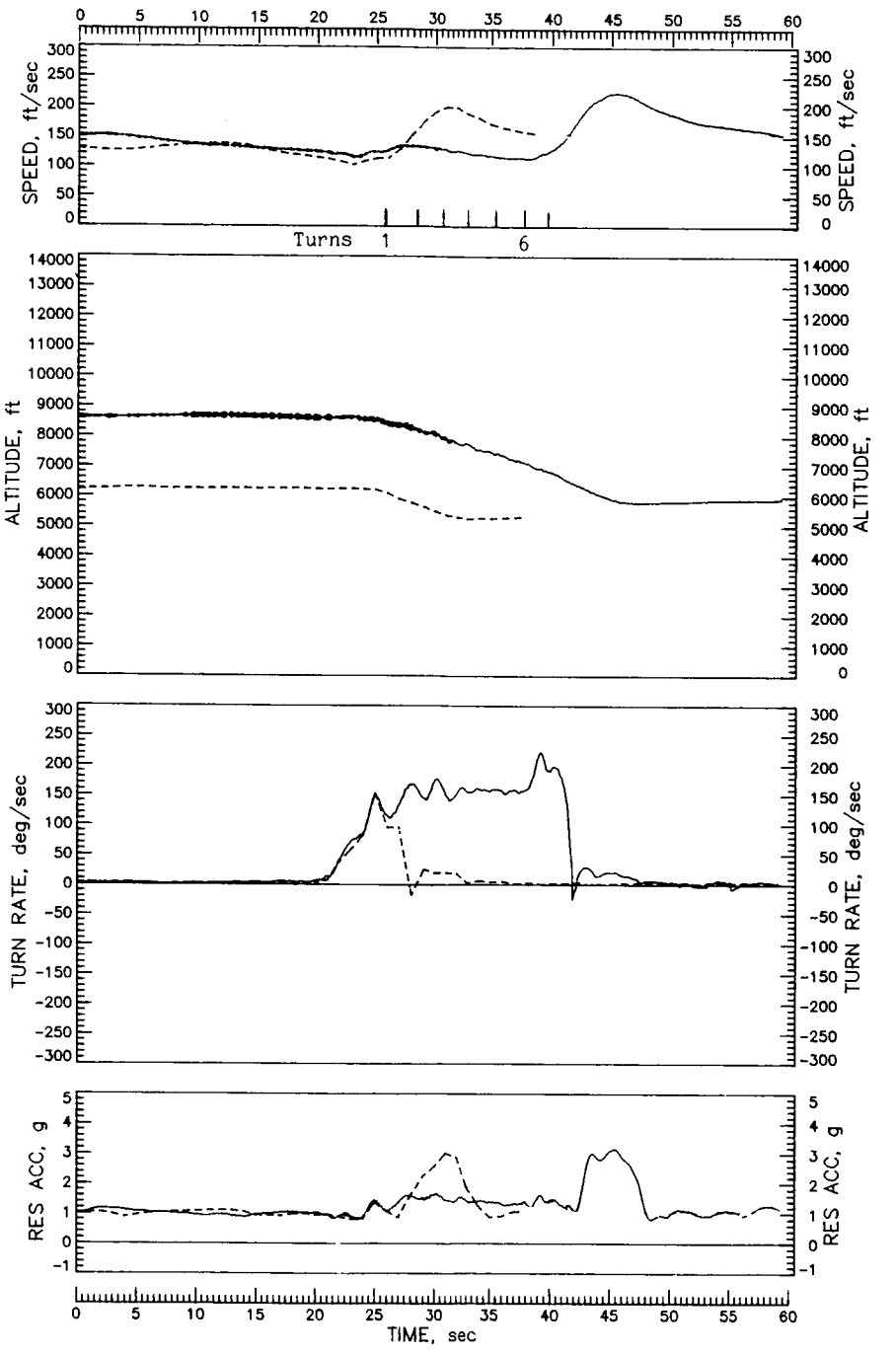

Figure 19.- Concluded.

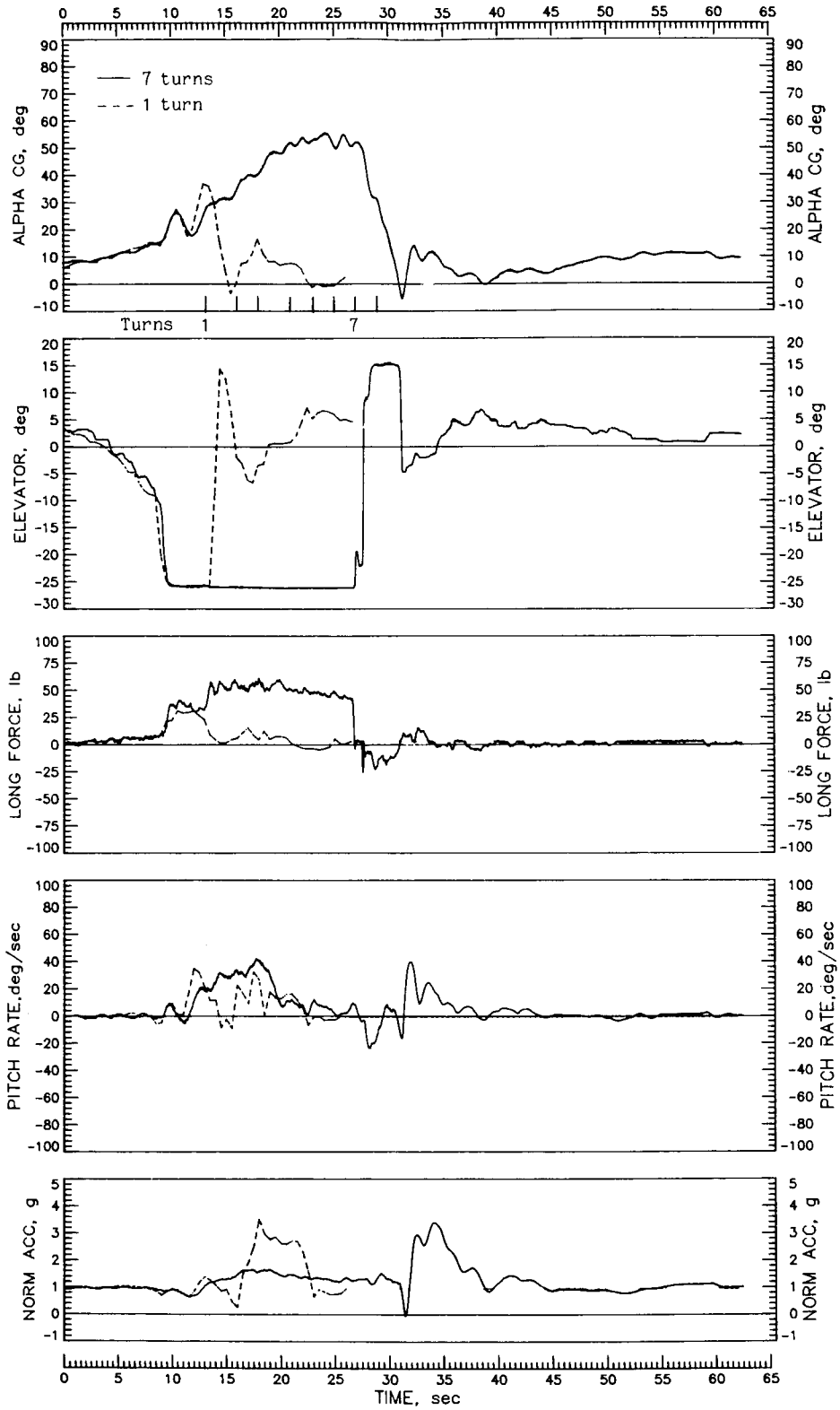

Figure 20.- Right spins of 1 and 7 turns with tail 6 at idle power with ailerons neutral. Normal recovery controls; IYMP = -50×10^{-4}; c.g. at $0.26\bar{c}$.

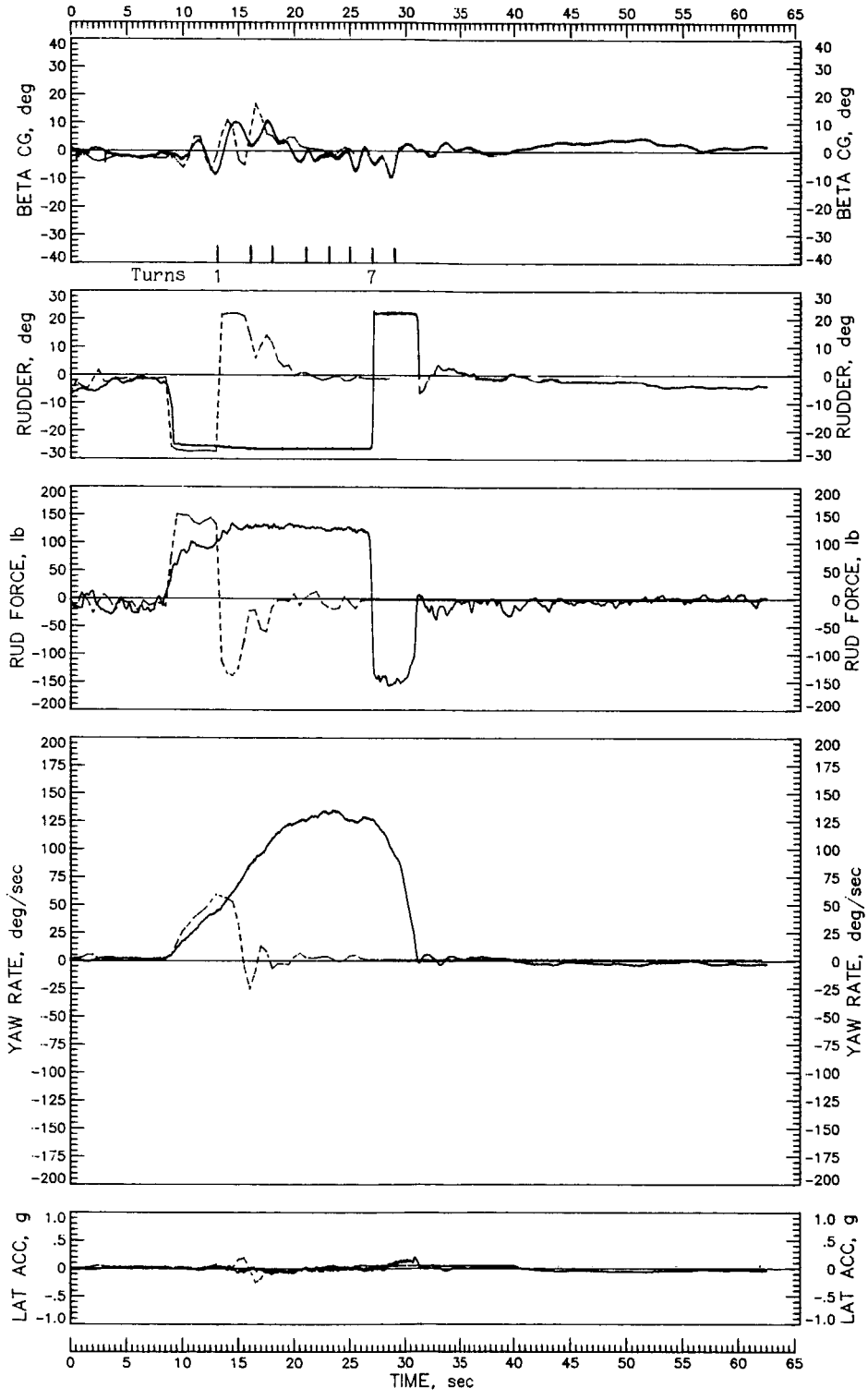

Figure 20.- Continued.

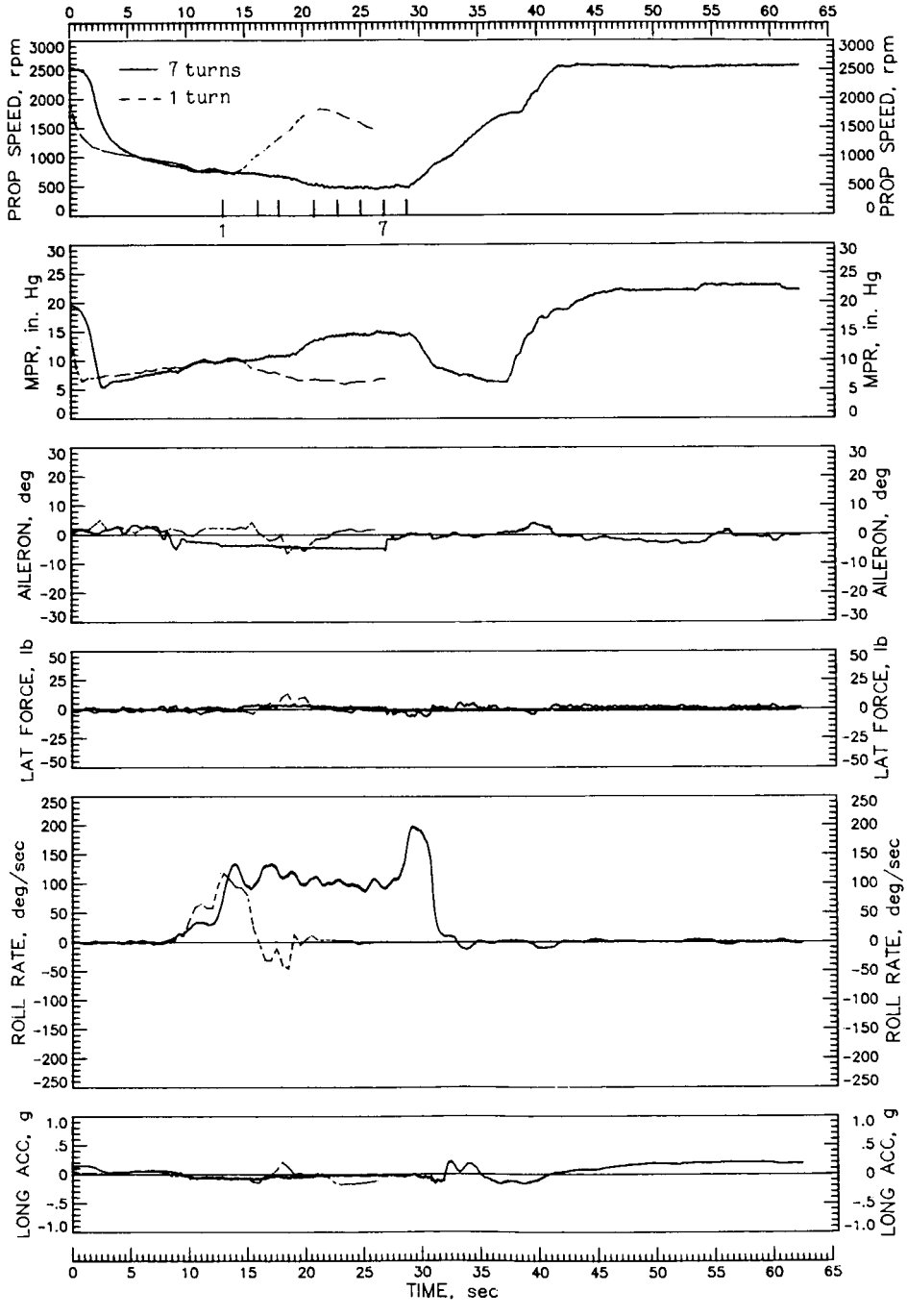

Figure 20.- Continued.

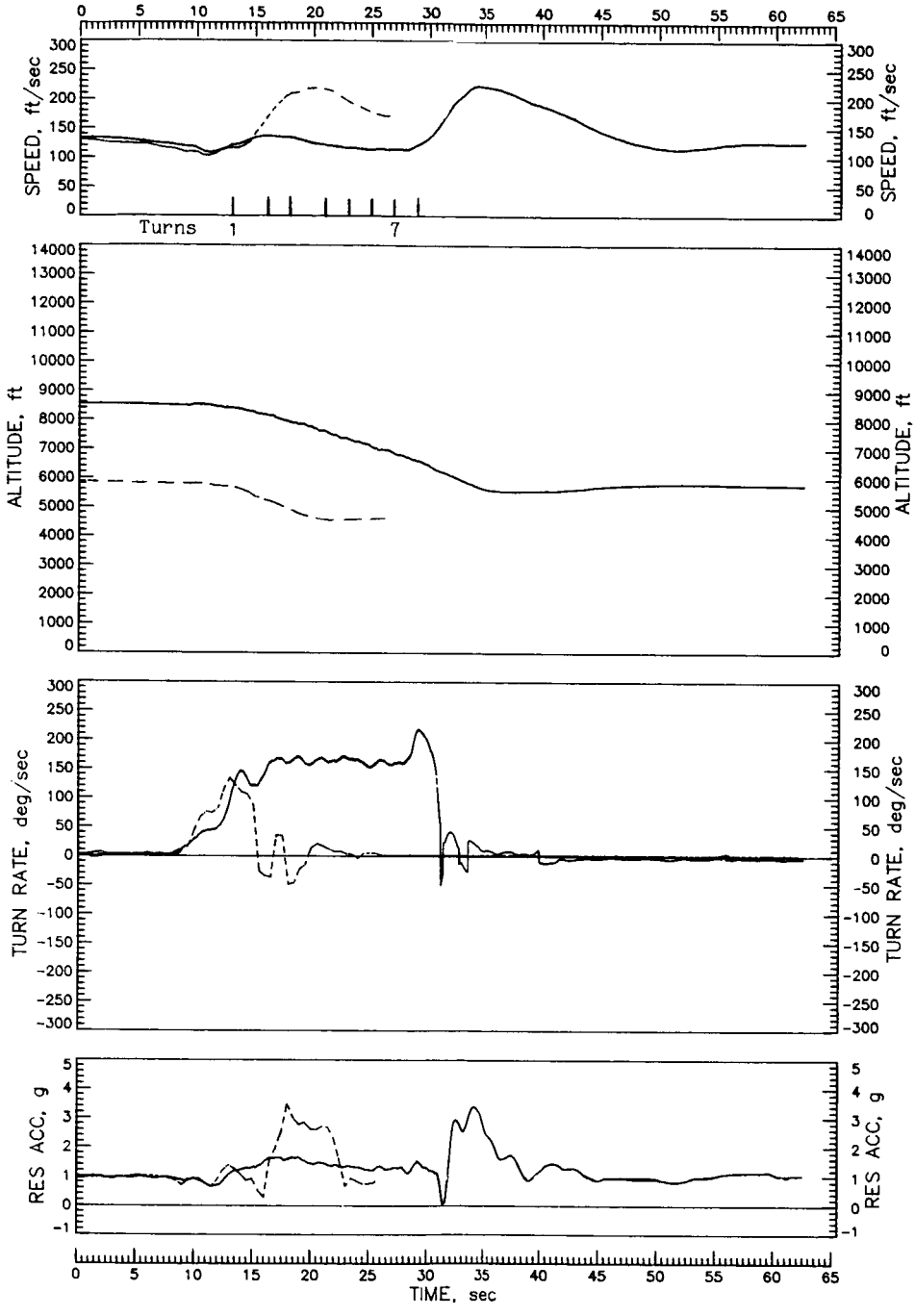

Figure 20.- Concluded.

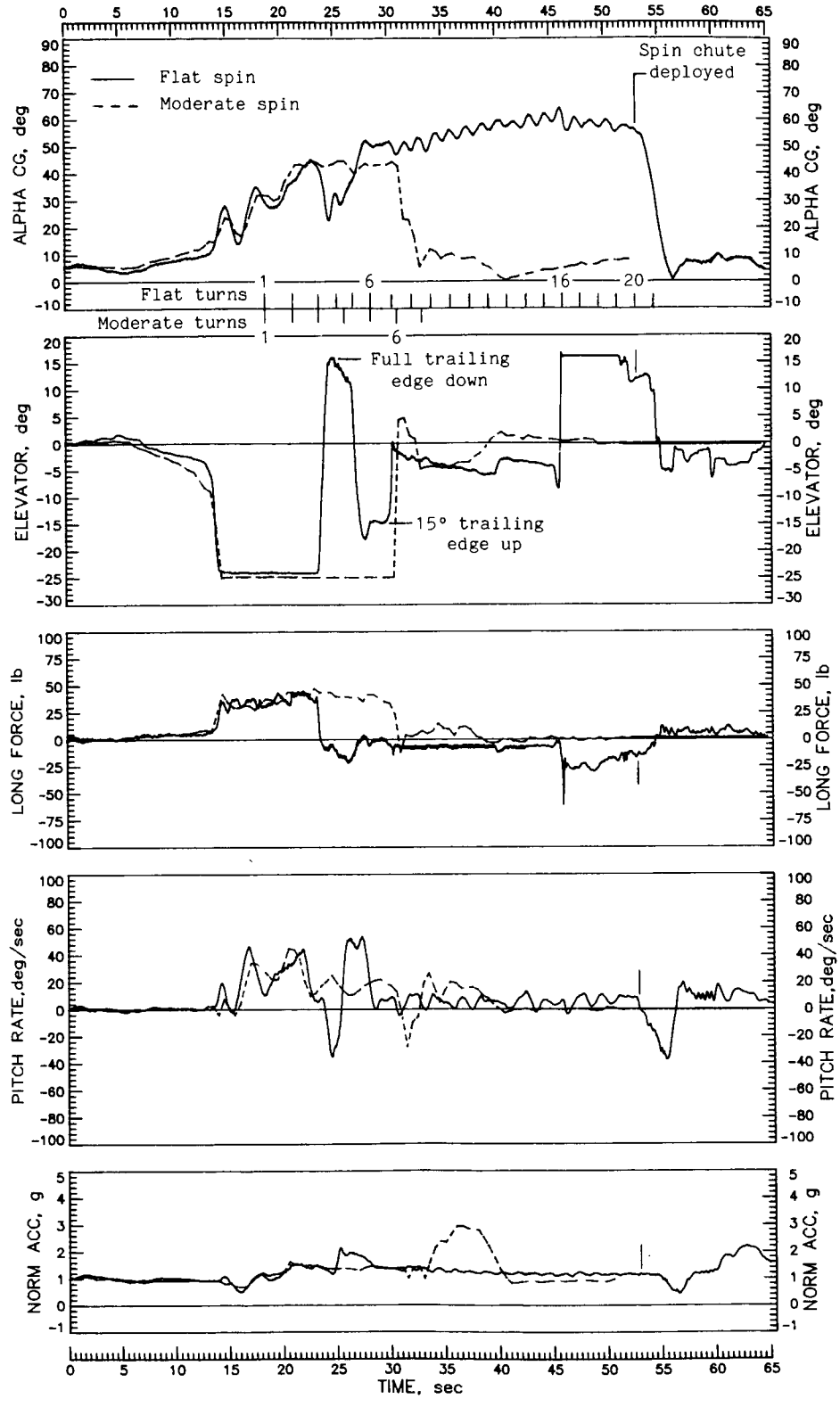

Figure 21.- Moderate and flat spins of baseline configuration at idle power with ailerons neutral. IYMP = -53×10^{-4}; c.g. at $0.26\bar{c}$.

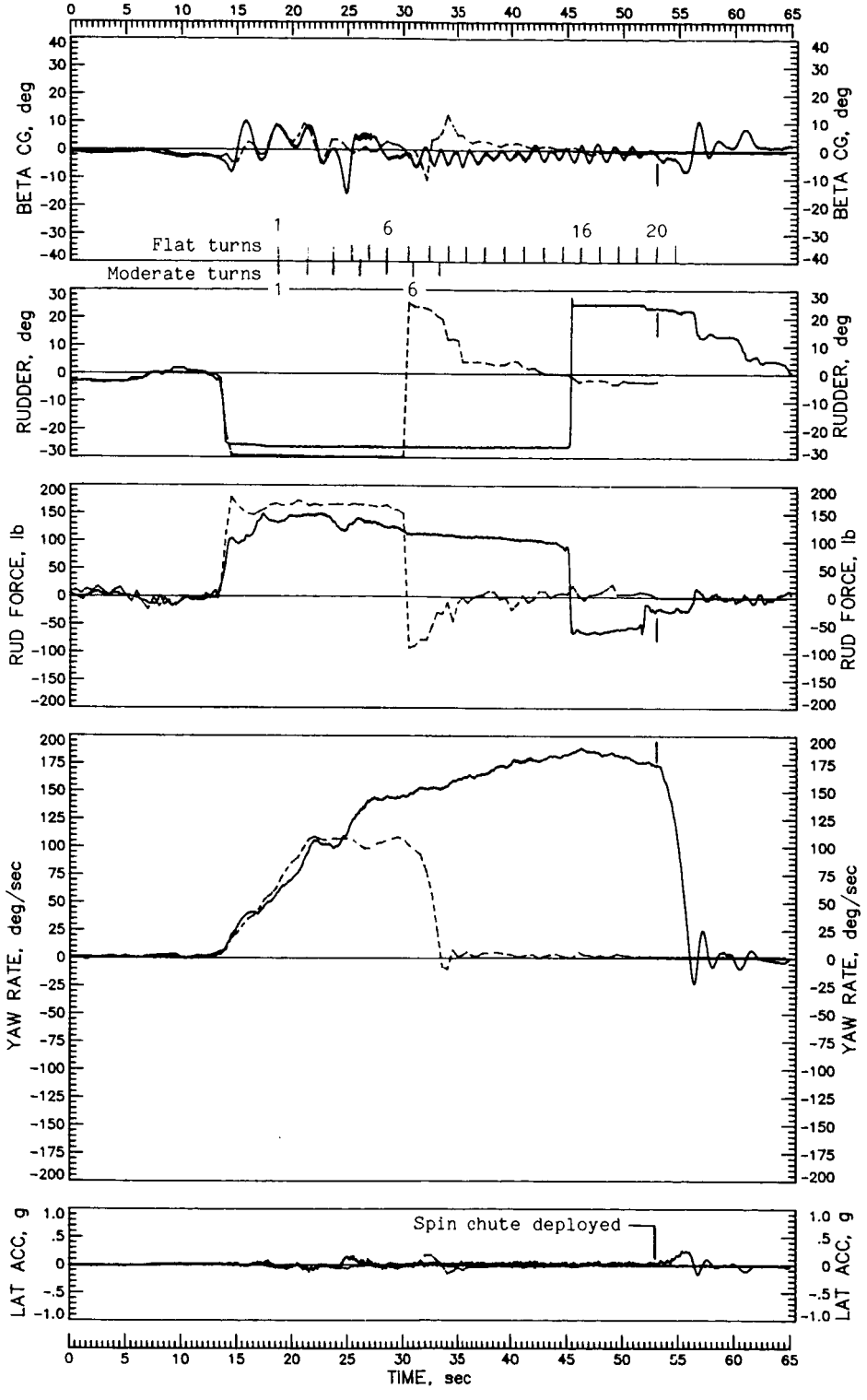

Figure 21.- Continued.

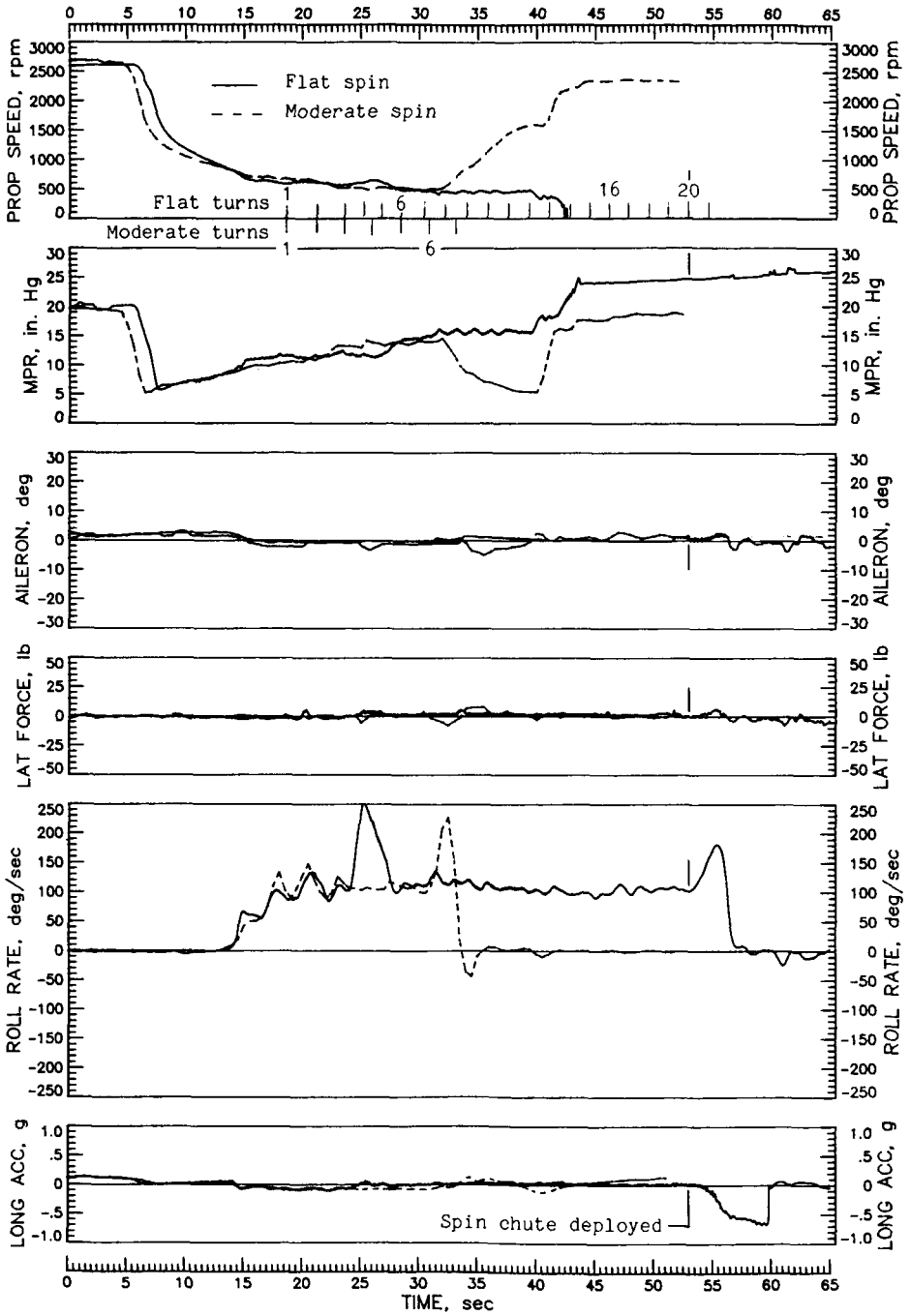

Figure 21.- Continued.

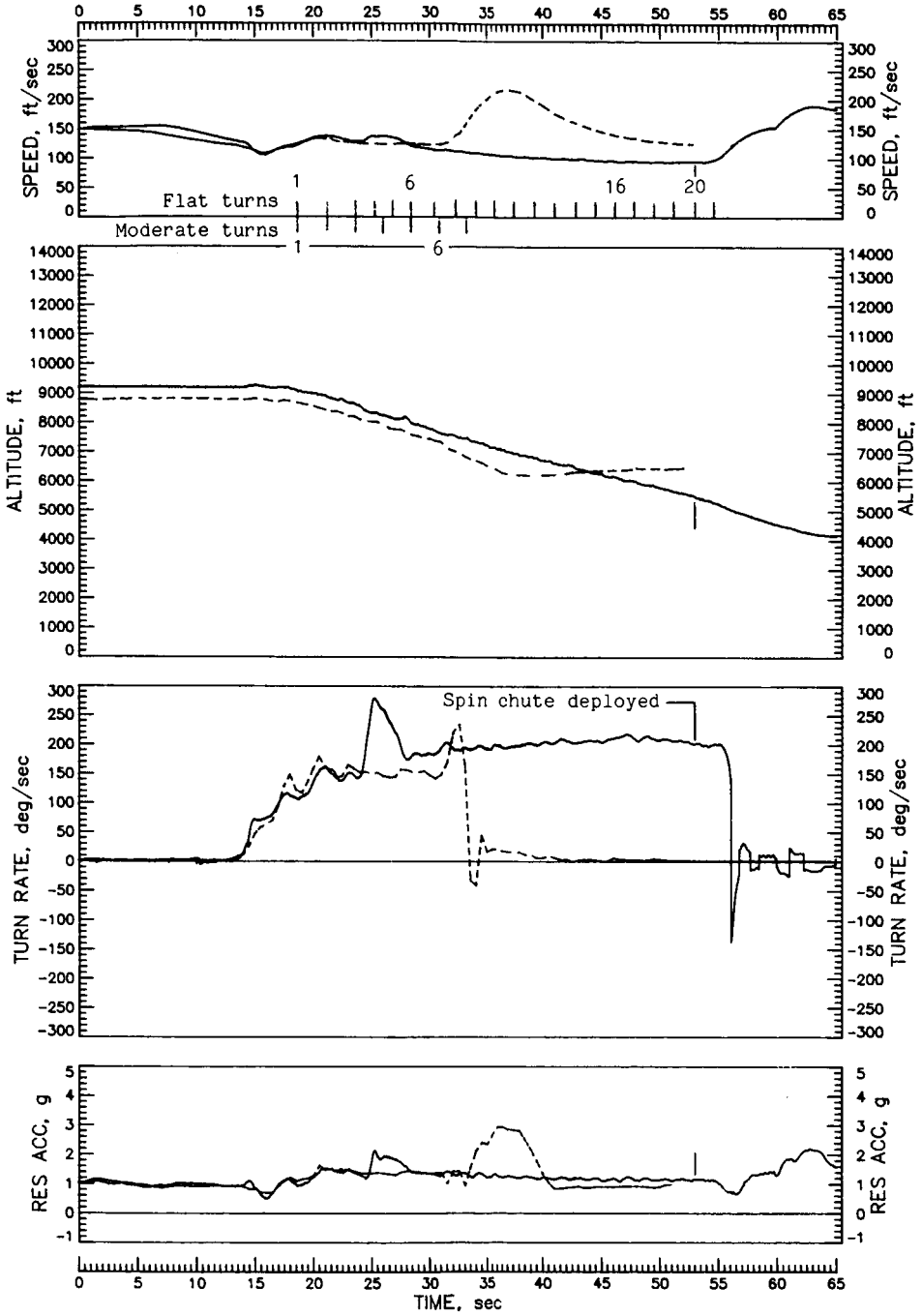

Figure 21.- Concluded.

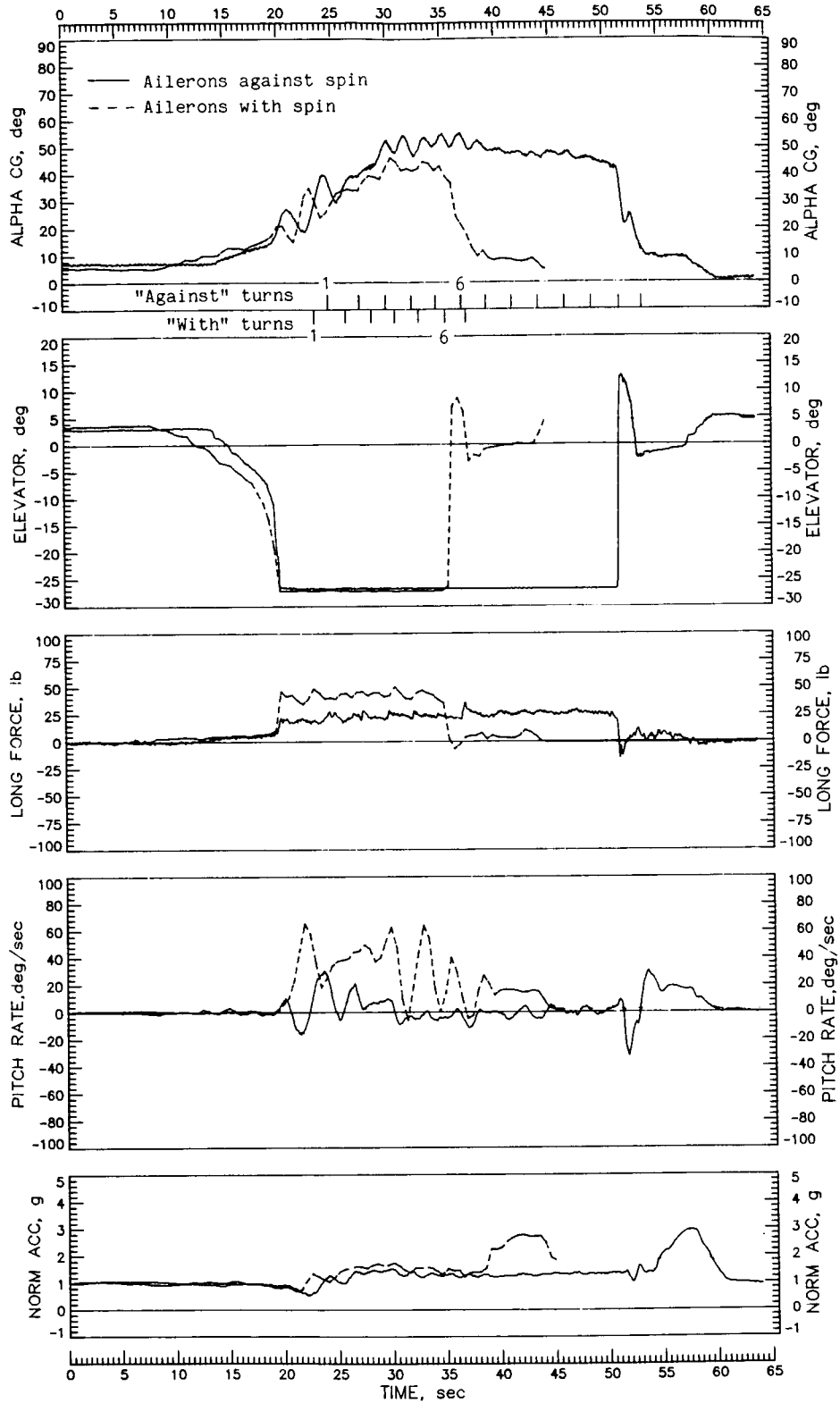

Figure 22.- Idle-power right spins with tail 2 for ailerons deflected against spin and with spin. IYMP = -50×10^{-4}; c.g. at $0.26\bar{c}$.

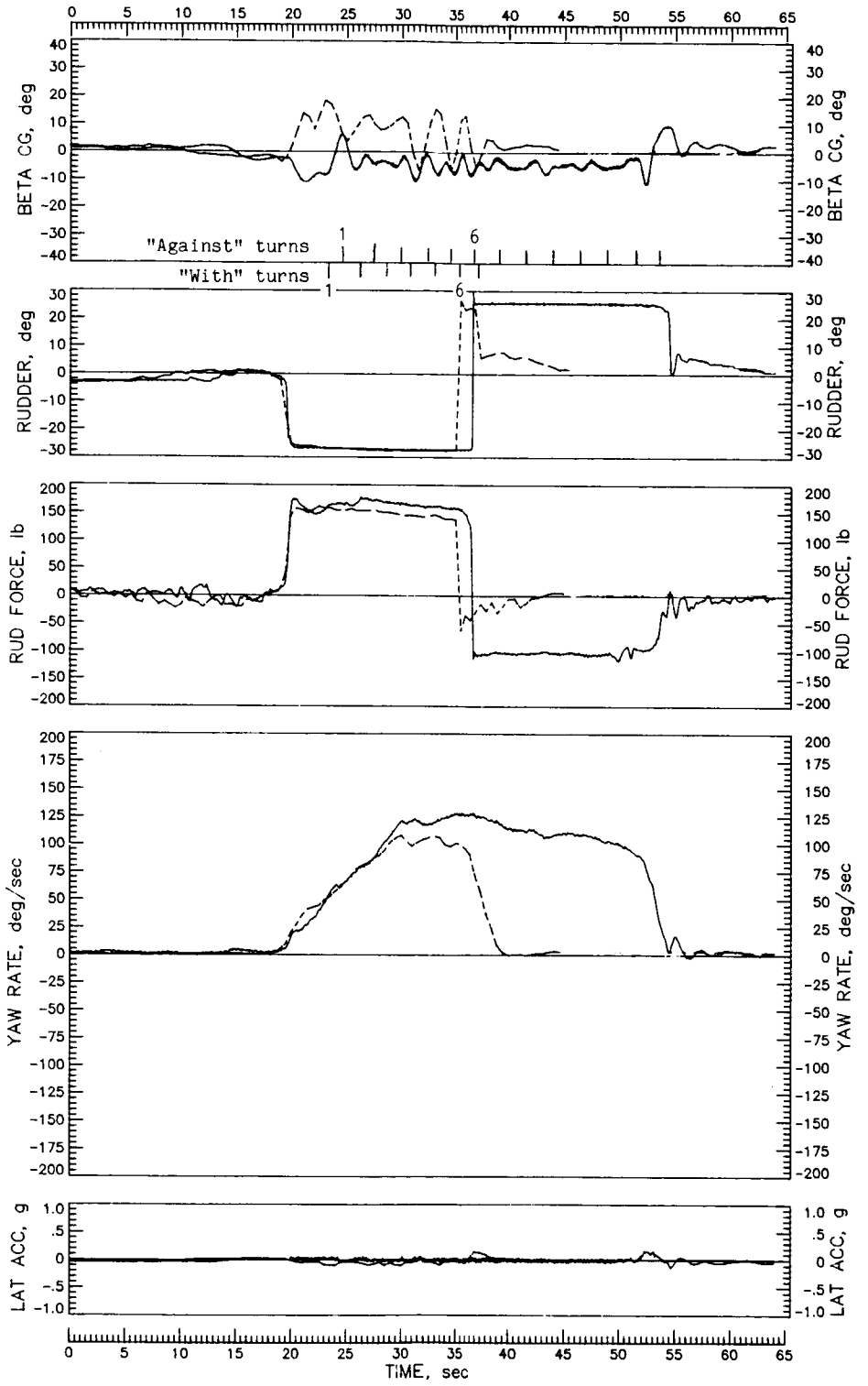

Figure 22.- Continued.

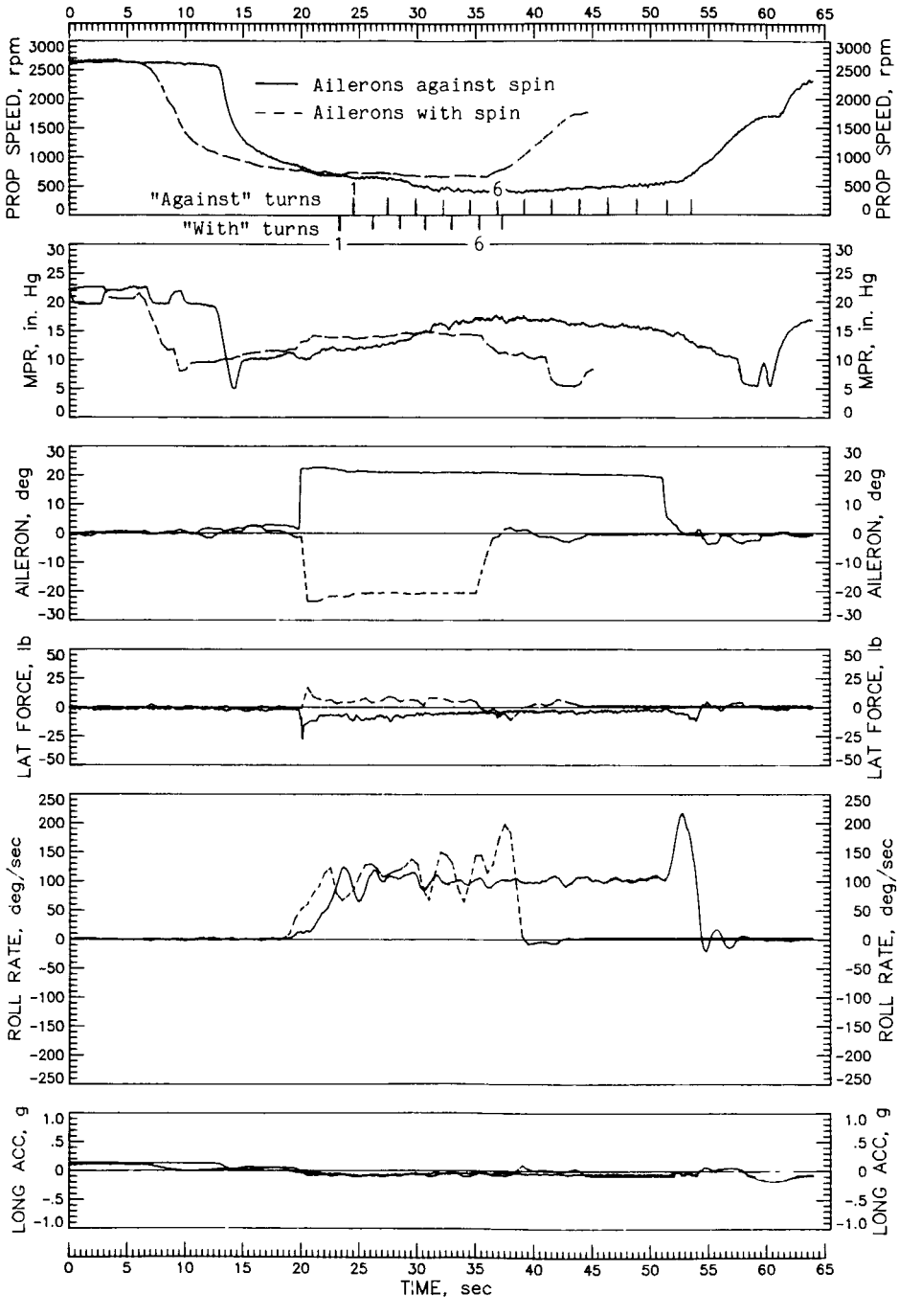

Figure 22.- Continued.

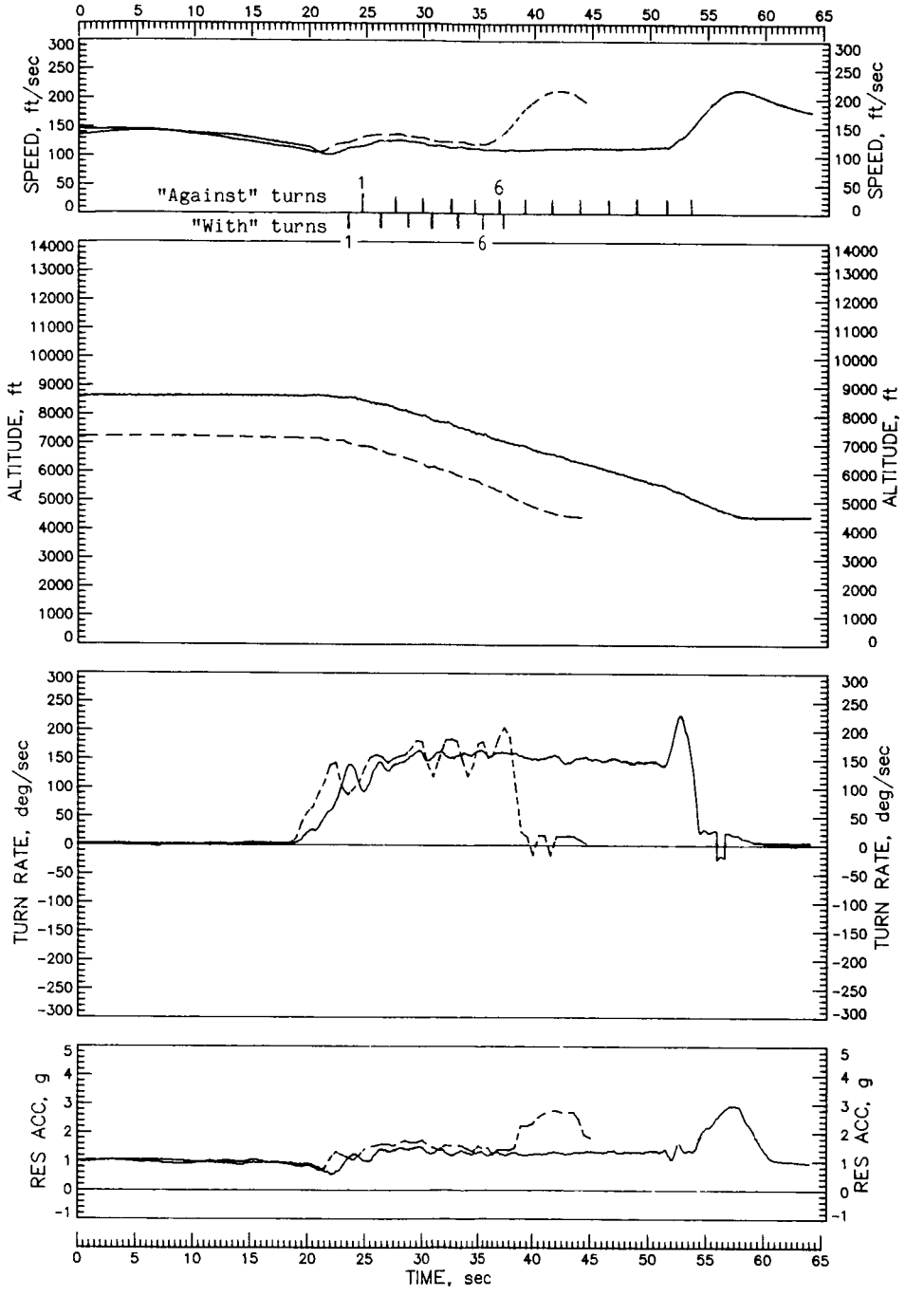

Figure 22.- Concluded.

C-2

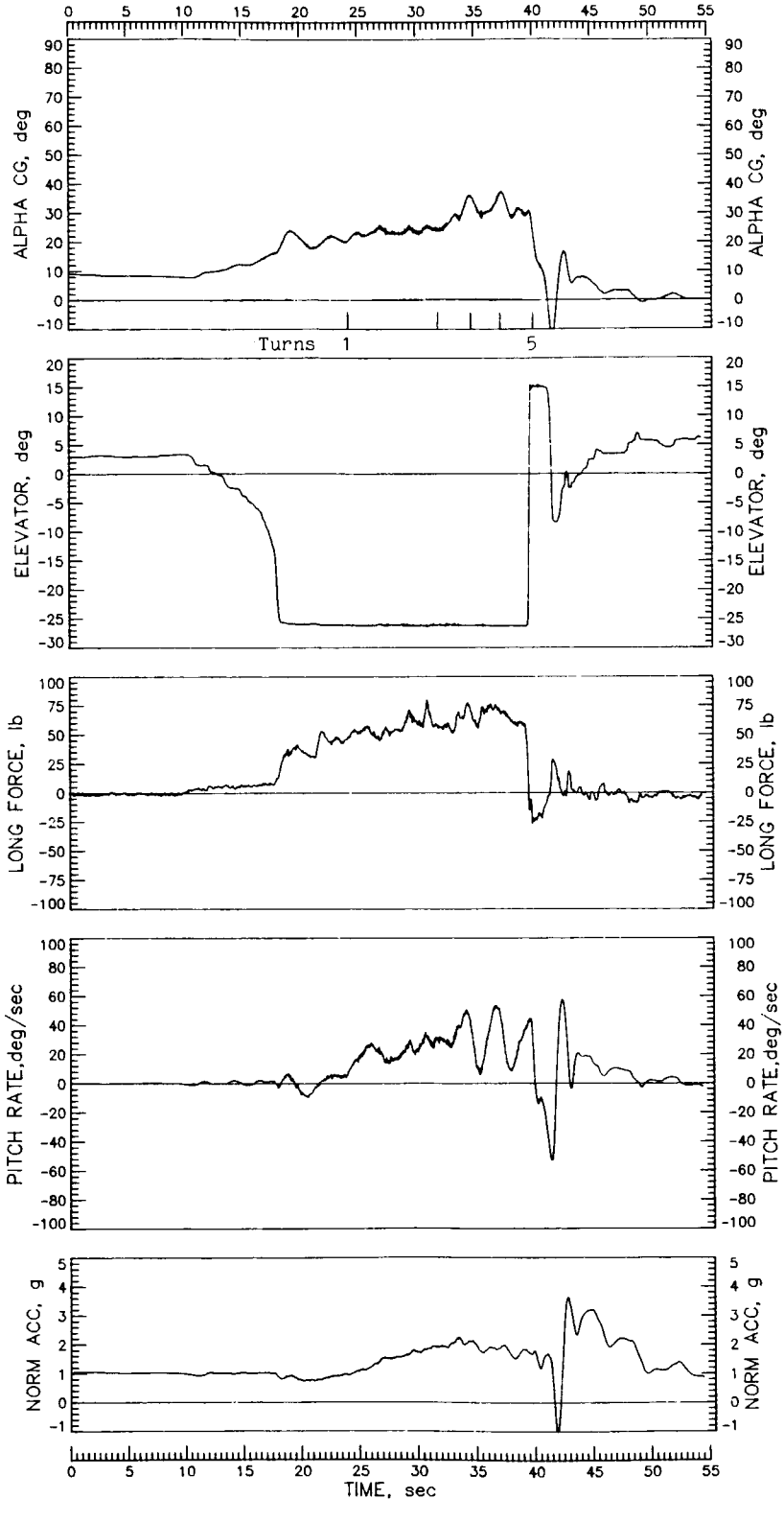

Figure 23.- Idle-power left spin with tail 6, entered with both rudder and ailerons neutralized. IYMP = -50×10^{-4}; c.g. at $0.26\bar{c}$.

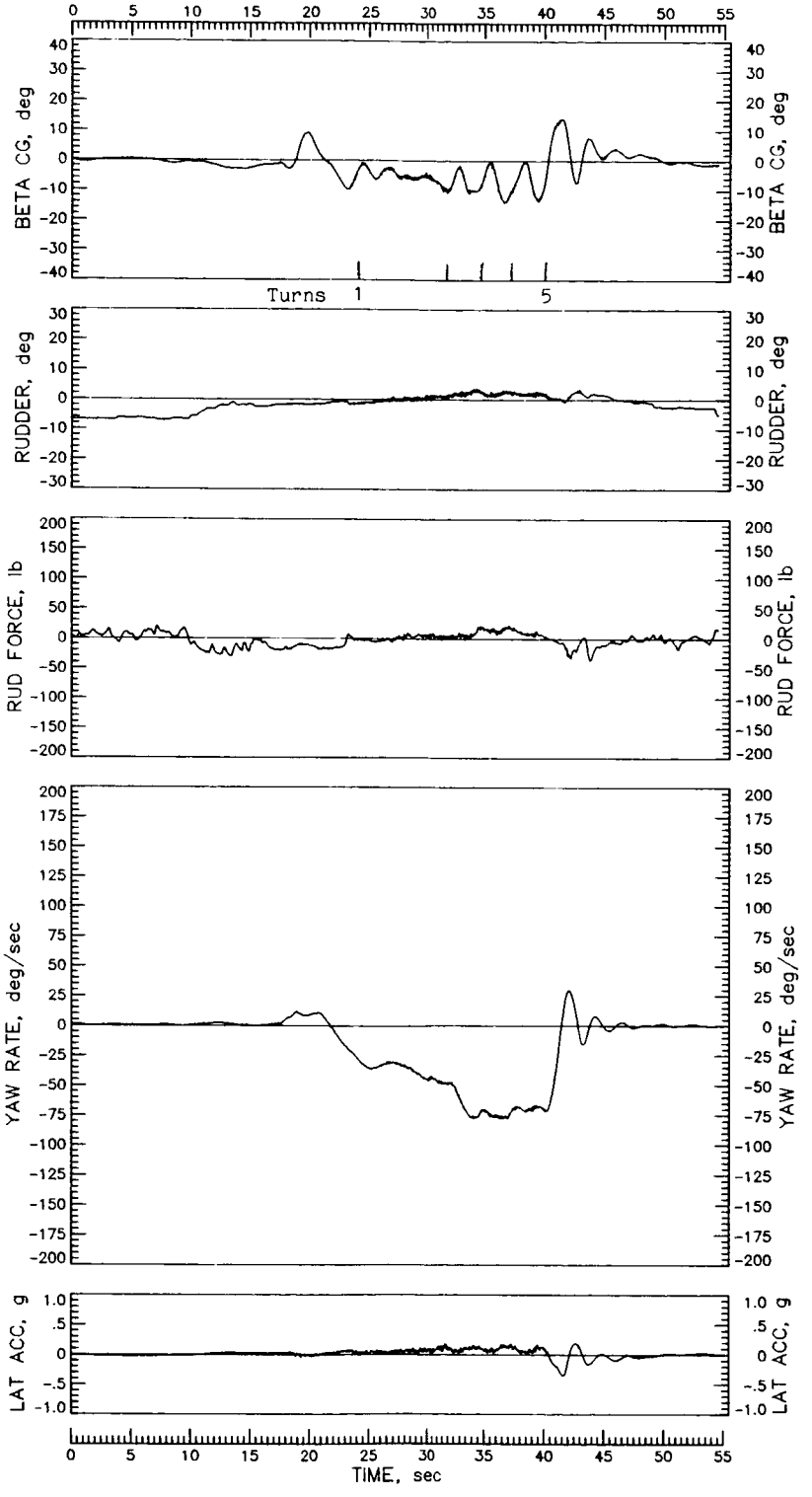

Figure 23.- Continued.

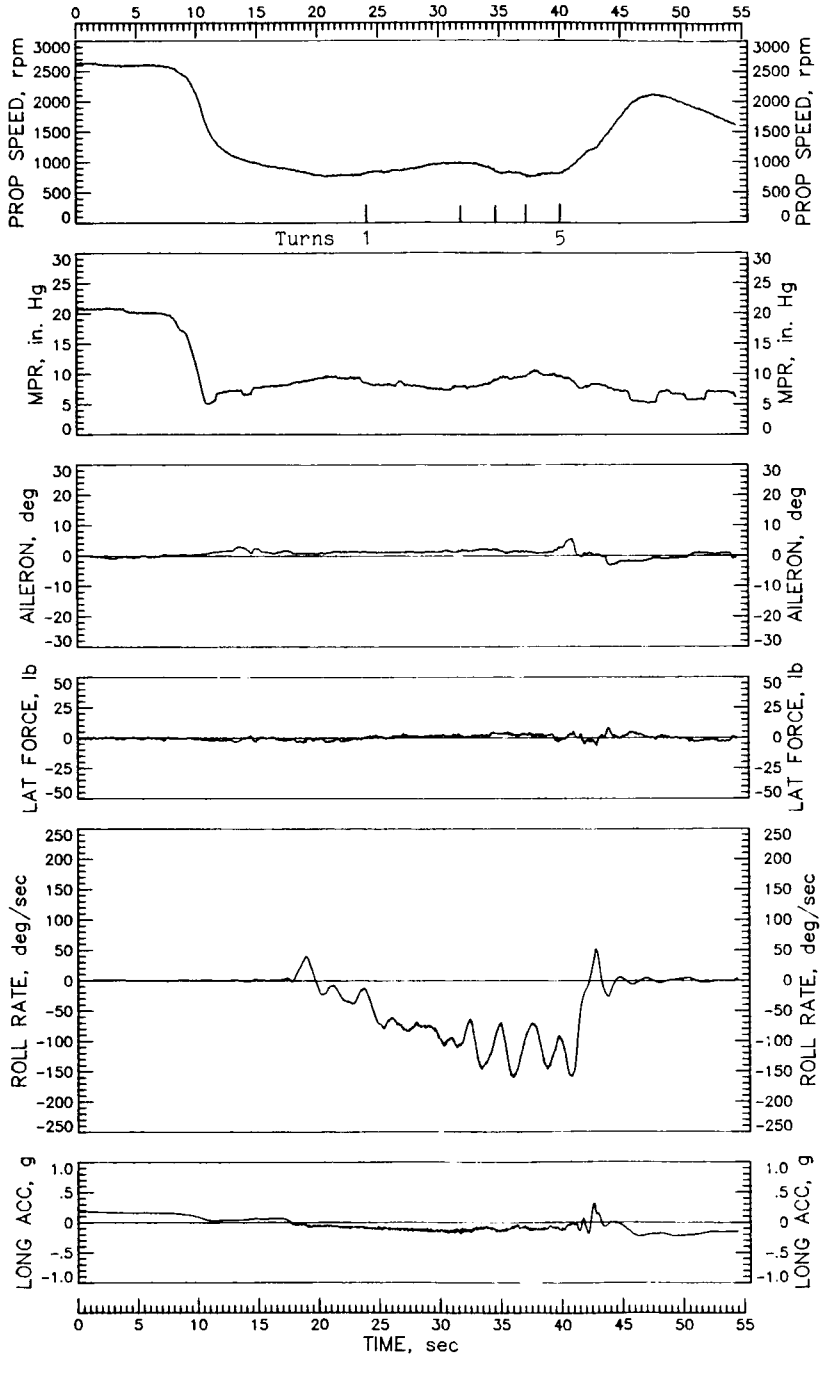

Figure 23.- Continued.

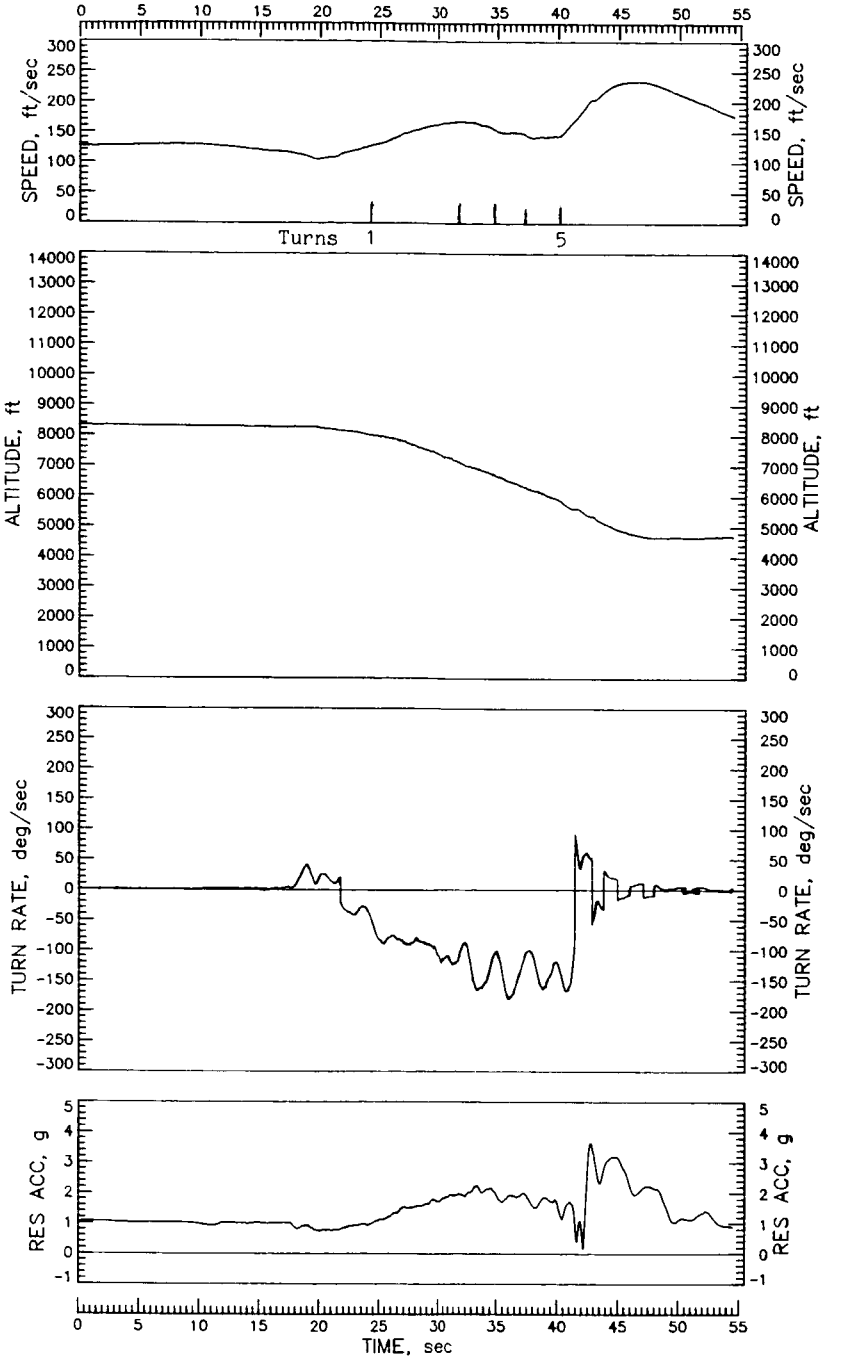

Figure 23.- Concluded.

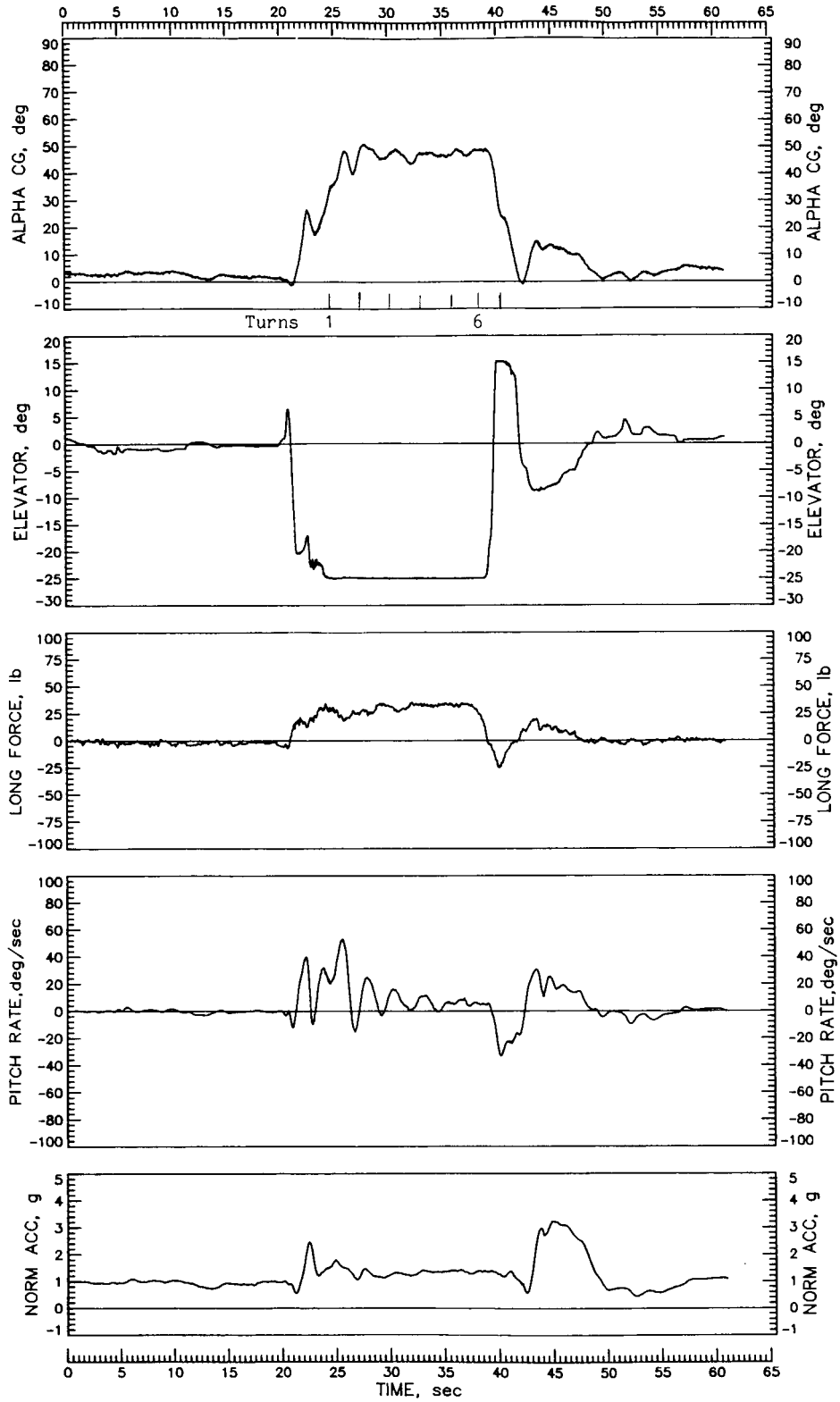

Figure 24.- Left spin with tail 4, entered from maximum-power stall with 14° left sideslip. Engine power decreased during spin even though maximum power was set throughout spin. IYMP = -53×10^{-4}; c.g. at $0.26\bar{c}$.

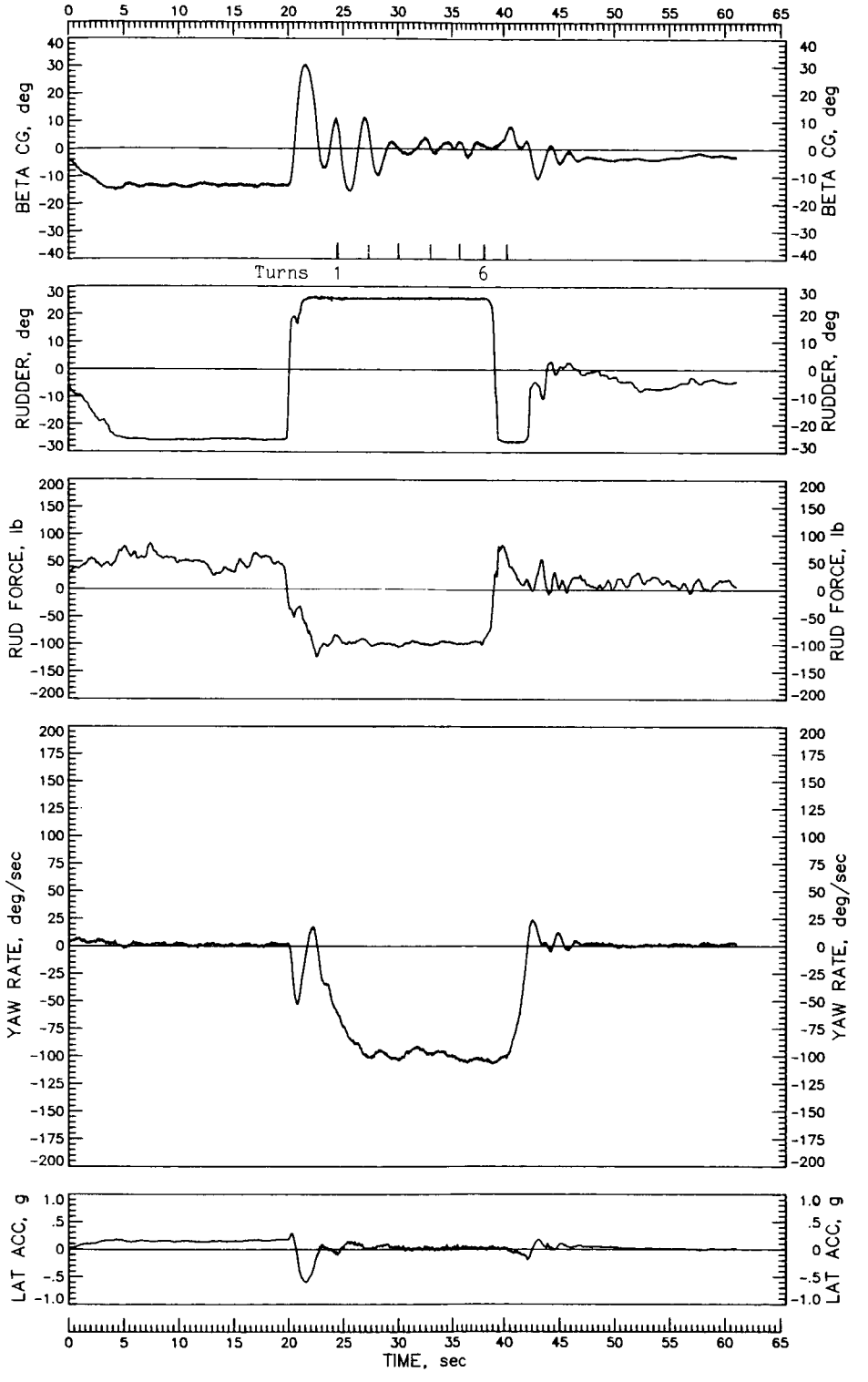

Figure 24.- Continued.

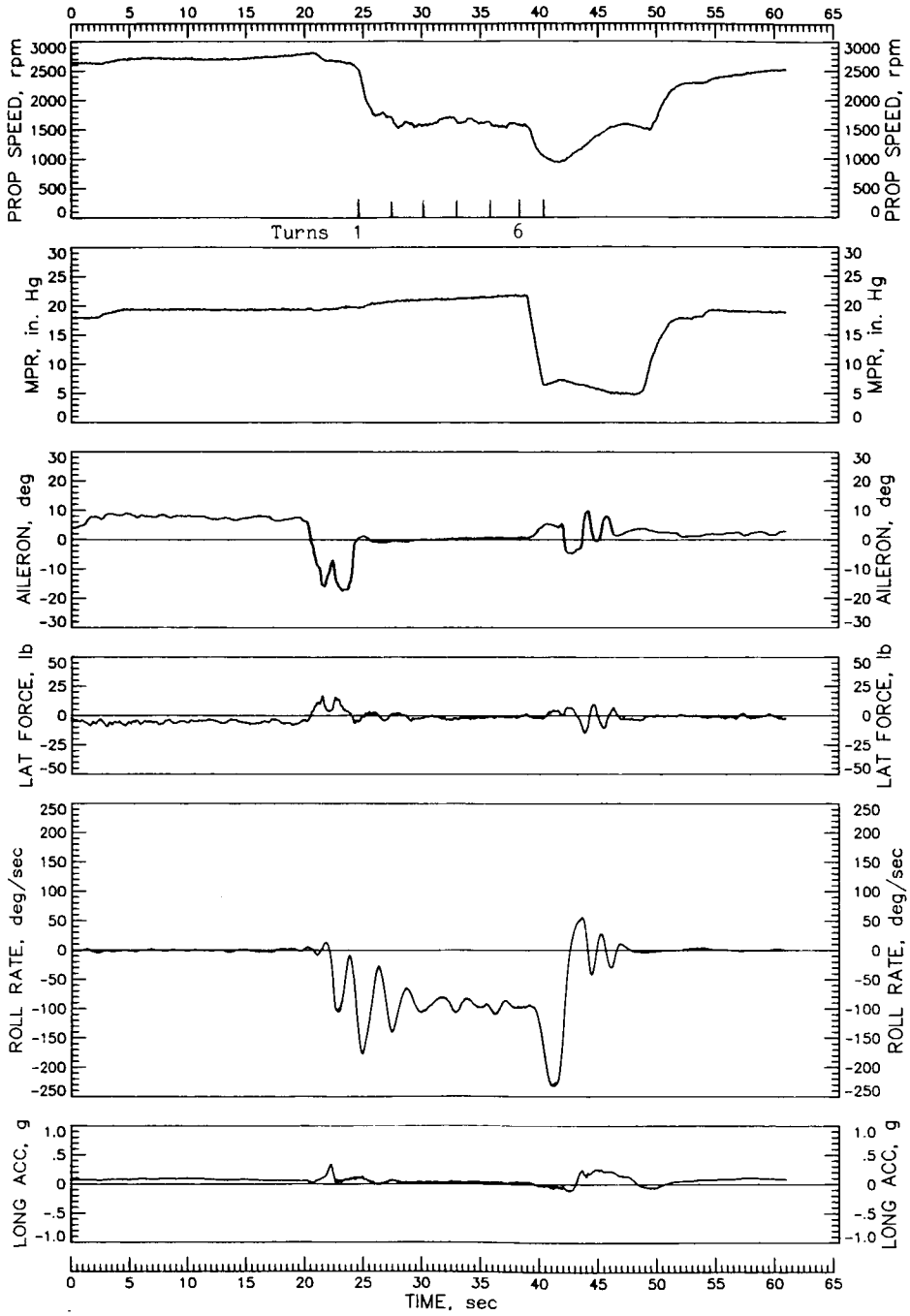

Figure 24.- Continued.

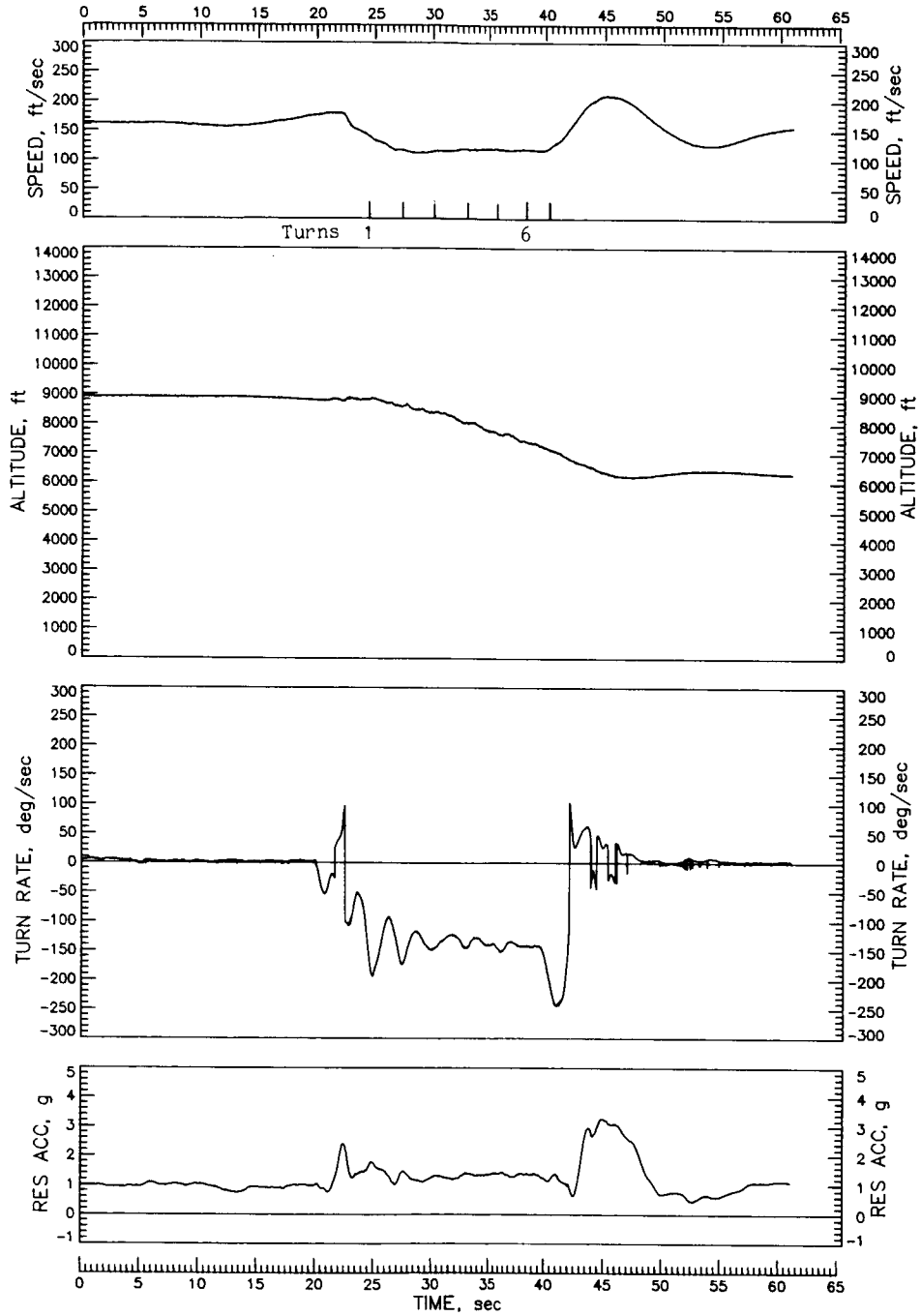

Figure 24.- Concluded.

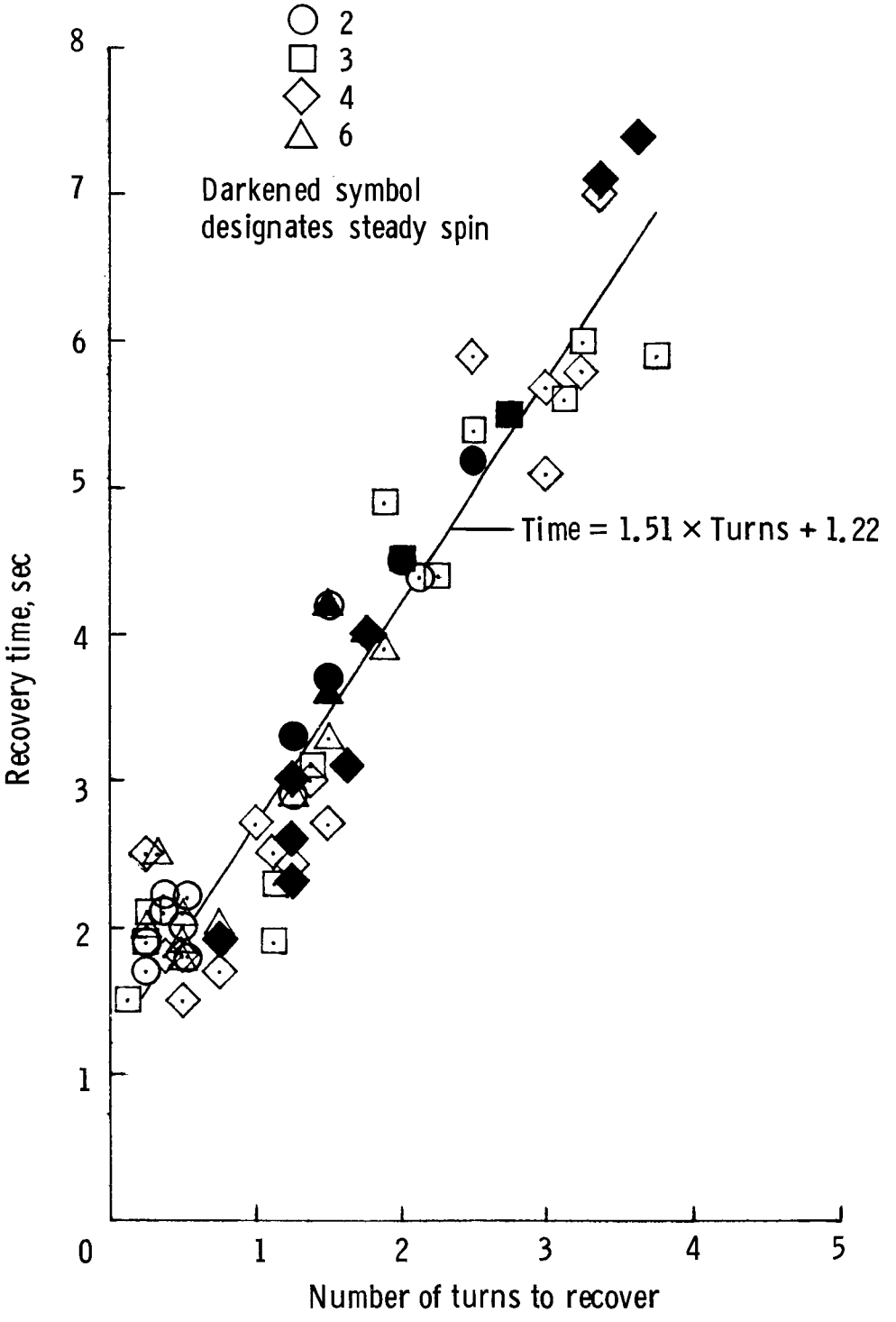

Figure 25.- Recovery time as function of number of turns required to recover from idle-power spins of 1 turn or more with normal recovery controls. Unrecoverable spin with tail 4 is not included. IYMP = -50×10^{-4}; c.g. at $0.26\bar{c}$.

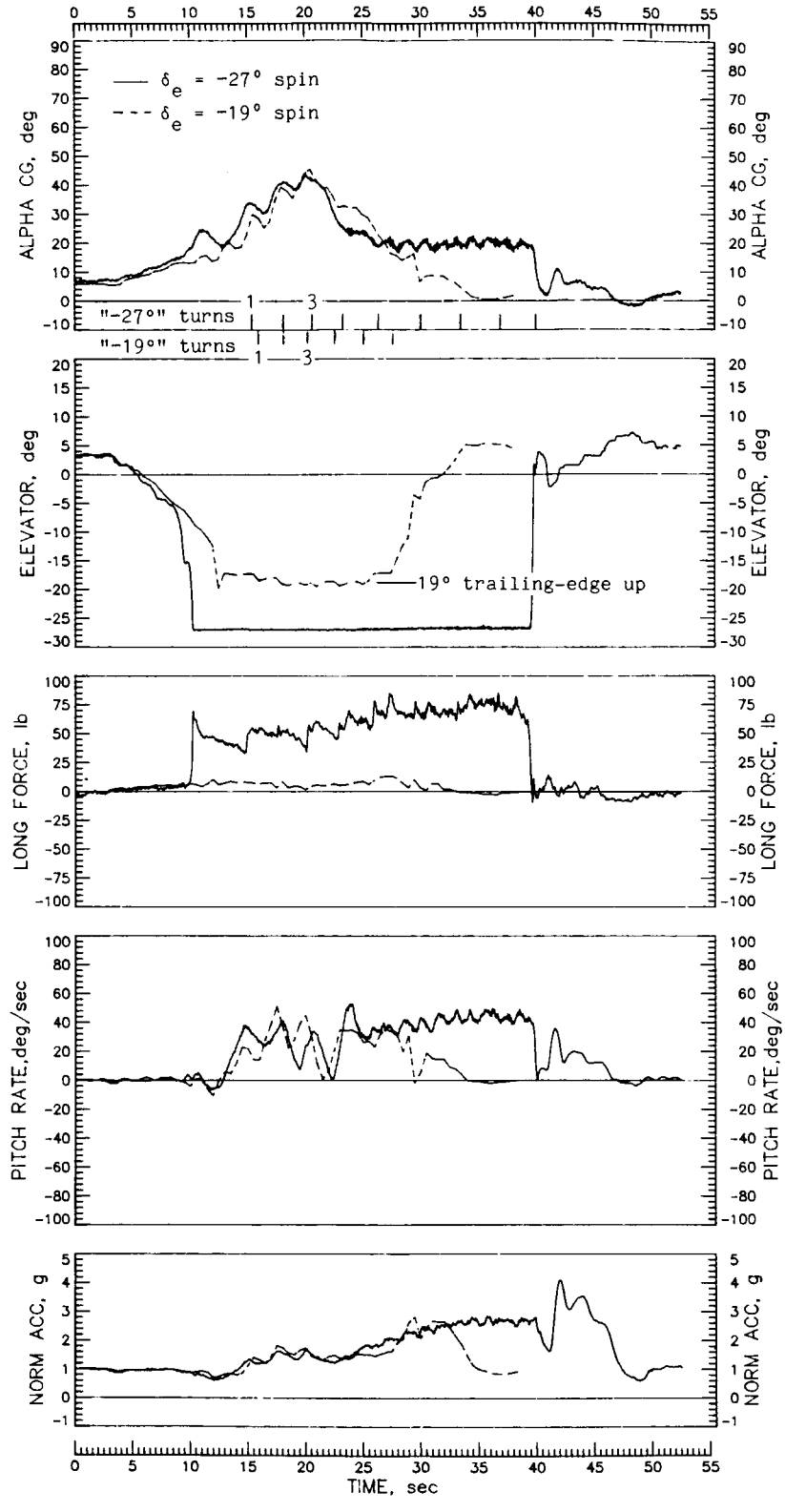

Figure 26.- Right spins with tail 2 for ailerons neutral, illustrating reduction of elevator deflection from -27° to -19° enabled rudder reversal to stop spin. IYMP = -50×10^{-4}; c.g. at $0.26\bar{c}$.

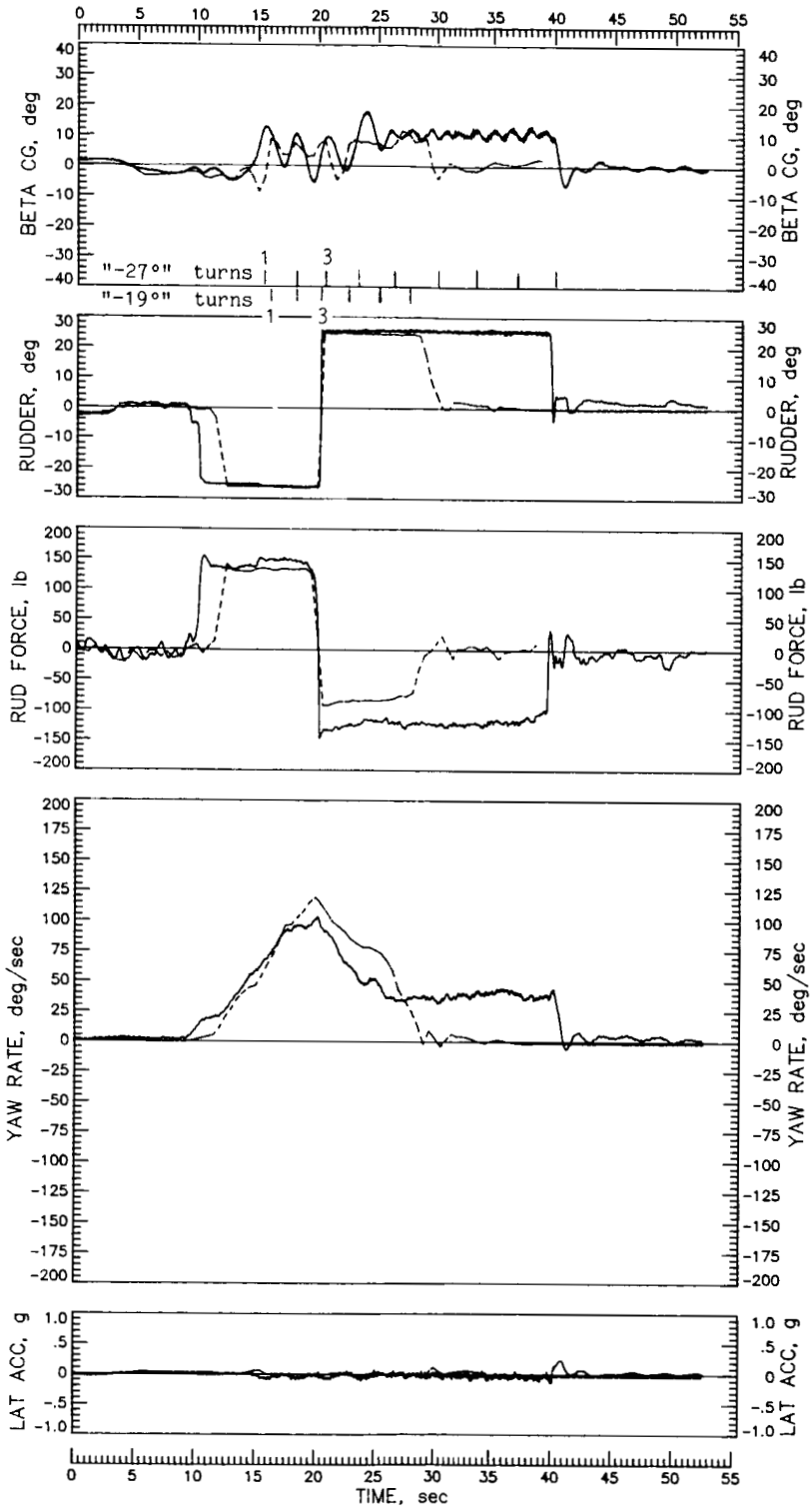

Figure 26.- Continued.

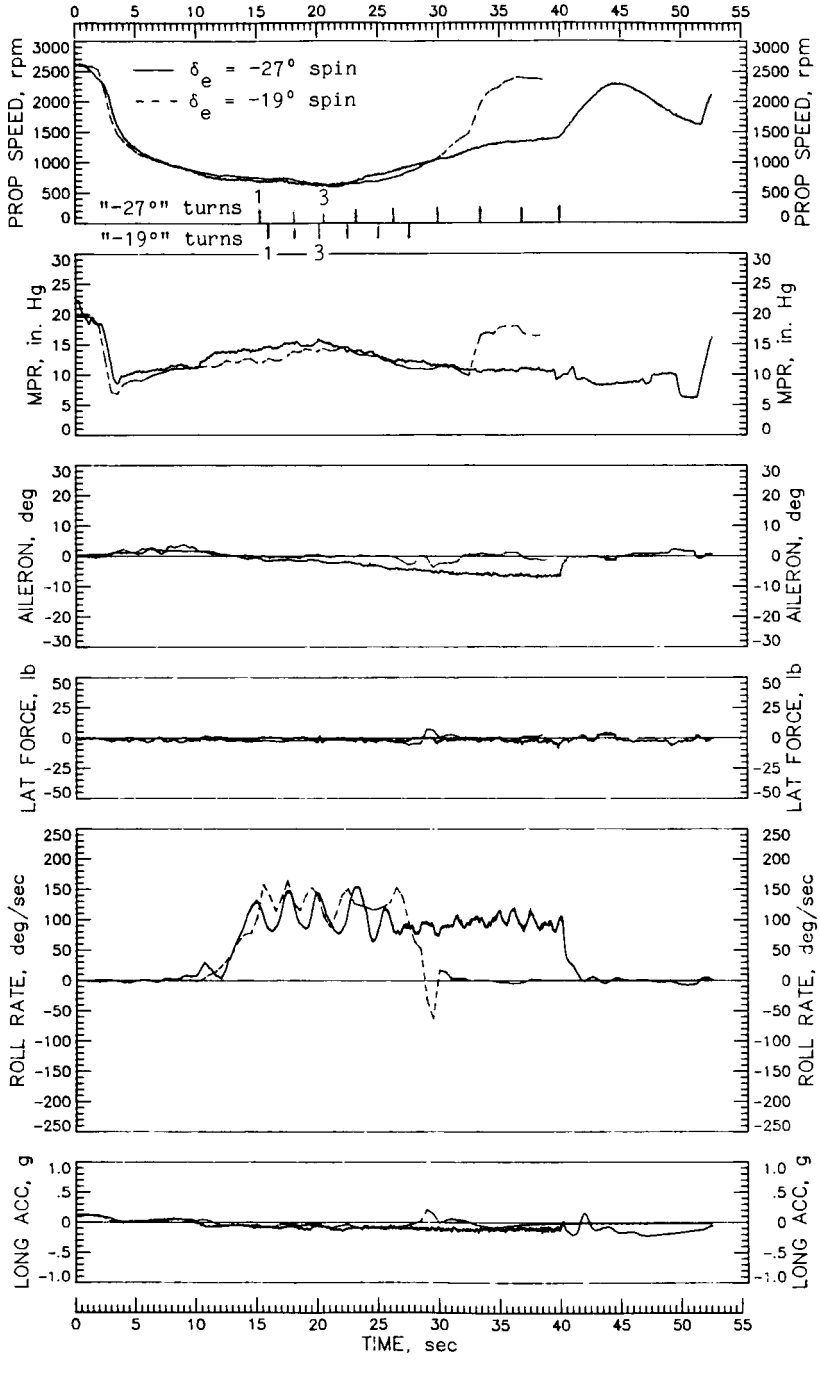

Figure 26.- Continued.

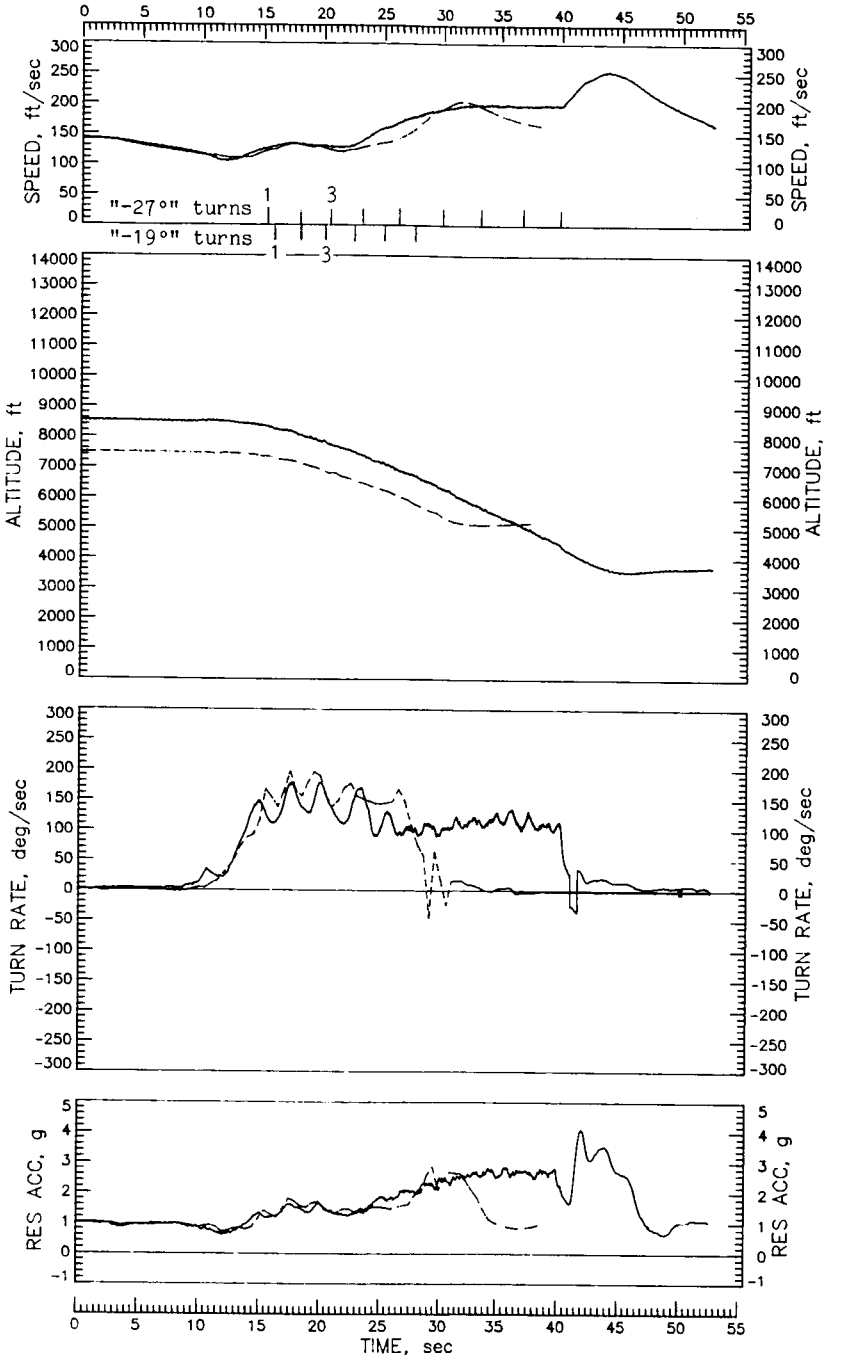

Figure 26.- Concluded.

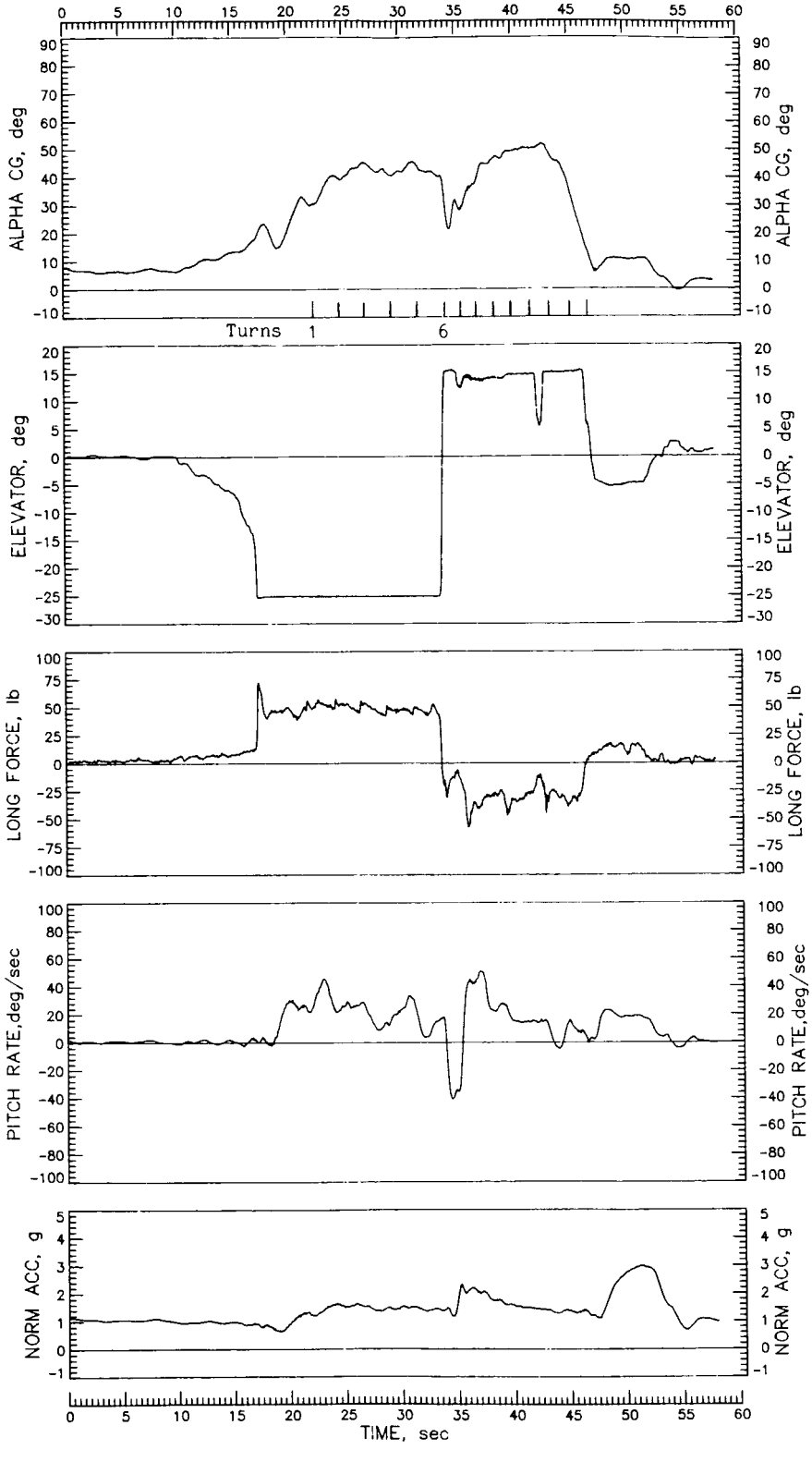

Figure 27.- Idle-power right spin with tail 4 for ailerons neutral, illustrating transition to higher angle-of-attack spin with increased yaw rate following elevator-alone recovery attempt. IYMP = -53×10^{-4}; c.g. at $0.26\bar{c}$.

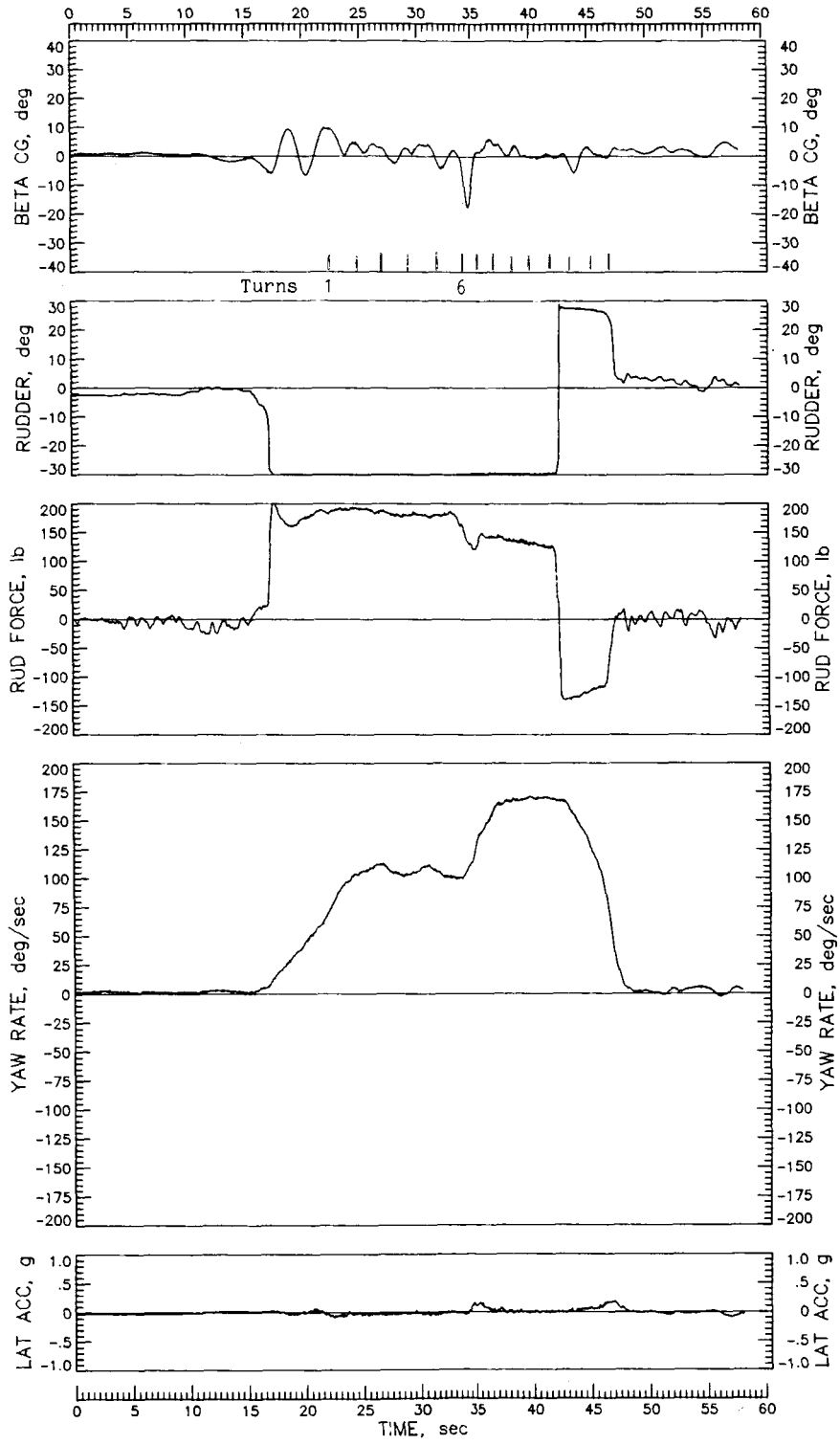

Figure 27.- Continued.

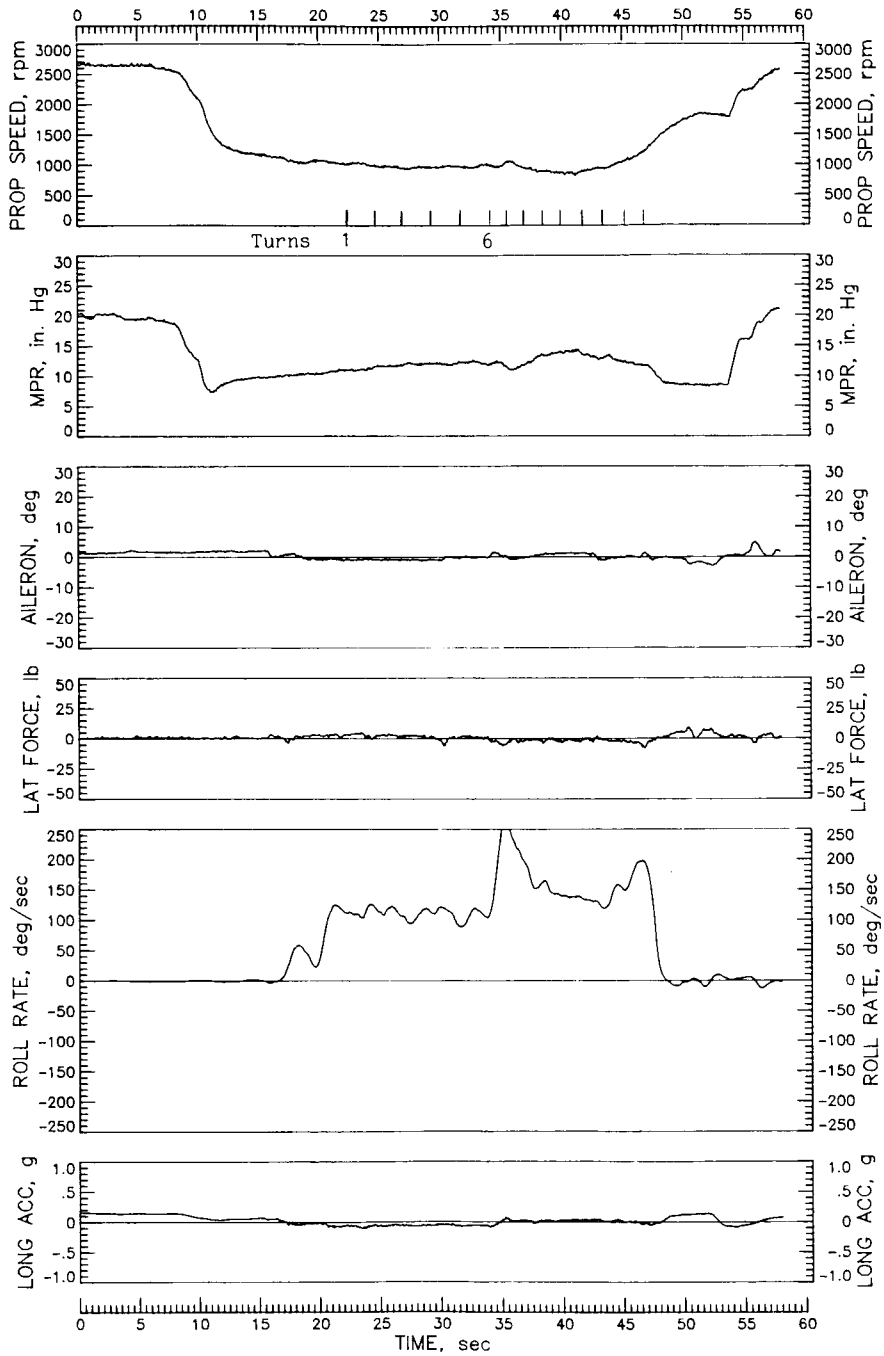

Figure 27.- Continued.

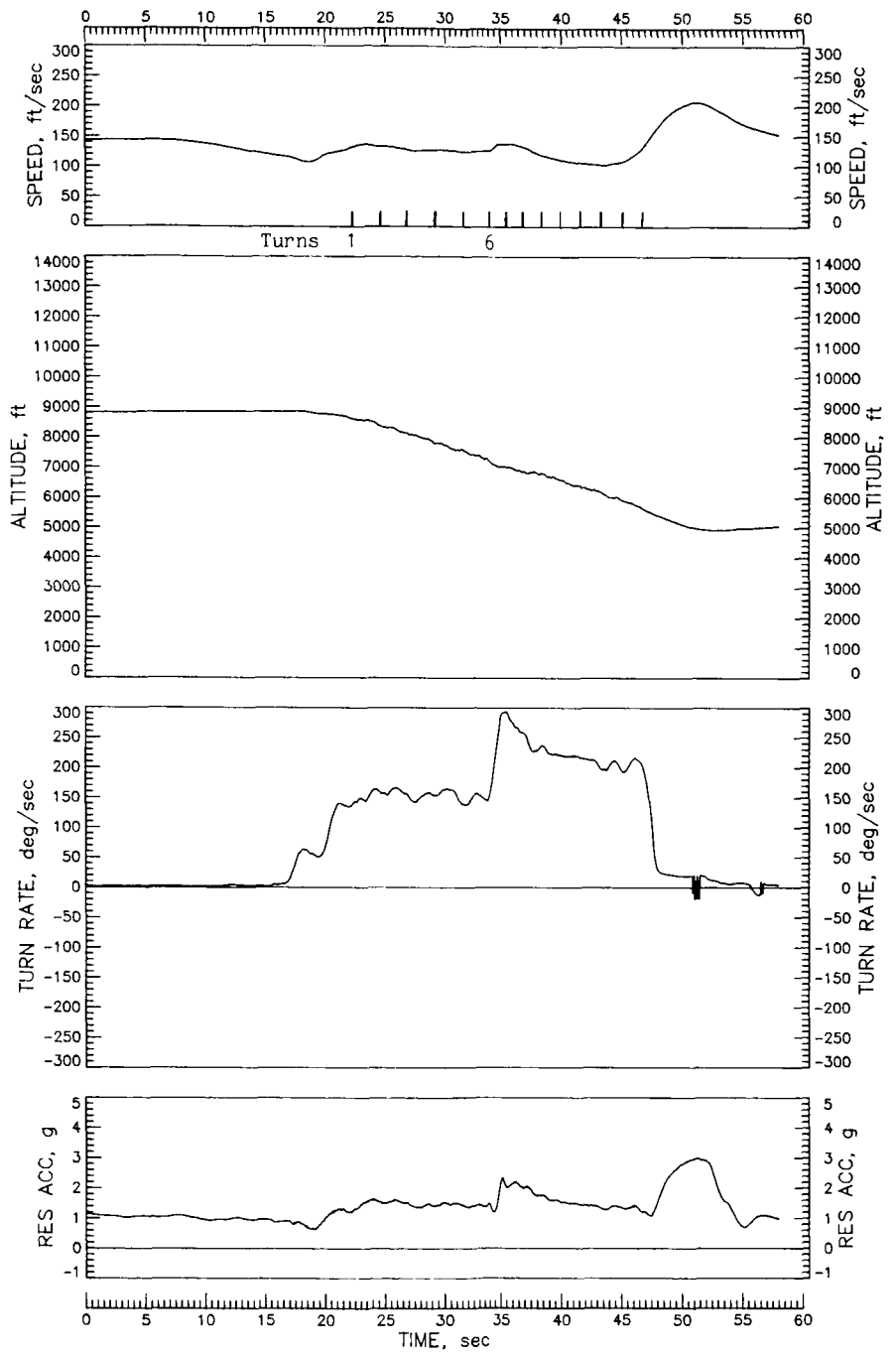

Figure 27.- Concluded.

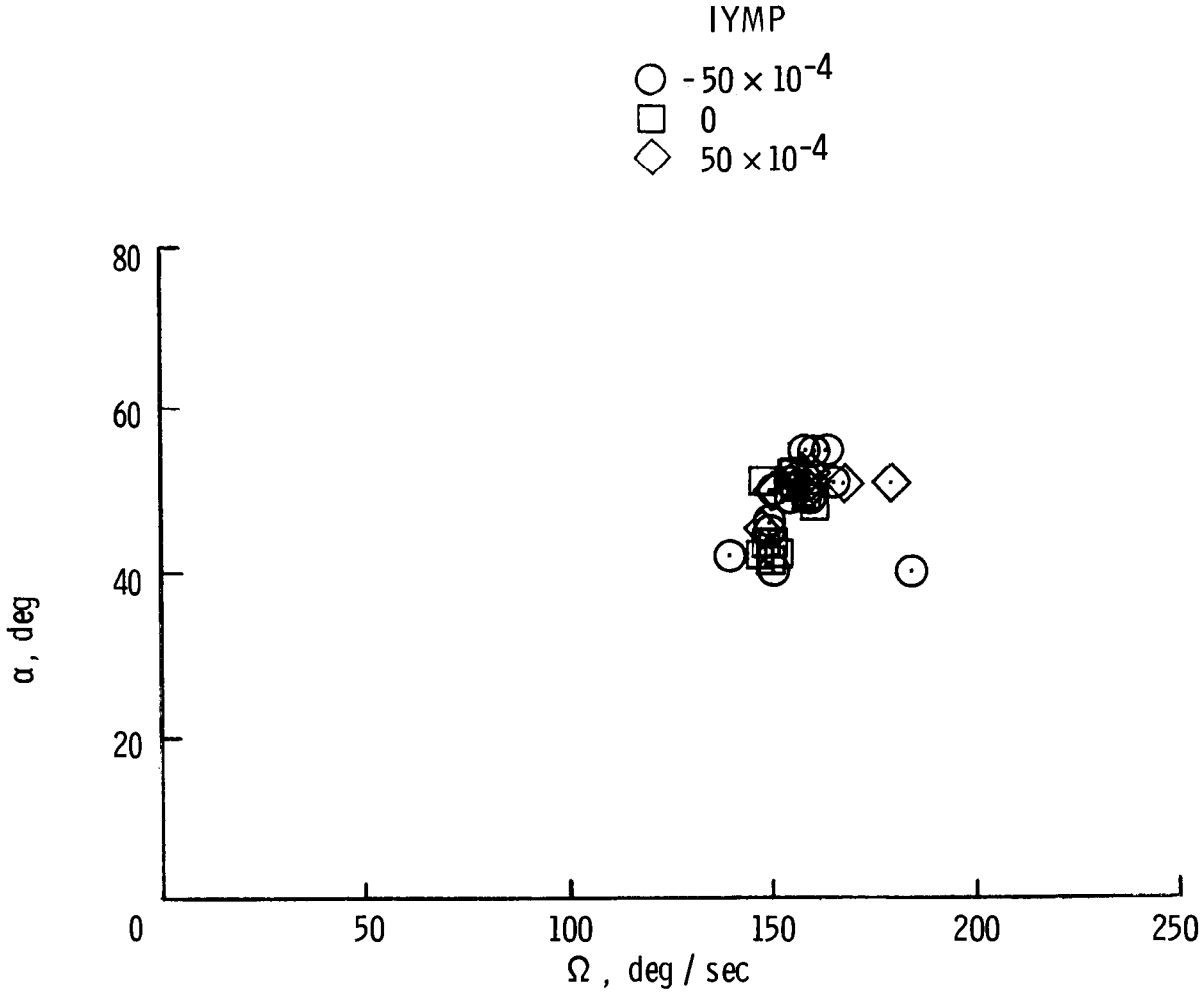

(a) Tail 2.

Figure 28.- Angle of attack and turn rate of fully developed spins for various mass loadings tested. Data include aileron deflections of neutral, with spin, and against spin. c.g. at 0.26$\bar{c}$.

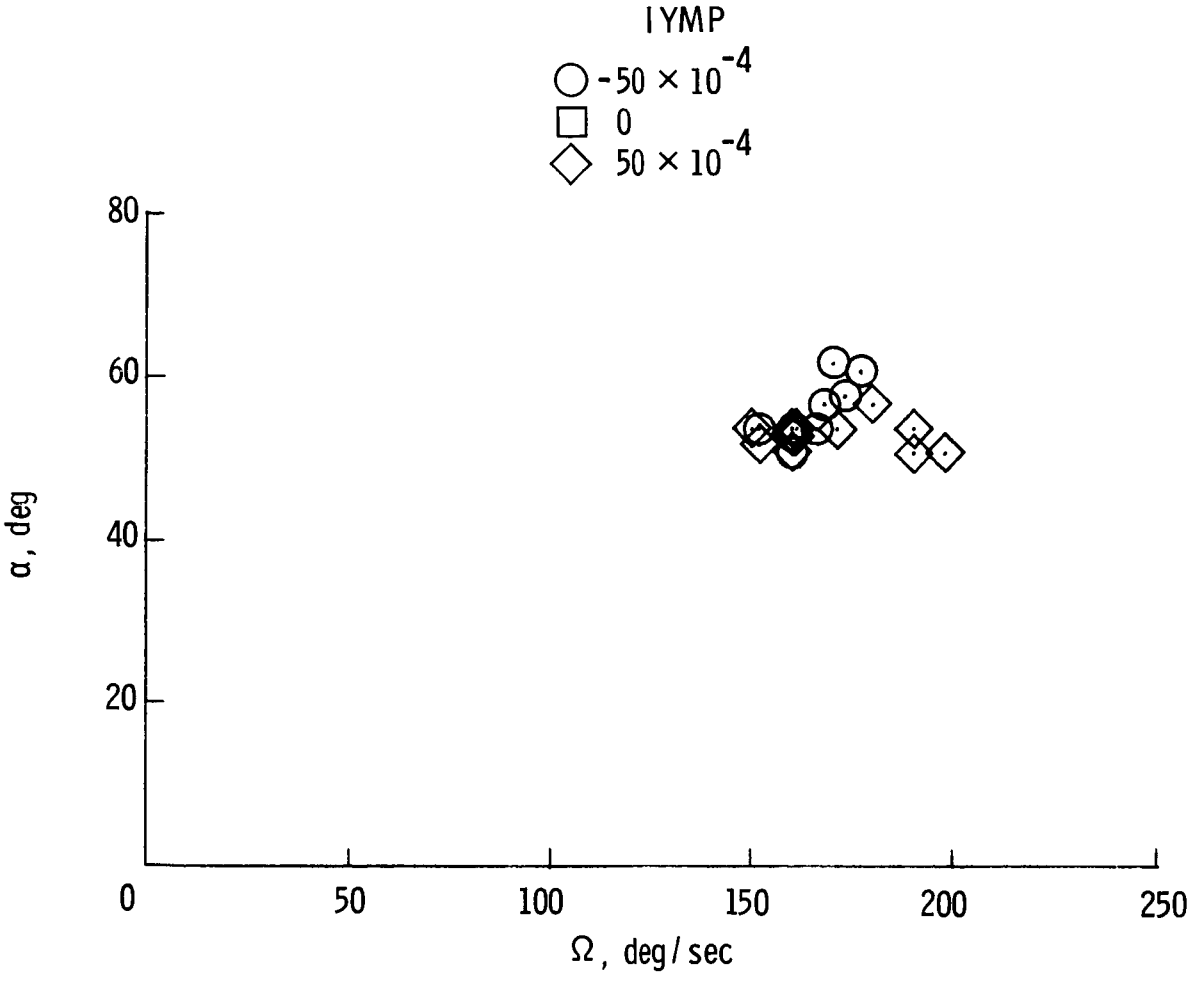

(b) Tail 3.

Figure 28.- Continued.

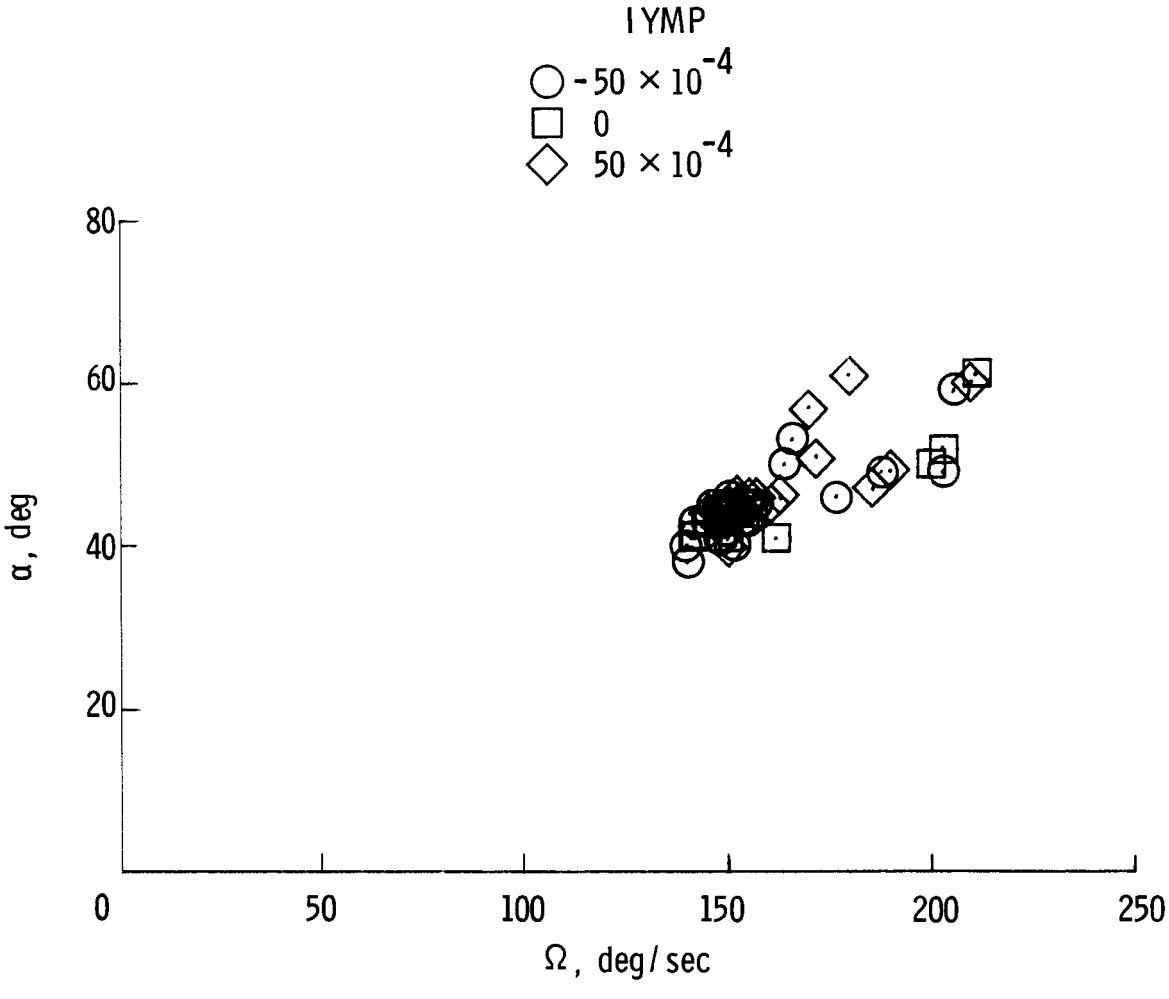

(c) Tail 4.

Figure 28.- Continued.

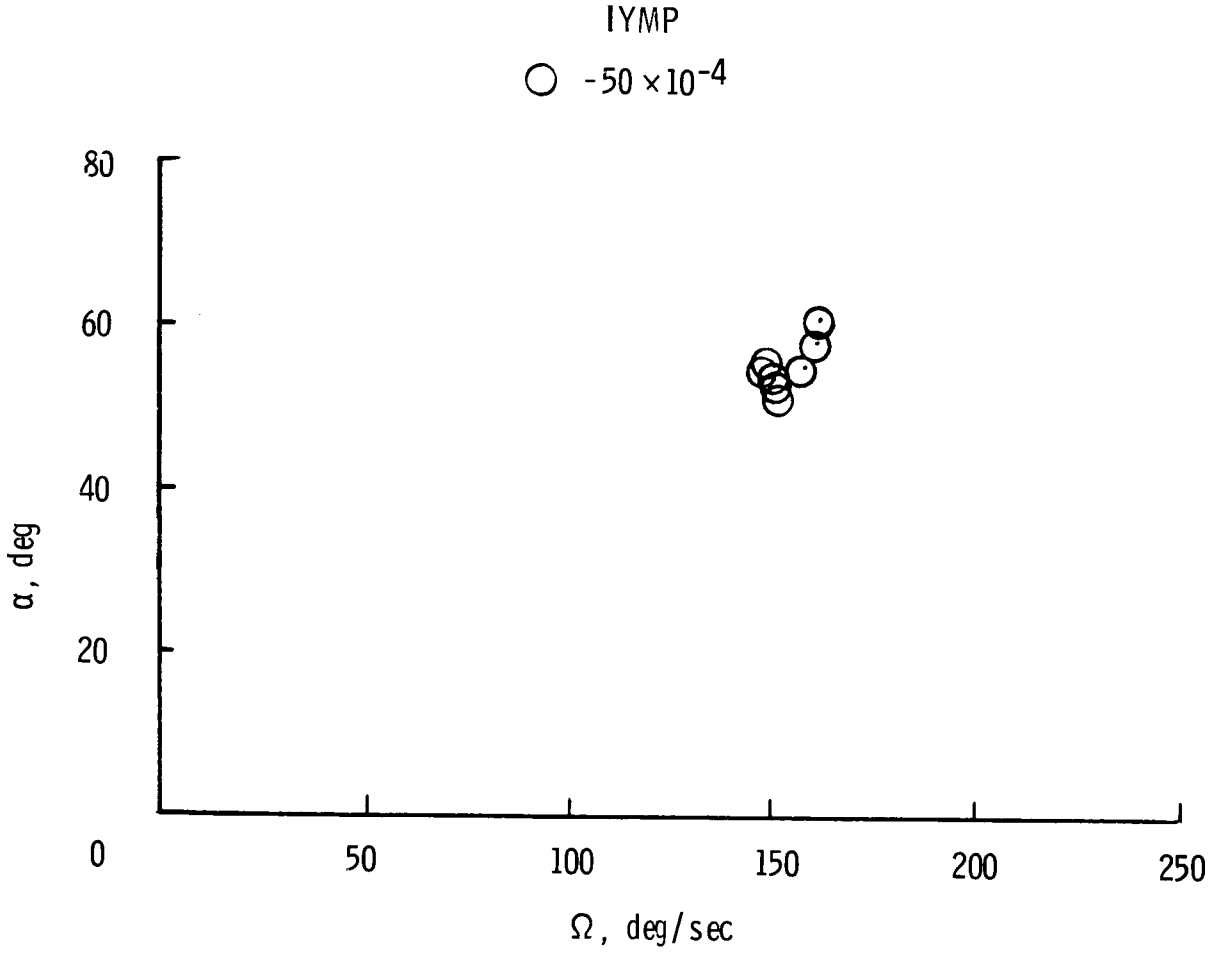

(d) Tail 6.

Figure 28.- Concluded.

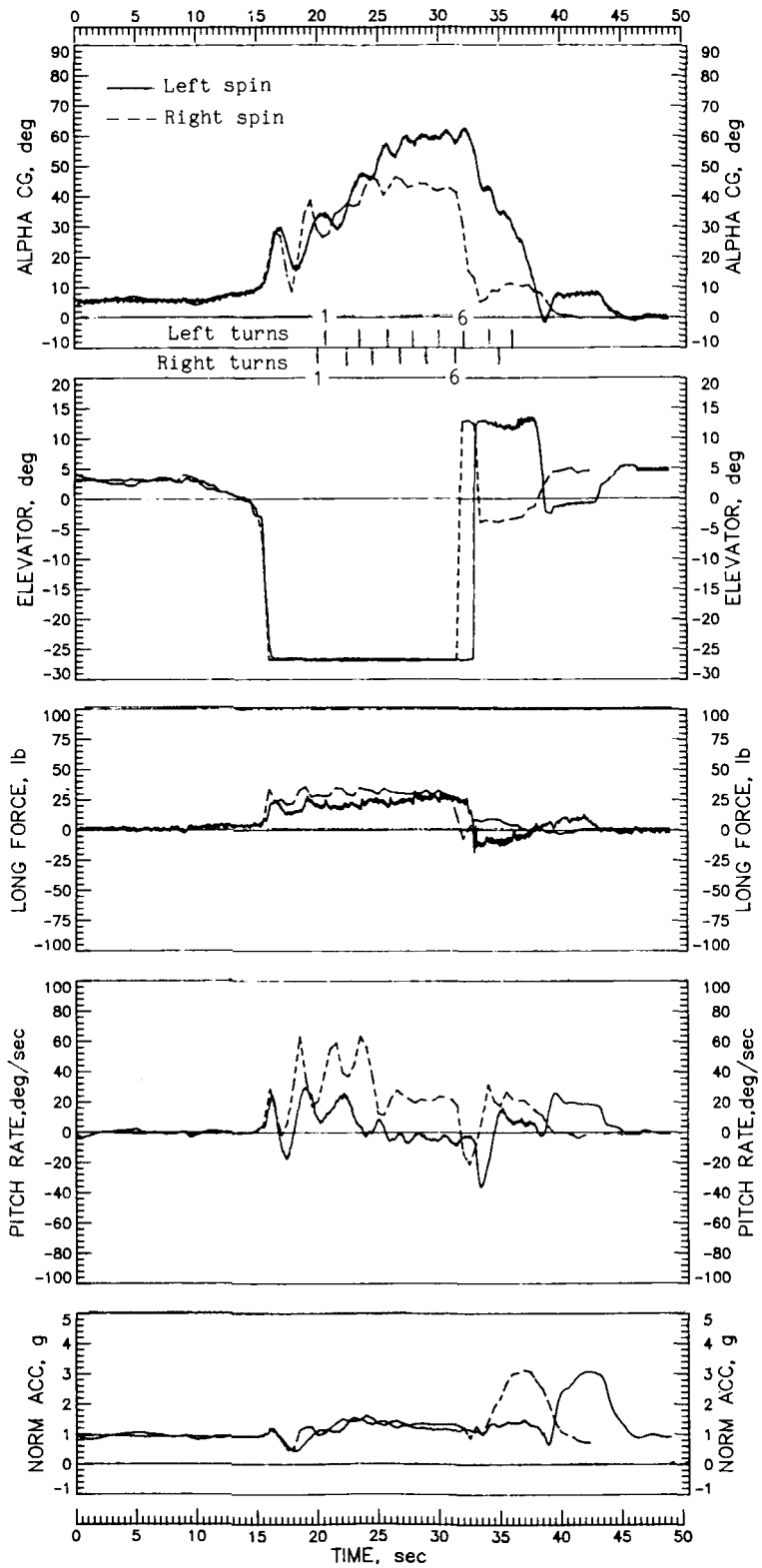

Figure 29.- Idle-power spins with tail 3 for ailerons neutral and right wing 40 lb heavy, illustrating change in spin and recovery with direction of spin. IYMP = -2×10^{-4}; c.g. at $0.26\bar{c}$.

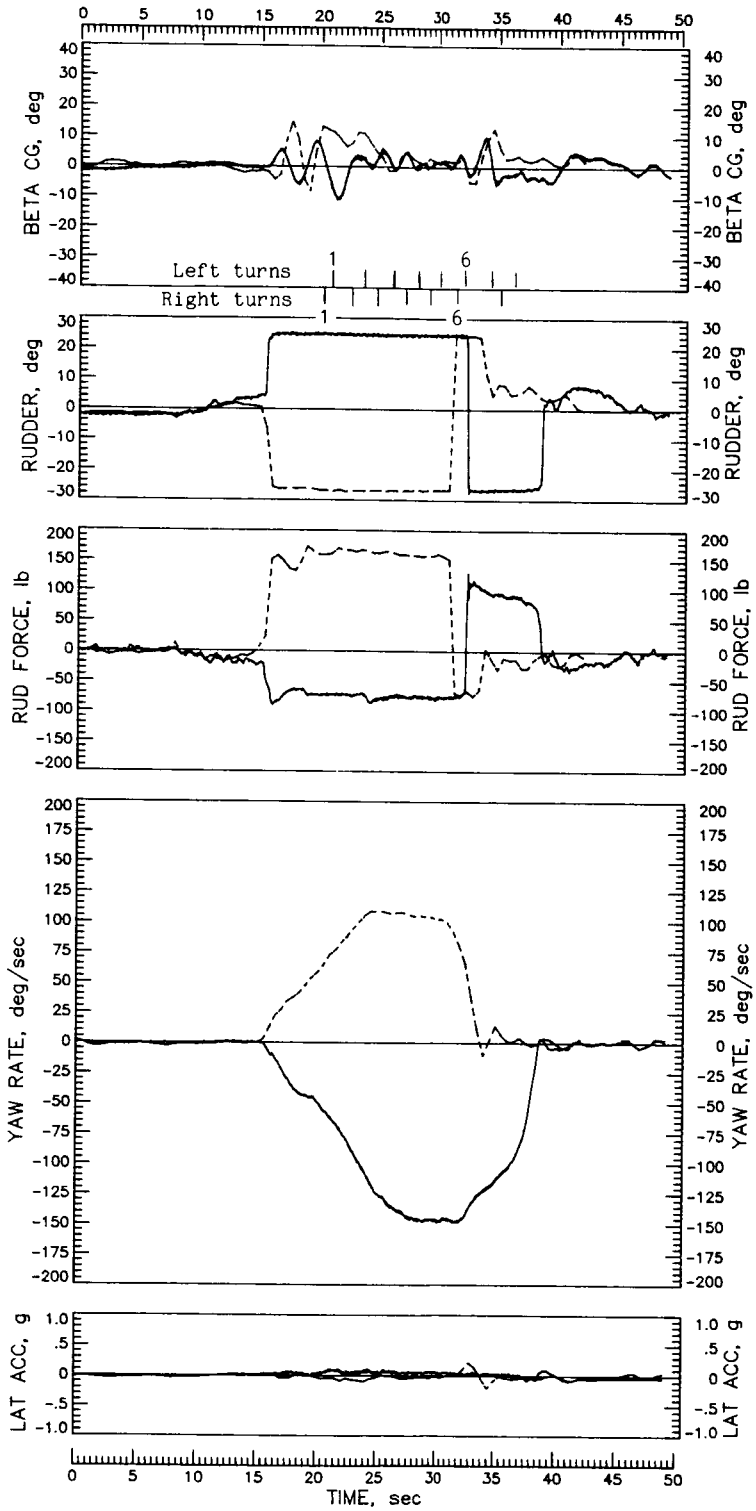

Figure 29.- Continued.

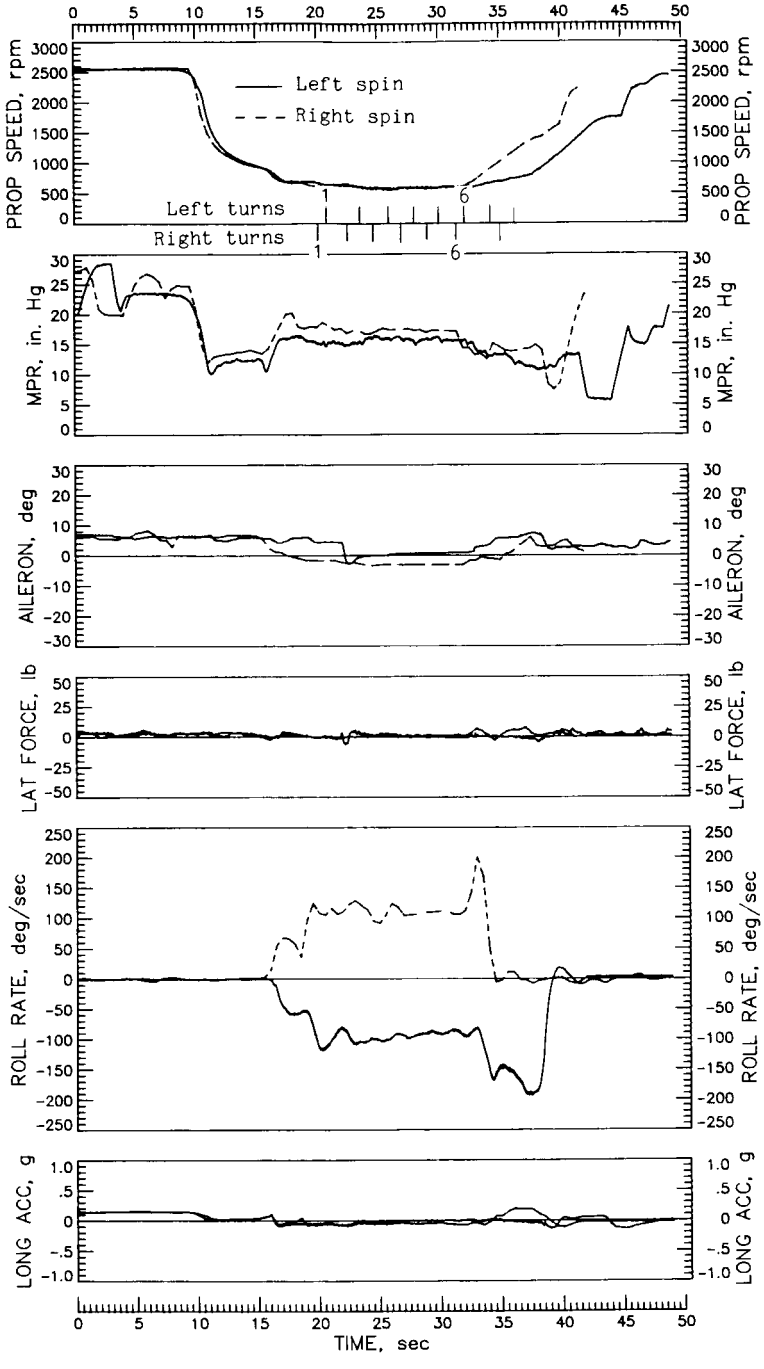

Figure 29.- Continued.

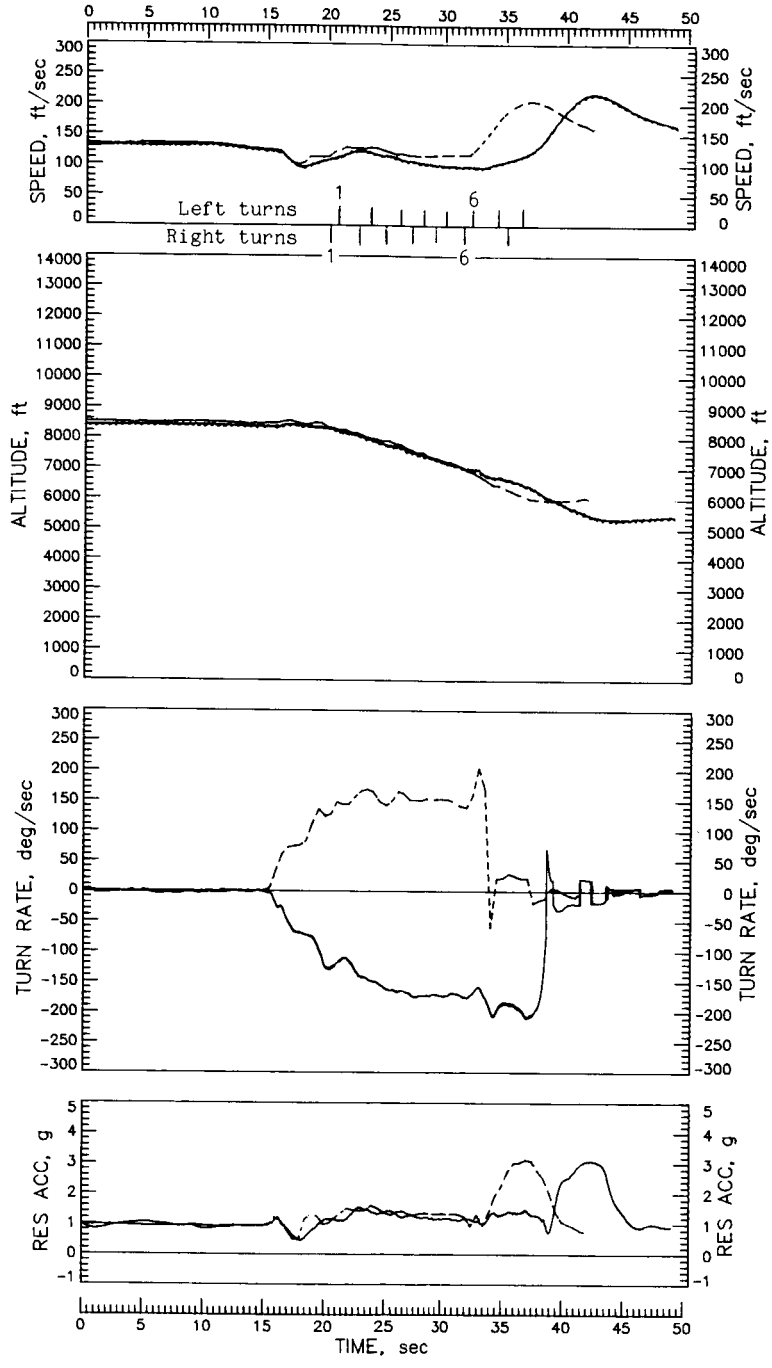

Figure 29.- Concluded.

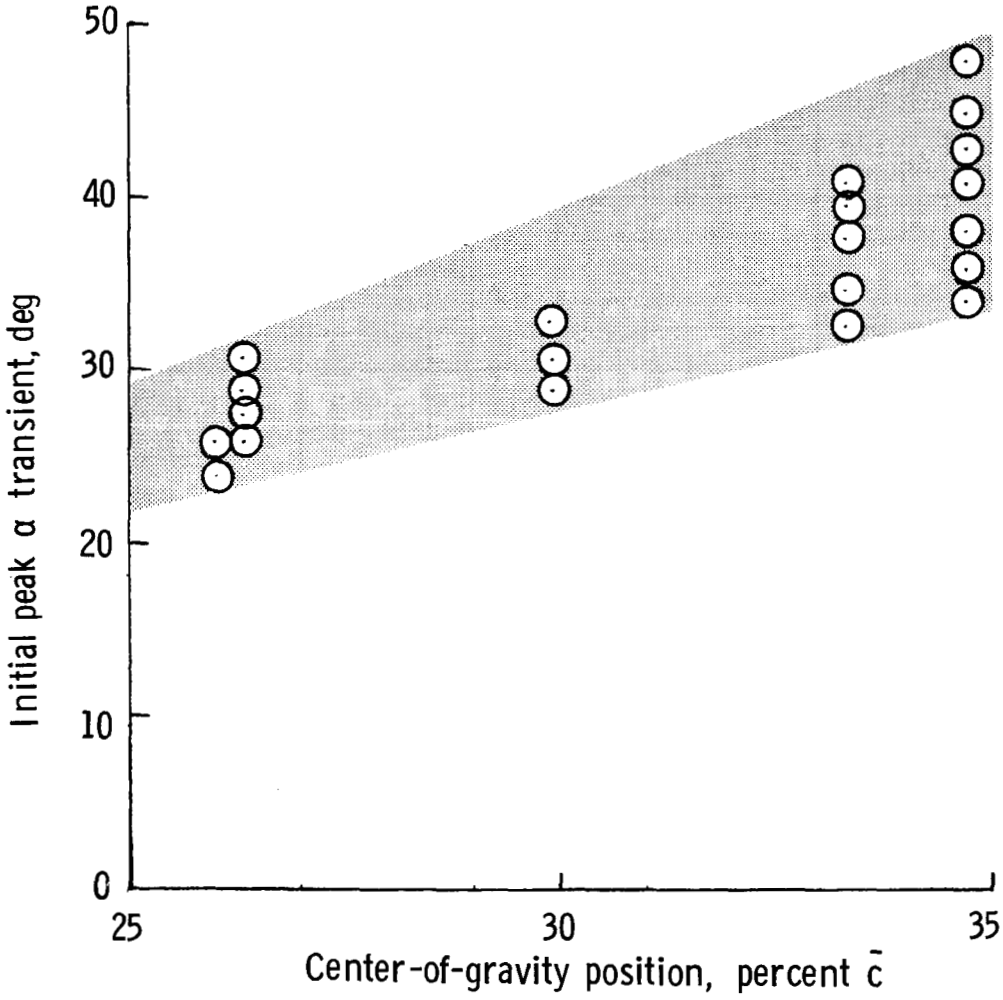

Figure 30.- Magnitude of initial angle-of-attack transient generated by prospin control input as function of center-of-gravity position for airplane with tail 4. Each point represents value for a single spin entry.

Standard Bibliographic Page

1. Report No.	2. Government Accession No.	3. Recipient's Catalog No.
NASA TP-2644		

4. Title and Subtitle	5. Report Date
Flight Investigation of the Effect of Tail Configuration on Stall, Spin, and Recovery Characteristics of a Low-Wing General Aviation Research Airplane	February 1987
	6. Performing Organization Code 505-61-41-01
7. Author(s) H. Paul Stough III, James M. Patton, Jr., and Steven M. Sliwa	8. Performing Organization Report No. L-16194
9. Performing Organization Name and Address NASA Langley Research Center Hampton, VA 23665-5225	10. Work Unit No.
	11. Contract or Grant No.
12. Sponsoring Agency Name and Address National Aeronautics and Space Administration Washington, DC 20546-0001	13. Type of Report and Period Covered Technical Paper
	14. Sponsoring Agency Code

15. Supplementary Notes

16. Abstract

Flight tests were performed to investigate the stall, spin, and recovery characteristics of a low-wing, single-engine, light airplane with four interchangeable tail configurations. The four tail configurations were evaluated for effects of varying mass distribution, center-of-gravity position, and control inputs. The airplane tended to roll-off at the stall. Variations in tail configuration produced spins ranging from 40° to 60° angle of attack and turn rates of about 145 to 208 deg/sec. Some unrecoverable flat spins were encountered which required use of the airplane spin chute for recovery. For recoverable spins, antispin rudder followed by forward wheel with ailerons centered provided the quickest spin recovery. The moderate spin modes agreed very well with those predicted from spin-tunnel model tests, however, the flat spin was at a lower angle of attack and a slower rotation rate than indicated by the model tests.

17. Key Words (Suggested by Authors(s))	18. Distribution Statement
Stall Spin General aviation	Unclassified - Unlimited Subject Category 05

19. Security Classif.(of this report)	20. Security Classif.(of this page)	21. No. of Pages	22. Price
Unclassified	Unclassified	126	A06

For sale by the National Technical Information Service, Springfield, Virginia 22161

NASA-Langley, 1987